

**UTILIZING ANTIGENIC PEPTIDE AND ADHESION MOLECULE  
CONJUGATES TO SUPPRESS AUTOIMMUNE DISEASE IN ANIMAL  
MODELS**

By

Barlas Büyüktimkin

Pharm.D., Pharmacy, The University of Kansas, 2005

M.S., Pharmaceutical Chemistry, The University of Kansas, 2008

Submitted to the Department of Pharmaceutical Chemistry and the Faculty of the  
Graduate School of the University of Kansas in partial fulfillment of the requirements  
for the degree of Doctor of Philosophy.

Dissertation Committee:

---

Chairperson                      Teruna J. Siahaan

---

Cory J. Berkland

---

Jennifer S. Laurence

---

David B. Volkin

---

Krzysztof Kuczera

Date Defended: October 7, 2011

The Dissertation Committee for Barlas Büyüktimkin  
certifies that this is the approved version of the following dissertation:

**Utilizing Antigenic Peptide and Adhesion Molecule Conjugates to Suppress  
Autoimmune Disease in Animal Models**

Dissertation Committee:

---

Chairperson            Teruna J. Siahaan

---

Cory J. Berkland

---

Jennifer S. Laurence

---

David B. Volkin

---

Krzysztof Kuczera

Date approved: October 7, 2011

**Utilizing antigenic peptide and adhesion molecule conjugates to suppress  
autoimmune disease in animal models**

Barlas Büyüktimkin

The University of Kansas, 2011

Peptides and proteins have been used as carriers to target and deliver molecules to sites of action. Conjugating a drug to a macromolecule offers the unique advantage of being able to target drug to a specific cell surface receptor with high affinity, thereby increasing efficacy and reducing side effects. Furthermore, conjugations between two different peptides, or between peptide and protein, that have activities to modulate two receptors have shown promising results in suppressing autoimmune diseases in animal models. Therefore, the objective of the dissertation was to explore the possibility of selectively targeting peptide and protein conjugates to antigen presenting cells to suppress autoimmune diseases. The I-domain of leukocyte function associated antigen-1 (LFA-1) conjugated to antigenic PLP<sub>139-151</sub> peptide (IDAC-3) suppressed experimental autoimmune encephalomyelitis (EAE) when delivered in a vaccine-like manner by shifting the immune balance away from Th17-mediated pathology by increasing involvement of T-reg cells (Chapter 2). PLP<sub>139-151</sub> conjugated to LABL adhesion peptide (Ac-PLP-BPI-NH<sub>2</sub>-2) was formulated in a colloidal gel for a one-time subcutaneous administration to suppress EAE. A vaccine-like administration of the peptide conjugate suppressed EAE as well as the relapse. *In vitro* cytokine studies suggested that the mechanism of suppression was due to the shift of the immune balance away from a Th17-

mediated response (Chapter 3). The utility of BPI to target other autoimmune diseases such as collagen-induced arthritis (CIA) was also investigated. Here, collagen type II peptides were conjugated to LBL (CII-BPI). It was found that suppression of disease is dependent upon the sequence of the antigen, and that the mechanism of disease suppression was linked to a shift in the immune balance from a proinflammatory to a regulatory response (Chapter 4).

*Dedicated to my Family*

## ACKNOWLEDGMENTS

I would like to thank my advisor, Dr. Teruna J. Siahaan. I feel extremely fortunate to have been able to join his group. Without his support, guidance, and patience, I would not be where I am today. He leads by example, and strongly believes in doing things the right way without sacrificing integrity. What I learned from him throughout my time as a scientist has made me a better person outside of the lab. I am thankful to him for helping me become the person I was meant to be.

I am also thankful for my dissertation committee members, Dr. Cory J. Berkland, Dr. Jennifer S. Laurence, Dr. David B. Volkin, and Dr. Krzysztof Kuczera. I appreciate the time and effort for the suggestions, comments, and corrections from Dr. Berkland and Dr. Laurence as readers of this dissertation.

Next, I would like to thank all of the past and present members of the Siahaan lab group. I appreciate their friendships and helpful discussions. I would like to thank the past Siahaan lab members, Drs. Prakash Manikwar, Maulik Trivedi, Sumit Majumdar, Kai Zheng, Naoki Kobayashi, Bimo Tejo, and Rahmawati Ridwan. I would also like to thank the current members of the Siahaan group, Dr. Paul Kiptoo, Ahmed Badawi, John Stewart, Marlyn Laksitorini, Ahmed Al Aofi, and Mohammed Al Salman.

I would like to especially thank Dr. Paul Kiptoo. I am grateful for his help and guidance in helping me get numerous projects off the ground. I will always remember his patience and willingness to help, even if it meant staying after hours or coming in during the weekends. I also want to convey my thanks to Dr. Prakash Manikwar. I thoroughly enjoyed the times we spent together in the lab, as well as outside of the lab. I will treasure

the memories of these days and look to create many more in the future. I am also grateful to have known Ahmed Badawi. His friendship and easy-going personality made life in the lab that much more fun.

I would also like to thank everyone involved with the Pharmaceutical Chemistry softball teams during my early years of graduate school. I am also grateful to everyone who participated in basketball during the latter part of my graduate career: Ahmed Badawi, Chris Kuehl, John Stewart, Josh Sestak, Justin Thomas, Amir Fakhari, Connor Dennis, and Tammi Vasiljevik.

I am sincerely appreciative of being the recipient of the NIGMS biotechnology predoctoral training grant, which generously supported me during the latter part of my graduate career. I am also indebted to Drs. Ajit D'Souza and Sumit Majumdar for allowing me to work as an intern at Becton Dickinson Technologies. I would also like to thank Dr. Qun Wang for helping me with the colloidal gel experiments.

I am also extremely grateful to all the staff, faculty, and students of the Department of Pharmaceutical Chemistry at the University of Kansas. I am especially grateful to the late Dr. J. Howard Rytting.

I would like to express my gratitude to Nancy Harmony for proofreading my dissertation.

Throughout my time in Lawrence, I made new friends. Many of these relationships have resulted in life-long friendships. I will cherish the memories we have already made, and look forward to many more in the years to come.

Finally, I want to thank my family. The patience, sacrifice, and love you have shown were inspiring and made me a better person.

## TABLE OF CONTENTS

<b>Chapter 1: Development of Therapeutic Macromolecule Conjugates to Make Better Drugs</b> .....	1
<b>1.1</b> Introduction.....	2
<b>1.2</b> Antibody-Drug Conjugates (ADC) .....	4
<b>1.2.1</b> Success of ADC in the market.....	4
<b>1.2.2</b> Examples of cargo molecules.....	5
<b>1.3</b> Chemistry of ADC.....	6
<b>1.3.1</b> Cleavable linkers.....	6
<b>1.3.1.1</b> Acidic linkers.....	6
<b>1.3.1.2</b> Reducing linkers.....	7
<b>1.3.1.3</b> Tumor-specific protease linkers.....	10
<b>1.3.2</b> Noncleavable linkers.....	13
<b>1.3.2.1</b> Thioether.....	13
<b>1.3.2.2</b> Peptibody.....	13
<b>1.4</b> Peptide-Drug Conjugates.....	16
<b>1.4.1</b> Cell-penetrating peptides.....	17
<b>1.4.2</b> Drug targeting with cell adhesion peptides.....	18
<b>1.4.3</b> Multifunctional peptides and proteins.....	18
<b>1.4.3.1</b> Bifunctional peptide inhibitors.....	19
<b>1.4.3.2</b> I-domain-antigenic peptide conjugate (IDAC).....	21
<b>1.5</b> Conclusions.....	22
<b>1.6</b> References.....	24



<b>Chapter 2: Utilizing the I-domain of LFA-1 to Target Antigenic Peptides for Suppressing the Immune Response in the EAE Animal Model.....</b>	<b>30</b>
2.1 Introduction.....	31
2.2 Materials and methods.....	33
2.2.1 Animals.....	33
2.2.2 Peptide synthesis.....	33
2.2.3 I-domain preparation.....	35
2.2.4 Synthesis of IDAC-1 and -3.....	35
2.2.5 Induction of EAE and efficacy studies.....	36
2.2.6 Determination of cytokine levels <i>in vitro</i> .....	36
2.2.7 Statistical analysis.....	37
2.3 Results.....	37
2.3.1 Synthesis and characterization of IDAC-1 and -3.....	37
2.3.2 Suppression of EAE by IDAC-1 and -3.....	38
2.3.3 Cytokine levels in SJL/J mice <i>in vitro</i> .....	53
2.4 Discussion.....	57
2.5 Conclusions.....	67
2.6 References.....	68
<b>Chapter 3: Vaccine-like Controlled-Release Delivery of an Immunomodulating Peptide to Treat Experimental Autoimmune Encephalomyelitis.....</b>	<b>72</b>
3.1 Introduction.....	73
3.2 Materials and methods.....	74
3.2.1 Materials.....	74

3.2.2	Animals.....	75
3.2.3	Peptide synthesis.....	75
3.2.4	Preparation of charged PLGA nanoparticles.....	76
3.2.5	Preparation of peptide-loaded colloidal gels.....	76
3.2.6	Characterization of nanoparticles and colloidal gels.....	76
3.2.7	<i>In vitro</i> peptide release from colloidal gel.....	77
3.2.8	Induction of EAE and efficacy evaluations.....	77
3.2.9	Determination of cytokine levels <i>in vitro</i> .....	78
3.2.10	Statistical analysis.....	79
3.3	Results.....	79
3.3.1	Characterization of coated nanoparticles and colloidal gel.....	79
3.3.2	<i>In vitro</i> peptide release from colloidal gel.....	82
3.3.3	Efficacy of Ac-PLP-BPI-NH <sub>2</sub> -2 in colloidal gel for suppression of EAE.....	82
3.3.4	<i>In vitro</i> cytokine production.....	88
3.4	Discussion.....	95
3.5	Conclusions.....	99
3.6	References.....	100
<b>Chapter 4: The Effects of Bifunctional Peptide Inhibitors in Suppressing Rheumatoid Arthritis in an Animal Model.....</b>		<b>104</b>
4.1	Introduction.....	105
4.2	Materials and methods.....	107
4.2.1	Animals.....	107

4.2.2	Peptide synthesis.....	109
4.2.3	Induction of CIA and therapeutic study.....	109
4.2.4	Determination of IL-6 levels in serum <i>in vivo</i> .....	110
4.2.5	Histopathology of the joints.....	111
4.2.6	Statistical analysis.....	111
4.3	Results.....	112
4.3.1	Suppression of CIA by CII-BPI.....	112
4.3.2	IL-6 serum levels in DBA mice <i>in vivo</i> .....	119
4.3.3	Histopathological analysis.....	123
4.4	Discussion.....	125
4.5	Conclusions.....	131
4.6	References.....	132
<b>Chapter 5:</b>	<b>Summary, Conclusions, and Future Directions.....</b>	<b>138</b>
5.1	Summary and conclusions.....	139
5.2	Future directions.....	142
5.2.1	Improving delivery of IDAC to suppress EAE.....	142
5.2.2	Optimizing Ac-PLP-BPI-NH <sub>2</sub> -2 formulation in colloidal gel.....	143
5.2.3	Exploring the mechanism of CIA suppression.....	143
5.3	References.....	144

## **CHAPTER 1**

### **Development of therapeutic macromolecule conjugates to make better drugs**

## 1.1 INTRODUCTION

Roche Chief Executive Officer Severin Schwan noted that the next generation of drugs to be developed must target specific groups of patients:

*“In 10 years we would see half of our portfolio be targeted therapies. And if anything, I would assume in 20 years this percentage is going to increase.”*

The current state of modern medicine is such that our understandings of the physiology of a human body and its complexities have grown exponentially. This dramatic growth in knowledge has allowed scientists to better understand and pinpoint the intricate differences between normally functioning cells and “diseased” cells. The differences between these cells could be due to cell-surface receptor changes, shifts in cytokine and hormone production, and differences in cell trafficking properties.<sup>1-5</sup> Targeted therapy utilizes these differences to guide the drug to a site of action on the diseased cell for its greatest impact.<sup>4,6,7</sup>

Peptides and proteins (e.g., antibodies) have been used as carrier and targeting molecules. The rationale for developing conjugates is to combine the specificity of the carrier (i.e., proteins or peptides) with the efficacy of the attached drug molecule. Currently, there are over 200 marketed protein products; however, the rate of approval of protein drugs has slowed down over the last five years.<sup>8</sup> Of the protein drugs in the market, 24 are antibodies.<sup>8</sup> Recently, more effort has been devoted to developing protein-drug conjugates (i.e., antibody-small drug and antibody-peptide conjugates (peptibodies)) and peptide-drug conjugates (**Fig. 1**).<sup>8</sup> However, the

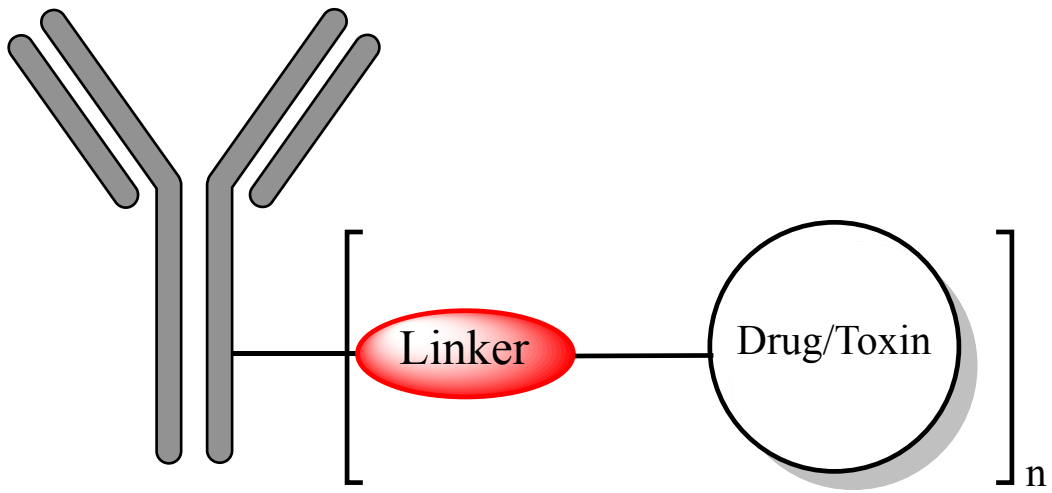


**Figure 1.** Structure of an antibody-drug conjugate (ADC).

development of these conjugates has been relatively slow; this is due to the lack of prior knowledge in developing these types of therapeutics. The major advantage of using a monoclonal antibody (mAb) for targeting drugs to a specific cell is that it has the ability to target a specific antigen on the cell surface with high binding affinity.

Understanding the physiological processes of diseases is an important step in developing macromolecule-drug conjugates. However, numerous other challenges need to be addressed before macromolecule-drug conjugates become candidates as therapeutics. An ideal conjugate should have the same binding properties to the target receptor in the cell surface as the parent macromolecule. Furthermore, the formation of conjugate should not impair or limit its biodistribution *in vivo*, and the drugs should not be released from the conjugate prior to reaching the target site. Once it is at the target site, and if the drug action is inside the cell, the conjugate should be internalized and the drug molecules should efficiently be released in their active form. A sufficient amount of drug must reach the site of action to produce optimal efficacy.

The aim of this chapter is to provide a review on the current state of development of the macromolecule-drug conjugate technology in improving drug delivery to a specific tissue or cell type. Ultimately, the hope is that macromolecule-drug conjugates should have greater efficacy than the parent drugs with a better safety profile.

## **1.2 ANTIBODY-DRUG CONJUGATES (ADC)**

### **1.2.1 Success of ADC in the Market**

The role of the antibody in antibody-drug conjugates (ADC) is to target the drug (cargo molecule) to an identified site, thereby reducing toxicity and increasing

effectiveness. The ideal characteristic of ADC is that the antibody has high specificity to the target molecule on the surface of target cells where the receptors are upregulated. Then, the drug molecules should be released at the appropriate site in the cell. Several ADC have been approved for treating patients. The first FDA-approved ADC was gentuzumab ozogamicin (Mylotarg<sup>®</sup>); this ADC was used for the treatment of acute myeloid leukemia (AML).<sup>9,10</sup> The antibody in Mylotarg targets the CD33 molecule, which is highly expressed in ~90% of malignant blast cells in AML.<sup>11</sup> Ideally, an ADC should not be a substrate for efflux pumps; unfortunately, Mylotarg has a DNA-binding calicheamicin derivative, which is a substrate for the MDR1/P-gp-1 efflux pump.<sup>12</sup> In 2010, Mylotarg was withdrawn from the market due to unsatisfactory patient benefit and increased patient death in post-approval clinical trials (SWOG S0106). Brentuximab vedotin (Adcetris<sup>®</sup>) was granted an accelerated approval in August 2011 for the treatment of systemic anaplastic large cell lymphoma (ALCL) and Hodgkin's lymphoma (HL). It is the first HL drug to receive FDA approval since 1977. Adcetris targets the drug to lymphoma cells via binding to CD30 molecules.<sup>13</sup> Another ADC, trastuzumab emtansine, is in clinical trials for treating metastatic breast cancer (*HER/neu*<sup>+</sup>). This ADC is a conjugate of trastuzumab (Herceptin<sup>®</sup>) mAb that targets Her2/neu receptor (CD340) and cytotoxic mertansine (DM1).<sup>14</sup>

### 1.2.2 Examples of Cargo Molecules

Chemotherapeutic ADC should be more effective than the free cargo drug alone because the cost to produce antibodies is high and there are limited conjugation sites on the mAb for the cargo molecules. There are several potent anticancer drugs used for



cargoes of ADC; they include DNA damaging agents (i.e., calicheamicin and duocarmycin) and microtubule inhibitors (i.e., auristatins, taxanes, and maytansinoids). These anticancer agents have nonspecific toxicity; therefore, conjugating them to mAb provides specificity for cancer cells and avoids side effects. Peptide sequences of diphtheria toxin have been fused with interleukin-2 (IL-2) to make denileukin diftitox (Ontak<sup>®</sup>), an approved drug for the treatment of cutaneous T-cell lymphoma (CTCL).<sup>4</sup> Other toxins such as ricin, RNase, and *Pseudomonas* exotoxin have been conjugated to monoclonal antibodies and are being investigated for cancer treatments.<sup>15-17</sup>

Radiolabeled atoms (i.e., <sup>131</sup>I, <sup>90</sup>Y, and <sup>177</sup>Lu) have been conjugated to mAbs for use in radiotherapy in cancer patients. For example, <sup>131</sup>I-tositumomab (Bexar<sup>®</sup>) and <sup>90</sup>Y-ibritumomab tiuxetan (Zevalin<sup>®</sup>) are both FDA-approved ADCs that target CD20 on the cancer cells of non-Hodgkin's lymphoma (NHL).<sup>18</sup> Currently, <sup>90</sup>Y-epratuzumab teraxetan, which is specific for CD22-expressing cancer cells, is in development.<sup>19</sup>

## **1.3 CHEMISTRY OF ADC**

### **1.3.1 Cleavable Linkers**

#### **1.3.1.1 Acidic Linkers**

Acid-sensitive cleavable linkers have been used to conjugate drugs to mAbs because the desire is to release the drug inside the lysosomes in an acidic pH environment. The hydrazone linker is relatively stable in blood (pH ~7.4), but it cleaves in acidic endosomes (pH 5.0 – 6.5) and lysosomes (pH 4.5 – 5.0), as well as in the more acidic environment inside cancer cell. An early example was doxorubicin conjugated to the cysteine residue of BR96 mAb via a combination of maleimide and hydrazone linkers

(**Fig. 2**).<sup>7</sup> BR96 binds to the Lewis Y receptor that is overexpressed on many carcinomas.<sup>7,20</sup> The thiol group of the cysteine residue of BR96 mAb was conjugated to a maleimide-hexanoic acid linker, and the carboxylic acid group of maleimide-hexanoic acid was coupled to the hydrazone group of hydrazone-derivatized doxorubicin to make the final BR96-Dox-ADC.

It was found that BR96-Dox-ADC had better antitumor efficacy than free doxorubicin. To achieve the same efficacy as that of doxorubicin, BR96-Dox-ADC was delivered at a dose equivalent to 13% of free doxorubicin.<sup>7</sup> This suggests that the antibody preferentially targets and carries the doxorubicin to the Lewis-Y-expressing tumor cell. It was suggested that, once inside the acidic tumor cell environment, doxorubicin is clipped off via hydrolysis of the hydrazone.<sup>21</sup>

### 1.3.1.2 Reducing Linkers

The cytotoxic drugs (i.e., calicheamicin class) in Mylotarg and inotuzumab ozogamizine were covalently linked to lysine residues of anti-CD33 IgG4 antibody via a combination of hydrazone and disulfide bond (**Fig. 3**). It was found that the drug was released from the ADC in lysosomes via acid hydrolysis of the hydrazone functional group. Finally, the drug was activated upon reduction of the disulfide bond.<sup>21</sup> One interesting aspect of the disulfide linker is that the sulfur atom of the thiol group is linked to a carbon with a gem-dimethyl group. The steric hindrance from the gem-dimethyl group slows the reduction of the disulfide bond by glutathione in plasma (**Fig. 3**). Upon entry into the cell, the disulfide bond can be released more rapidly than in plasma

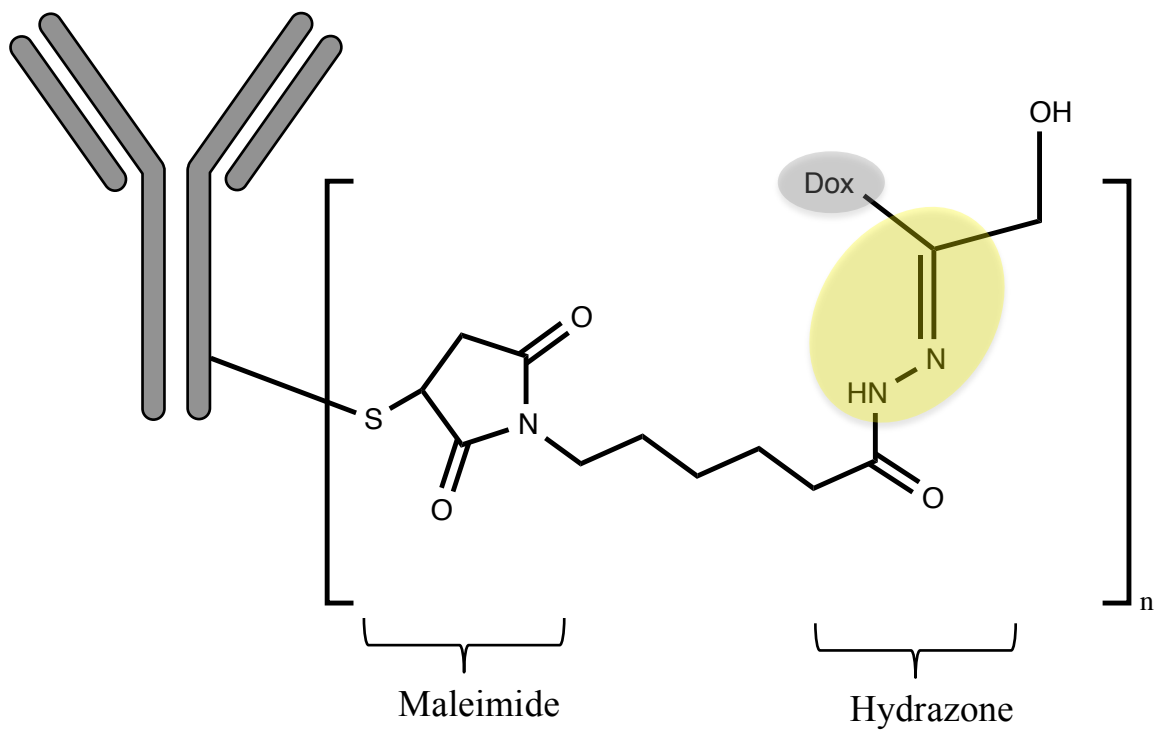


**Figure 2.** Structure of Br96-Dox-ADC immunconjugate. A cysteine residue of BR96 mAb forms a thioether bond with maleimide. The acid-labile hydrazone forms a linker between maleimide-hexanoic acid and doxorubicin.

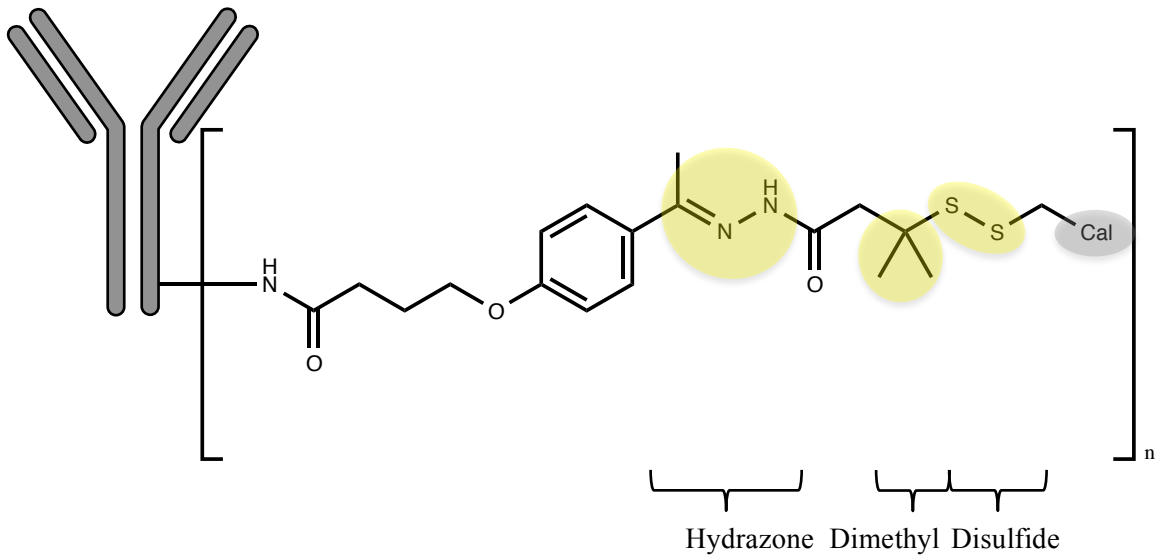


**Figure 3.** Cytotoxic calicheamicin (Cal) cargo is attached to an anti-CD33 antibody via a hydrazone linker. The disulfide bond is stabilized by two geminal methyl groups to prevent calicheamicin release prior to reaching its target.

because the concentration of glutathione is a thousand times higher in the cytoplasm of tumor cells than in the plasma.<sup>22</sup>

A similar concept using a steric disulfide bond conjugation was used in maytansinoids, where DM1 or DM4 drug was conjugated to mAbs via the lysine residues (**Fig. 4**). The amino group of surface lysine residues was conjugated to 4-thiolbutanoate via a peptide bond. The thiol group on mAb was conjugated to DM1 or DM4 drug via a disulfide bond. In this case, the gem-dimethyl group is on the DM4 drug molecule but not in the DM1 drug molecule. The DM4-ADC has a longer half-life (102 hours) compared DM1-ADC (47 hours); this is due to the presence of a gem-dimethyl group in DM4-ADC that slows the reduction of the disulfide bond by glutathione.<sup>23,24</sup>

### **1.3.1.3 Tumor-Specific Protease Linkers**

Generally, ADCs that contain an acid-labile linker or a disulfide bond have poor plasma stability because the linker can be rapidly hydrolyzed or reduced, respectively, in the plasma to release the drug prior to reaching the target site. To overcome this problem, a peptide bond linker was developed because proteases normally are not very active outside of the cell cytoplasm.<sup>25</sup> Monomethyl auristatin E (MMAE) was linked to valine-citrulline dipeptide that was connected to a maleimide group; the maleimide linker was attached to cysteine residues on the antibody to give MMAE-ADC (**Fig. 5**). The dipeptide is recognized by cathepsin B for hydrolysis to release MMAE in its active form.<sup>26</sup> It has been shown that the use of a dipeptide linker (i.e., valine-citrulline) increases the half-life of the ADC in the human plasma by nearly 100-fold compared to the MMAE linked to antibody by a hydrazone linker.<sup>27</sup> Because the rate of enzymatic

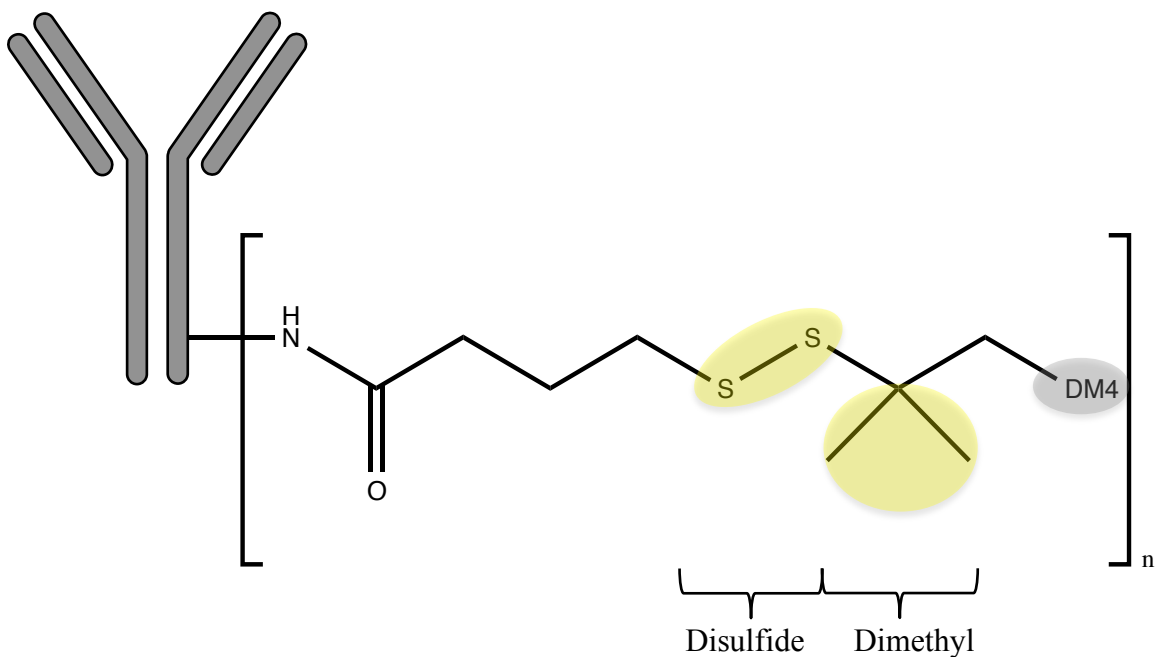


**Figure 4.** Conjugation of DM1 or DM4 drug was achieved using lysine residues near the surface of the mAb. The presence of gem-dimethyl groups adjacent to the disulfide group in DM4 drug increased the half-life by more than twofold compared to DM1, which does not have gem-dimethyl groups.

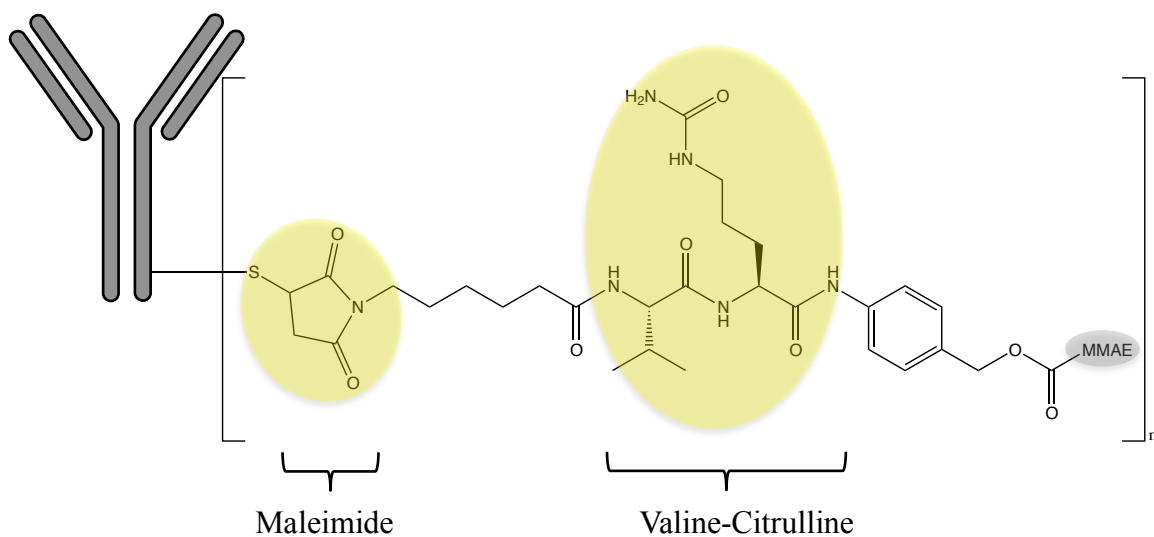


**Figure 5.** Monomethyl auristatin E (MMAE) was conjugated to a dipeptide consisting of valine and citrulline as the enzyme-cleavable linker. The MMAE-dipeptide is conjugated to cysteine residue(s) of the mAb via a maleimide linker.

cleavage depends on the dipeptide sequence, the half-life the MMAE ADC can be partly regulated by sequence of the dipeptide linker.

### **1.3.2 Noncleavable Linkers**

#### **1.3.2.1 Thioether**

DM1 was conjugated to a mAb via a thioether bond (**Fig. 6**). Because this linker cannot be cleaved by enzyme or acid, it is proposed that the drug is released in the lysosome after the mAb is degraded. It is thought that the active substance is the DM1 drug linked to the lysine residue of the mAb via a maleimide group. The thioether-linked DM1 conjugate has a half-life of 134 hours.<sup>28</sup> One caution in using this type of linker is that, if the mAb has poor cellular uptake, the non-cleavable linker should not be used because the drug cannot be released from the conjugate.

#### **1.3.2.2 Peptibody**

Peptibody is a conjugate between peptides and antibodies or antibody fragments (**Fig. 7**). Unlike conventional ADCs with chemical conjugation, a peptibody is produced upon expression of the antibody with a peptide sequence attached to it.<sup>29</sup> This process eliminates the need to separately synthesize the peptide and express the protein. Currently, peptibody formation is being utilized to improve the half-life of the peptide in systemic circulation.<sup>29</sup> Romiplostim (Nplate<sup>®</sup>) is the only FDA-approved peptibody on the market.<sup>30</sup> It was approved in 2008 for the treatment of chronic immune thrombocytopenic purpura (ITP).<sup>30</sup> Romiplostim is the result of a fusion between an Fc-fragment of mAb (IgG1) and a 14-amino acid peptide agonist of a thrombopoietin (TPO), receptor called



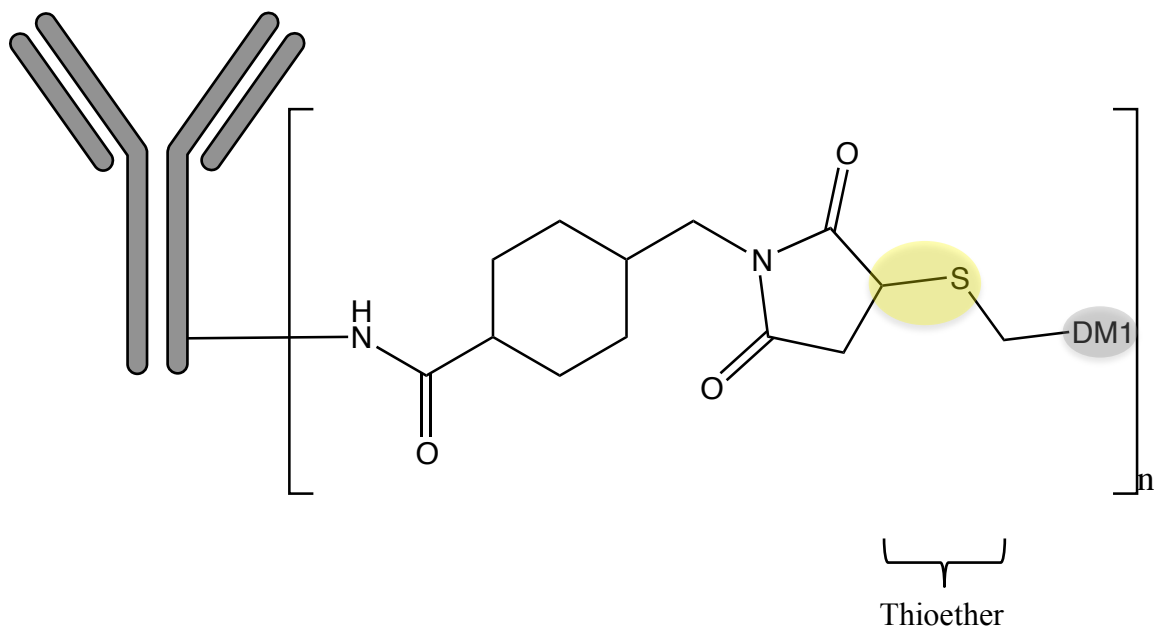


**Figure 6.** To increase the drug half-life, DM1 is conjugated to a thioether linker to the mAb via a maleimide group that is attached to lysine residues.

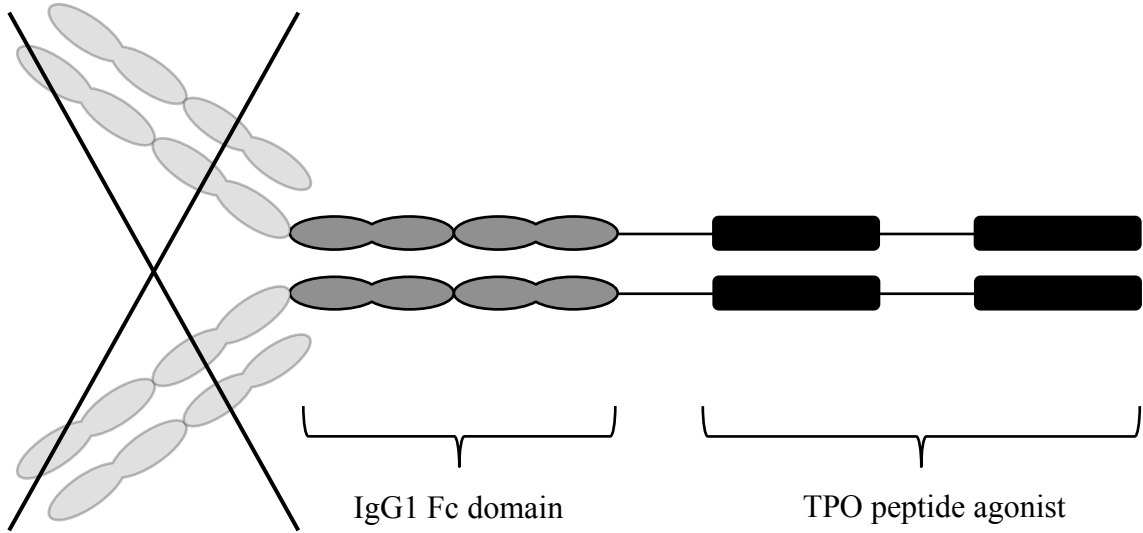


**Figure 7.** The Fc domain of the IgG1 antibody (dark gray) prolongs the half-life of Romiplostim *in vivo*, whereas the TPO agonist (black) provides biological activity.

AF12505, which stimulates platelet production.<sup>30</sup> Here, two molecules of AF12505 are fused to an Fc-fragment of mAb to enhance peptibody activity because the two peptide fragments presumably bind simultaneously to the dimeric form of the receptor. This idea was modeled after the finding that the dimeric form of the peptide agonist was more active than the monomeric form.<sup>29</sup> This is the first design of a peptibody for increasing receptor-binding affinity as well as extending the circulation half-life of the peptide.

#### **1.4 PEPTIDE-DRUG CONJUGATES**

Peptides are generally defined as having a chain of no more than 50 amino acids. Unlike proteins, peptides may exhibit a high degree of secondary structure, but may or may not have tertiary structure.<sup>31</sup> The advantage of a peptide over an antibody is the relative ease of synthesis and structure manipulation compared to an antibody. Once a target has been identified, peptide synthesis and purification can be achieved in a matter of just a few weeks. In contrast, it takes years to develop an efficient method to produce and purify large quantity of antibodies. However, peptides tend to have lower specificities than antibodies in recognizing target cell surface receptors. A major disadvantage of a peptide compared to an antibody is its rapid rate of renal clearance because kidneys do not filter out proteins larger than 50 kDa.<sup>32</sup> Furthermore, peptides normally have low half-lives ranging anywhere from a few hours to minutes.<sup>32</sup> To combat against renal clearance and exposure to exopeptidases, scientists have attached polyethylene glycol (PEG) to the N- and C-termini of peptides to add bulk and protect from enzymes.<sup>33</sup> A variety of peptides have been investigated for delivering drugs to

specific cells, including cell-penetrating peptides, bombesin peptide, LHRH peptide, RGD peptide, and ICAM-1 peptide.<sup>34-38</sup>

#### **1.4.1 Cell-Penetrating Peptides**

Highly cationic cell-penetrating peptides (CPP) can cross the cell lipid bilayer without the need for a specific receptor.<sup>39</sup> Although the mechanism of cellular uptake of CPP has not been fully elucidated, this is an ideal molecule to deliver drugs to a site of action where no suitable receptors exist. CPP contain either a predominant population of arginine residues or largely lysine residues.<sup>32</sup> Penetratin, TAT, and VP22 have been used to deliver biologically active proteins.<sup>39</sup> TAT is a trans-activator of transcription derived from HIV, and the arginine-rich (11 amino acid) peptide sequence (TAT<sub>47-57</sub>; YGRKKRRQRRR) is involved in cellular transduction.<sup>38</sup> As mentioned above, the mechanism of CPP crossing cell membranes is not exactly clear, but evidence for both endosomal and non-endosomal mechanisms has been reported.<sup>40,41</sup> The endosomal pathway of CPP occurs due to a decrease in pH in the endosome, trapping the positively charged amino acid residues.<sup>42</sup> If the goal of delivery is to avoid transport to the nucleus, both the CPP and the drug cargo must not be highly positively charged and, therefore, formulated to avoid this possibility. An application of a CPP-drug conjugate is illustrated using a  $\delta$ PKC inhibitor, KAI-9803, which is used in stroke patients. Here, the compound is conjugated to TAT<sub>47-57</sub> via a disulfide bond where the conjugate showed a reduction in apoptotic cell death after ischemia.<sup>42</sup> Although cell-penetrating peptides have provided success in delivering drugs into cells, they lack specificity to recognize receptors as

targets to deliver drugs to the optimal site of action. Up to now, no successful clinical applications of CPP-drug conjugates are available for treating patients.

#### **1.4.2 Drug Targeting With Cell Adhesion Peptides**

The upregulation of adhesion molecules on the surface of leukocytes and endothelial cells has been correlated with inflammation and some forms of cancers (i.e., lung and pancreatic cancers).<sup>3,5</sup> LFA-1 receptor is exclusively expressed on leukocytes, and has been shown to uptake and internalize cIBR peptide derived from the ICAM-1 protein.<sup>35,43,44</sup> Methotrexate (MTX) has been linked to cIBR peptide to give MTX-cIBR conjugate for delivering MTX to activated leukocytes to suppress inflammation in rheumatoid arthritis (RA). MTX is being used to treat RA; however, chronic use of MTX produces adverse side effects. Therefore, targeting MTX using peptides may alleviate unwanted side effects and improve efficacy. MTX-cIBR was effective in suppressing rheumatoid arthritis in the collagen-induced arthritis (CIA) mouse model and rat adjuvant arthritis model.<sup>45</sup> MTX-cIBR has lower *in vivo* toxicity than MTX alone in CIA mouse model, suggesting that cIBR peptide selectively targets MTX to leukocytes *in vivo*. *In vitro*, MTX-cIBR was more toxic to LFA-1-expressing cells than to cells without LFA-1 on the cell surface, indicating that LFA-1 receptor contributes to the activity of MTX-cIBR.

#### **1.4.3 Multifunctional Peptides and Proteins**

Recently, the concept of simultaneously modulating two different receptors to control biological mechanism was explored in autoimmune diseases. Siahaan *et al.*

explored the possibility of altering the differentiation and proliferation of T cells by controlling the formation of immunological synapse.<sup>46</sup> Bifunctional peptide inhibitors and insert-domain (I-domain) antigen conjugates (IDAC) are respective peptide-peptide and peptide-protein conjugates that can bind two different receptors (MHC-II and ICAM-1) on the surface of antigen-presenting cells (APC) and can alter the differentiation of naïve T cells to favor regulatory T cells and generate immune tolerance in autoimmune diseases.

#### **1.4.3.1 Bifunctional Peptide Inhibitors**

A bifunctional peptide inhibitor (BPI; **Fig. 8A**) molecule is a conjugate between an antigenic peptide and a cell adhesion peptide that can simultaneously bind to their respective receptors (MHC-II and ICAM-1) on APC to elicit biological activity. One example of BPI molecules is PLP-BPI, which is a conjugate of PLP peptide and LABL peptide that is linked via a chain of aminocaproic acids. In PLP-BPI, PLP and LABL peptides were proposed to simultaneously bind to MHC-II and ICAM-1, respectively, on the surface of APC.<sup>47</sup> Therefore, linking PLP and LABL peptide is hypothesized to prevent the formation of the immunological synapse during the interaction of APC and T cells for T-cell activation.<sup>47</sup> The immunological synapse is a bull's eye structure at the interface of APC and T cells made of a cluster of Ag-MHC-II/TCR (Signal-1) at the center and a cluster of ICAM-1/LFA-1 (Signal-2) at the periphery.<sup>47</sup> Several different bifunctional peptide inhibitor (BPI) molecules such as PLP-BPI, GAD-BPI, and CII-BPI have been shown to suppress experimental autoimmune encephalomyelitis (EAE), Type-1 diabetes, and rheumatoid arthritis, respectively.<sup>2,6,46,48</sup> The common mechanism of BPI

**Figure 8A.**

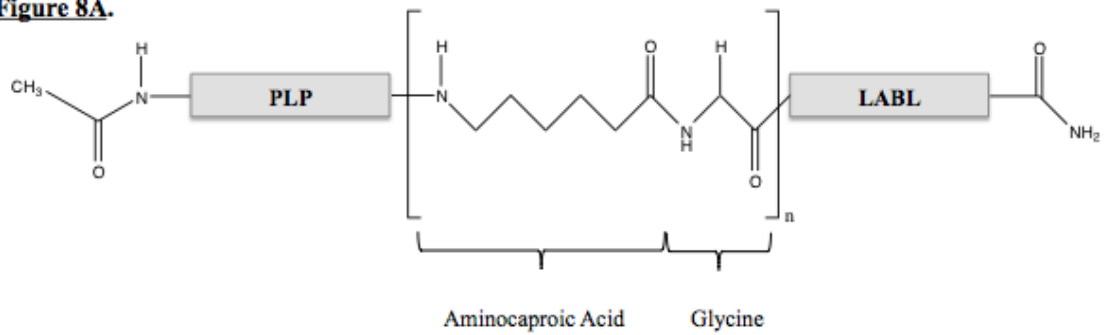


**Figure 8B.**

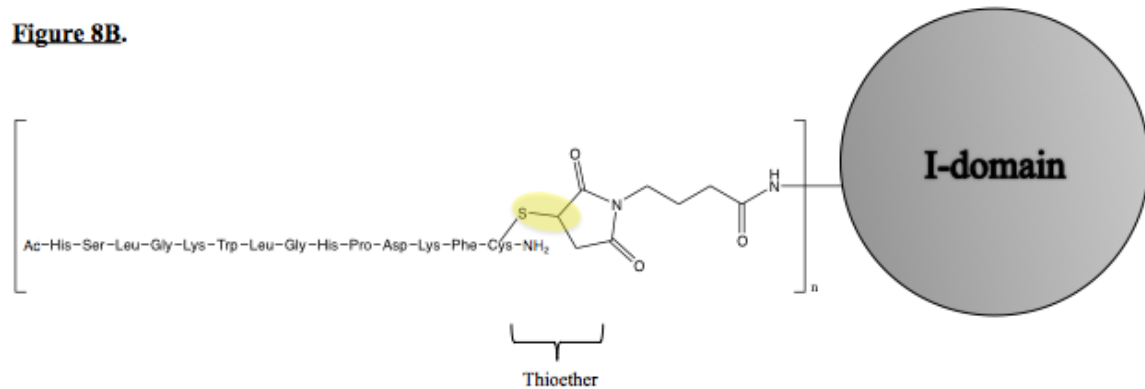


**Figure 8.** (A) Representative construct of bifunctional peptide inhibitors. Aminocaproic acid with an alternating glycine residue is commonly used as the spacer. The N-terminus is capped with an acetyl group, and the C-terminus is capped with an amide group. (B) IDAC is a conjugate between an antigenic peptide and the I-domain. The linker between the two compounds is *N*-[ $\gamma$ -maleimidobutyryloxy]-succinimide ester.

molecules is that they induce tolerance by stimulating the differentiation/proliferation of T-regs and suppressing the inflammatory Th17 cells.<sup>2,48</sup>

#### **1.4.3.2 I-domain-Antigenic Peptide Conjugate (IDAC)**

Proteins (i.e., cytokines and mAbs) have been successfully used as therapeutics to treat various diseases. Proteins are known to bind specific receptors and have been investigated as conjugates for delivering drugs to specific types of cells. As mentioned above, peptibodies, which are conjugates between a peptide and a fragment of antibody, have been used to improve systemic circulation of peptide drugs. However, the peptide-protein conjugation has not been evaluated for simultaneous binding to two different cell surface receptors for controlling pathological conditions. The Siahaan group designed IDAC molecules as conjugates between antigenic peptides and the I-domain protein. The I-domain is a fragment of the alpha subunit of LFA-1 that binds to domain-1 of ICAM-1.<sup>47</sup> Using fluorescein-5'-isothiocyanate (FITC)-I-domain conjugate, it was found that the I-domain can bind to ICAM-1 and become internalized by the effector cell.<sup>49</sup> Recently, the I-domain has been conjugated to an antigenic peptide (PLP<sub>139-151</sub>) to give IDAC molecules. This was accomplished by utilizing *N*-[ $\gamma$ -maleimidobutyryloxy]succinimide ester (GMBS), where the free lysines of the I-domain were conjugated to the succinimide group of GMBS, and the maleimide group was subsequently reacted with the sulfur group of the cysteine residue located on the C-terminus of PLP<sub>139-151</sub>-Cys (**Fig. 8B**). As in PLP-BPI, it is proposed that the IDAC molecules simultaneously bind to target receptors MHC-II and ICAM-1 on the surface of antigen-presenting cells.<sup>49</sup> The IDAC molecules effectively suppressed experimental autoimmune encephalomyelitis (EAE) in the mouse



model, an animal model for multiple sclerosis. It was found that IDAC molecules suppress EAE by enhancing the production of regulatory T cells (T-reg) and suppressing Th17 cells.

## 1.5 CONCLUSIONS

Using peptides and proteins as cargoes to carry drugs has generated an increasing amount of interest, especially in the field of cancer research. Although success has varied, the results have been promising. One strategy is to consider developing conjugates that have dual activities to potentially modulate two or more receptors. For many immune disorders, effector cells require two or more signals to become activated. Proof-of-concept studies suggested that BPI and IDAC could be used to suppress autoimmune diseases. Liposomal and polymer technologies containing conjugates of multiple peptide sequences specific for different receptors have also had success.<sup>31,50</sup> The hope is that conjugates will provide a new avenue for the development of better drugs. Therefore, the overall objective of this work was to investigate the ability of peptide/protein conjugates to deliver antigenic peptides to antigen-presenting cells to suppress autoimmune disease in mouse models. To investigate this, the following specific aims were undertaken:

**Specific Aim 1 (Chapter 2):** To investigate the ability of an LFA-1 I-domain antigen conjugate (IDAC) to target APC and suppress EAE in both vaccine-like and prophylactic fashions.

**Specific Aim 2 (Chapter 3):** To design a colloidal gel formulation of a BPI molecule for controlled-release delivery in a vaccine-like manner to suppress EAE.

**Specific Aim 3 (Chapter 4):** To investigate the utility of BPI to target APC to suppress other autoimmune diseases such as rheumatoid arthritis in the mouse model.

## 1.6 REFERENCES

- 1 Kaufmann, A. M. & Krise, J. P. Lysosomal sequestration of amine-containing drugs: analysis and therapeutic implications. *J Pharm Sci* **96**, 729-746 (2007).
- 2 Kobayashi, N. *et al.* Prophylactic and therapeutic suppression of experimental autoimmune encephalomyelitis by a novel bifunctional peptide inhibitor. *Clin Immunol* **129**, 69-79 (2008).
- 3 Lee, S. J. & Benveniste, E. N. Adhesion molecule expression and regulation on cells of the central nervous system. *J Neuroimmunol* **98**, 77-88 (1999).
- 4 Olsen, E. *et al.* Pivotal phase III trial of two dose levels of denileukin diftitox for the treatment of cutaneous T-cell lymphoma. *J Clin Oncol* **19**, 376-388 (2001).
- 5 Seidel, M. F., Keck, R. & Vetter, H. ICAM-1/LFA-1 expression in acute osteodestructive joint lesions in collagen-induced arthritis in rats. *J Histochem Cytochem* **45**, 1247-1253 (1997).
- 6 Kobayashi, N., Kobayashi, H., Gu, L., Malefyt, T. & Siahaan, T. J. Antigen-specific suppression of experimental autoimmune encephalomyelitis by a novel bifunctional peptide inhibitor. *J Pharmacol Exp Ther* **322**, 879-886 (2007).
- 7 Trail, P. A. *et al.* Cure of xenografted human carcinomas by BR96-doxorubicin immunoconjugates. *Science* **261**, 212-215 (1993).
- 8 Walsh, G. Biopharmaceutical benchmarks 2010. *Nat Biotechnol* **28**, 917-924 (2010).
- 9 Hamann, P. R. *et al.* An anti-CD33 antibody-calicheamicin conjugate for treatment of acute myeloid leukemia. Choice of linker. *Bioconjug Chem* **13**, 40-46 (2002).

- 10 Hamann, P. R. *et al.* Gemtuzumab ozogamicin, a potent and selective anti-CD33 antibody-calicheamicin conjugate for treatment of acute myeloid leukemia. *Bioconjug Chem* **13**, 47-58 (2002).
- 11 Linenberger, M. L. CD33-directed therapy with gemtuzumab ozogamicin in acute myeloid leukemia: progress in understanding cytotoxicity and potential mechanisms of drug resistance. *Leukemia* **19**, 176-182 (2005).
- 12 Linenberger, M. L. *et al.* Multidrug-resistance phenotype and clinical responses to gemtuzumab ozogamicin. *Blood* **98**, 988-994 (2001).
- 13 Younes, A. *et al.* Brentuximab vedotin (SGN-35) for relapsed CD30-positive lymphomas. *N Engl J Med* **363**, 1812-1821 (2010).
- 14 Niculescu-Duvaz, I. Trastuzumab emtansine, an antibody-drug conjugate for the treatment of HER2+ metastatic breast cancer. *Curr Opin Mol Ther* **12**, 350-360 (2010).
- 15 Hursey, M. *et al.* Specifically targeting the CD22 receptor of human B-cell lymphomas with RNA damaging agents: a new generation of therapeutics. *Leuk Lymphoma* **43**, 953-959 (2002).
- 16 Kreitman, R. J. Recombinant immunotoxins for the treatment of chemoresistant hematologic malignancies. *Curr Pharm Des* **15**, 2652-2664 (2009).
- 17 Pastan, I., Hassan, R., FitzGerald, D. J. & Kreitman, R. J. Immunotoxin treatment of cancer. *Annu Rev Med* **58**, 221-237 (2007).
- 18 Goldsmith, S. J. Radioimmunotherapy of lymphoma: Bexxar and Zevalin. *Semin Nucl Med* **40**, 122-135 (2010).

- 19 Linden, O. *et al.* Dose-fractionated radioimmunotherapy in non-Hodgkin's lymphoma using DOTA-conjugated, <sup>90</sup>Y-radiolabeled, humanized anti-CD22 monoclonal antibody, epratuzumab. *Clin Cancer Res* **11**, 5215-5222 (2005).
- 20 Tolcher, A. W. *et al.* Randomized phase II study of BR96-doxorubicin conjugate in patients with metastatic breast cancer. *J Clin Oncol* **17**, 478-484 (1999).
- 21 Stella, V. J. *Prodrugs : challenges and rewards.* (Springer, 2007).
- 22 Ducry, L. & Stump, B. Antibody-drug conjugates: linking cytotoxic payloads to monoclonal antibodies. *Bioconjug Chem* **21**, 5-13 (2010).
- 23 Erickson, H. K. *et al.* Antibody-maytansinoid conjugates are activated in targeted cancer cells by lysosomal degradation and linker-dependent intracellular processing. *Cancer Res* **66**, 4426-4433 (2006).
- 24 Xie, H., Audette, C., Hoffee, M., Lambert, J. M. & Blattler, W. A. Pharmacokinetics and biodistribution of the antitumor immunoconjugate, cantuzumab mertansine (huC242-DM1), and its two components in mice. *J Pharmacol Exp Ther* **308**, 1073-1082 (2004).
- 25 Koblinski, J. E., Ahram, M. & Sloane, B. F. Unraveling the role of proteases in cancer. *Clin Chim Acta* **291**, 113-135 (2000).
- 26 Toki, B. E., Cervený, C. G., Wahl, A. F. & Senter, P. D. Protease-mediated fragmentation of p-amidobenzyl ethers: a new strategy for the activation of anticancer prodrugs. *J Org Chem* **67**, 1866-1872 (2002).
- 27 Doronina, S. O. *et al.* Development of potent monoclonal antibody auristatin conjugates for cancer therapy. *Nat Biotechnol* **21**, 778-784 (2003).

- 28 Polson, A. G. *et al.* Antibody-drug conjugates for the treatment of non-Hodgkin's lymphoma: target and linker-drug selection. *Cancer Res* **69**, 2358-2364 (2009).
- 29 Cwirla, S. E. *et al.* Peptide agonist of the thrombopoietin receptor as potent as the natural cytokine. *Science* **276**, 1696-1699 (1997).
- 30 Molineux, G. & Newland, A. Development of romiplostim for the treatment of patients with chronic immune thrombocytopenia: from bench to bedside. *Br J Haematol* **150**, 9-20 (2010).
- 31 Majumdar, S. & Siahaan, T. J. Peptide-mediated targeted drug delivery. *Med Res Rev* (2010).
- 32 Sato, A. K., Viswanathan, M., Kent, R. B. & Wood, C. R. Therapeutic peptides: technological advances driving peptides into development. *Curr Opin Biotechnol* **17**, 638-642 (2006).
- 33 Werle, M. & Bernkop-Schnurch, A. Strategies to improve plasma half life time of peptide and protein drugs. *Amino Acids* **30**, 351-367 (2006).
- 34 Chen, X., Plasencia, C., Hou, Y. & Neamati, N. Synthesis and biological evaluation of dimeric RGD peptide-paclitaxel conjugate as a model for integrin-targeted drug delivery. *J Med Chem* **48**, 1098-1106 (2005).
- 35 Gursoy, R. N. & Siahaan, T. J. Binding and internalization of an ICAM-1 peptide by the surface receptors of T cells. *J Pept Res* **53**, 414-421 (1999).
- 36 Nagy, A. *et al.* Design, synthesis, and in vitro evaluation of cytotoxic analogs of bombesin-like peptides containing doxorubicin or its intensely potent derivative, 2-pyrrolinodoxorubicin. *Proc Natl Acad Sci U S A* **94**, 652-656 (1997).

- 37 Nagy, A. *et al.* Cytotoxic analogs of luteinizing hormone-releasing hormone containing doxorubicin or 2-pyrrolinodoxorubicin, a derivative 500-1000 times more potent. *Proc Natl Acad Sci U S A* **93**, 7269-7273 (1996).
- 38 Vives, E., Brodin, P. & Lebleu, B. A truncated HIV-1 Tat protein basic domain rapidly translocates through the plasma membrane and accumulates in the cell nucleus. *J Biol Chem* **272**, 16010-16017 (1997).
- 39 Lindgren, M., Hallbrink, M., Prochiantz, A. & Langel, U. Cell-penetrating peptides. *Trends Pharmacol Sci* **21**, 99-103 (2000).
- 40 Magzoub, M. & Graslund, A. Cell-penetrating peptides: [corrected] from inception to application. *Q Rev Biophys* **37**, 147-195 (2004).
- 41 Wagstaff, K. M. & Jans, D. A. Protein transduction: cell penetrating peptides and their therapeutic applications. *Curr Med Chem* **13**, 1371-1387 (2006).
- 42 Langel, U. I. *Cell-penetrating peptides : methods and protocols*. (Humana Press, 2011).
- 43 Jois, D. S. *et al.* Inhibition of homotypic adhesion of T-cells: secondary structure of an ICAM-1-derived cyclic peptide. *J Pept Res* **49**, 517-526 (1997).
- 44 Majumdar, S., Kobayashi, N., Krise, J. P. & Siahaan, T. J. Mechanism of internalization of an ICAM-1-derived peptide by human leukemic cell line HL-60: influence of physicochemical properties on targeted drug delivery. *Mol Pharm* **4**, 749-758 (2007).
- 45 Majumdar, S. *Targeted drug delivery to leukocytes with ICAM-1 derived peptides* Ph.D. thesis, University of Kansas, (2008).

- 46 Murray, J. S. *et al.* Suppression of type 1 diabetes in NOD mice by bifunctional peptide inhibitor: modulation of the immunological synapse formation. *Chem Biol Drug Des* **70**, 227-236 (2007).
- 47 Manikwar, P., Kiptoo, P., Badawi, A. H., Buyuktimkin, B. & Siahaan, T. J. Antigen-specific blocking of CD4-specific immunological synapse formation using BPI and current therapies for autoimmune diseases. *Med Res Rev* (2011).
- 48 Ridwan, R. *et al.* Antigen-specific suppression of experimental autoimmune encephalomyelitis by a novel bifunctional peptide inhibitor: structure optimization and pharmacokinetics. *J Pharmacol Exp Ther* **332**, 1136-1145 (2010).
- 49 Manikwar, P. *et al.* Utilization of I-domain of LFA-1 to Target Drug and Marker Molecules to Leukocytes. *Theranostics* **1**, 277-289 (2011).
- 50 Chittasupho, C., Shannon, L., Siahaan, T. J., Vines, C. M. & Berkland, C. Nanoparticles targeting dendritic cell surface molecules effectively block T cell conjugation and shift response. *ACS Nano* **5**, 1693-1702 (2011).



## **CHAPTER 2**

**Utilizing the I-domain of LFA-1 to target antigenic peptides for suppressing the  
immune response in the EAE animal model**

## 2.1 INTRODUCTION

Multiple sclerosis (MS) is an autoimmune disease caused by demyelination of the myelin sheath, which protects the neurons in the central nervous system (CNS). Without the protection of the myelin sheath proteins, nerve impulses are either disrupted or slowed down. While the triggers of MS have not been clearly elucidated, several factors such as Epstein-Barr virus (EBV) infection, genetic predisposition, and environmental effects are thought to play key roles in its development.<sup>1-4</sup> Just as in rheumatoid arthritis and type-1 diabetes, MS is a result of activation of a subpopulation of autoreactive T cells that demyelinate the nerve fibers in CNS.<sup>1,4,5</sup> While there is no cure for MS, many of today's therapies, including biologic drugs such as such as interferons (Avonex<sup>®</sup>, Betaseron<sup>®</sup>), antibodies (Tysabri<sup>®</sup>), and antineoplastics (mitoxantrone), focus on slowing down or altering the disease progression.<sup>6</sup> A criticism of these current therapies is that they do not target the cause of MS but rather suppress the general immune system, leading to potential serious side effects. Therefore, there is a need to investigate a new and more specific way to control the immune response generated in an autoimmune disease such as MS without suppressing the general immune response.

To investigate new therapeutics, the Siahaan lab group developed a novel way to target antigenic peptides to antigen presenting cells (APC) to control the activation of a subpopulation of T cells specific to a particular autoimmune disease. In this approach, a cell adhesion peptide was conjugated to an antigenic peptide to make bifunctional peptide inhibitors (BPI) with the hypothesis that the BPI molecules target the APC and shift the activation of T cells from an inflammatory to a regulatory phenotype.<sup>7-9</sup> Previously, BPI molecules have been shown to successfully suppress the progression of autoimmune

diseases such as MS, Type 1 diabetes, and rheumatoid arthritis in animal models.<sup>7-10</sup> It was proposed that BPI molecules bind simultaneously to the major histocompatibility complex class II (MHC-II) and ICAM-1 on APC to block immunological synapse formation at the T cell-APC interface, subsequently altering T cell differentiation from inflammatory to regulatory.<sup>7-10</sup> PLP-BPI is a conjugate between an antigenic peptide (PLP<sub>139-151</sub>) and a cell adhesion peptide (LABL) derived from the I-domain of lymphocyte function-associated antigen-1 (LFA-1) and tethered together by a linker molecule. Unfortunately, BPI molecules can deliver only one antigenic peptide at a time and cannot deliver multiple antigens when antigenic spreading has occurred. Therefore, there is also a need to find a way to simultaneously deliver multiple antigens to APC to overcome the problem of antigenic spreading in a particular autoimmune disease.

In this study, I-domain-antigen conjugate (IDAC) molecules derived from the I-domain protein were conjugated with multiple proteolipid protein (PLP) peptides. The experimental autoimmune encephalomyelitis (EAE) mouse model was treated with IDAC using prophylactic and vaccine-like delivery methods. The I-domain of LFA-1 interacts with the first domain (D1) of ICAM-1 thus providing a scheme to target PLP antigen to APC.<sup>11</sup> Because the I-domain has multiple lysine residues, several PLP peptides can be conjugated to one molecule of the I-domain. In this study, IDAC-1 and IDAC-3 molecules were synthesized by conjugating PLP-Cys-OH and Ac-PLP-Cys-NH<sub>2</sub> peptides, respectively, to several lysine groups of the I-domain. The purified IDAC molecules were characterized using mass spectrometry and circular dichroism (CD) spectroscopy, and their efficacies were evaluated in the EAE mouse model. In both prophylactic and vaccine-like delivery methods, IDAC molecules effectively suppressed EAE compared to

PBS. The cytokine production data suggested that IDAC molecules stimulate the proliferation of regulatory and suppressor cells.

## **2.2 MATERIALS AND METHODS**

### **2.2.1 Animals**

SJL/J female mice were purchased from Charles River Laboratories, Inc. (Wilmington, MA) and subsequently housed under specific pathogen-free conditions at the animal facility at The University of Kansas approved by the Association for Assessment and Accreditation of Laboratory Animal Care (AAALAC). All experimental procedures using live mice were approved by the Institutional Animal Care and Use Committee (IACUC) at The University of Kansas.

### **2.2.2 Peptide Synthesis**

All peptides used in this study (**Table 1**) were synthesized using a 9-fluorenylmethyloxycarbonyl-protected solid-phase peptide chemistry on an automated peptide synthesizer (Pioneer; Perceptive Biosystems, Framingham, MA). The peptides along with the protecting group were removed from the resin using trifluoroacetic acid (TFA) in the presence of appropriate scavengers. The crude peptides were purified using semi-preparative reversed-phase high-performance liquid chromatography (RP-HPLC) with a C18 column. A gradient method was used for purification with solvent A (94.9%

<b>Table 1. The sequences of peptides and proteins used in the present study</b>	
<b>Peptide/Protein</b>	<b>Sequence</b>
Ac-PLP-BPI-NH <sub>2</sub> -2	<i>Ac</i> -HSLGKWLGHDPKF-(AcpGAcpGAcp) <sub>2</sub> -ITDGEATDSG-NH <sub>2</sub>
Ac-PLP-cIBR1-NH <sub>2</sub>	<i>Ac</i> -HSLGKWLGHDPKF-(AcpGAcpGAcp) <sub>2</sub> -Cyclo(1,12)-PenPRGGSVLVTGC-NH <sub>2</sub>
IDAC-1	(HSLGKWLGHDPKFC) <sub>n</sub> -linker-I-domain
IDAC-3	(Ac-HSLGKWLGHDPKFC-NH <sub>2</sub> ) <sub>n</sub> -linker-I-domain
GMB-I-domain	[ <i>N</i> -( $\gamma$ -maleimido)-1-oxybutyl] <sub>n</sub> -I-domain
I-domain	MGNVDLVFLFDGMSLQPDEFQKILDFMKDVMKK LSNTSYQFAAVQFSTSYKTEFDFSDYVKRKDPDALL KHKHMLLLTNTFGAINYVATEVFREELGARPDAT KVLIIITDGEATDSGNIDAAKDIIRYIIGIGKHFQTKES QETLHKFASKPASEFVKILDTFEKLKDLFTELQKKIY
Ac = Acetyl and Acp = Aminocaproic acid	

water, 5% acetonitrile, and 0.1% trifluoroacetic acid) and solvent B (100% acetonitrile). HPLC with an analytical C18 column was used to determine the peptide purity (>96%). The identity of the peptides was confirmed using matrix-assisted laser desorption/ionization time-of-flight (MALDI-TOF) mass spectrometry.

### **2.2.3 I-domain Preparation**

The I-domain protein was over-expressed, refolded, and purified as previously described.<sup>12</sup> The identity, purity, and secondary structure of the protein were confirmed by mass spectrometry, SDS-PAGE, and CD, respectively.

### **2.2.4 Synthesis of IDAC-1 and -3**

*N*-[ $\gamma$ -maleimidobutyryloxy]succinimide ester (GMBS) was first reacted at a tenfold molar excess with the free lysine residues of the I-domain (2 mg/ml) for 1 h in PBS to generate GMB-I-domain. Subsequent purification of the reaction mixture was done using size-exclusion chromatography (SEC). Then, the thiol group on the Cys residue of PLP-Cys-OH and Ac-PLP-Cys-NH<sub>2</sub> peptides was reacted at a 15-molar excess with the newly formed maleimide groups on the GMB-I-domain (2 mg/ml) at pH 8.5 to give IDAC-1 and -3, respectively. After a 1-hour reaction, the pH of the solution was adjusted to 7.4, and the resulting mixture was purified using SEC. The purity, identity, and conformation of IDAC-1 and -3 were determined using SDS-PAGE, mass spectrometry (LC ESI-MS), and CD, respectively.

### **2.2.5 Induction of EAE and Efficacy Studies**

Six-to-eight week old SJL/J female mice were immunized subcutaneously with 200 µg PLP<sub>139-151</sub> peptide in a 0.2 ml emulsion consisting of equal volumes of PBS and complete Freund's adjuvant (CFA) containing killed *mycobacterium tuberculosis* strain H37RA at a final concentration of 4 mg/ml (Difco, Detroit, MI). The PLP/CFA emulsion was administered to regions above the shoulder and the flanks (total of 4 sites, 50 µl at each injection site). In addition, 200 ng of pertussis toxin was injected intraperitoneally on the day of immunization (day 0) and 2 days post-immunization.

The mice then received either intravenous or subcutaneous injections of IDAC (10 or 26 nmol/injection) or peptides (100 nmol/injection for Ac-PLP-BPI-NH<sub>2</sub>-2 or 50 nmol/injection/mouse for Ac-PLP-cIBR1-NH<sub>2</sub>). The prophylactic disease suppression was carried out with subcutaneous or intravenous injections of IDAC molecules on days 4 and 7, or BPI molecules on days 4, 7, and 10. Mice receiving vaccine-like treatment were given subcutaneous injections of IDAC and BPI molecules at 11, 8, and 5 days prior to the induction of disease. As negative controls, mice were treated with PBS, I-domain, and GMB-I-domain. Disease progression was evaluated by monitoring the change in weight of the mice and clinical scoring based on the severity of nerve damage ranging from 0 to 5: 0–no clinical symptoms of disease; 1–tail weakness or limp tail; 2–paraparesis (weakness or partial paralysis of one or two hind limbs); 3–paraplegia (complete paralysis of two hind limbs); 4–paraplegia with forelimb weakness or paralysis; 5–moribund (at this point, the affected mice were euthanized).

### **2.2.6 Determination of Cytokine Levels *In Vitro***

Representative spleens for each group (IDAC-3 or PBS) from Study 2 were harvested from female SJL/J (H-2<sup>S</sup>) mice on days 13 and 35. Splenocytes were dispersed by gently smashing the spleen using the coarse portion of a 1 ml syringe in a petri dish containing RPMI 1640 medium (10% FBS, 0.05 M BME). The cells were then filtered through a 40 micrometer strainer. After centrifugation, the red blood cells were lysed using “ACK lysis buffer,” and the remaining white blood cells were washed three times with medium. Splenocytes ( $5 \times 10^6$  cells/ml) were cultured in parallel in the presence of 20  $\mu$ M PLP and blank RPMI medium. Supernatants were collected at a 72 h time-point for the measurement of cytokine levels. The samples were then analyzed using a fully quantitative ELISA-based Q-Plex<sup>TM</sup> Mouse Cytokine-Screen (Quansys Biosciences, Logan, UT).

### **2.2.7 Statistical Analysis**

Statistical differences among the groups in clinical disease scores were determined by calculating the average score for each mouse from day 12 to day 17 by one-way analysis of variance followed by Fisher’s least significant difference. Statistical differences in body weight among groups were also analyzed in the same fashion, but from day 12 to day 24. Comparison of cytokine concentrations was also performed by one-way analysis of variance. All analyses were performed using StatView (SAS Institute, Cary, NC).

## **2.3 RESULTS**

### **2.3.1 Synthesis and Characterization of IDAC-1 and -3**



IDAC-1 and -3 were prepared by randomly conjugating the free amine groups of the I-domain with the N-hydroxysuccinimide group of GMBS, yielding GMB-I-domain. The resulting GMB-I-domain was then reacted with the thiol group of the Cys residue on PLP-Cys-OH or Ac-PLP-Cys-NH<sub>2</sub>, yielding IDAC-1 and -3, respectively. Then, the resulting mixture was purified using size-exclusion column chromatography, and the eluted fractions were subsequently analyzed using SDS-PAGE (**Fig. 2.1A**). Multiple bands were seen on SDS-PAGE due to the varying number of conjugated peptides on the I-domain. The earlier lanes on the gel have bands at a higher molecular weight compared to the later lanes, which corresponded to the order of elution of IDAC from the SEC. Analysis with circular dichroism showed that both IDAC-1 and -3 have spectra similar to that of the I-domain, indicating that multiple conjugations did not alter the secondary structure (**Fig. 2.1B**). The deconvoluted LC-MS data showed that both IDAC molecules had 0–5 PLP-Cys peptides conjugated per I-domain, with an average of 2.5 PLP-Cys peptides per I-domain molecule (**Fig. 2.1C**).

### **2.3.2 Suppression of EAE by IDAC-1 and -3**

To test whether the I-domain and GMB-I-domain had *in vivo* efficacy, three groups of mice were treated with two intravenous injections of the I-domain or GMB-I-domain (26 nmol/injection) as well as PBS on days 4 and 7. Although there was a slight delay in the onset of the disease, neither the I-domain nor GMB-I-domain

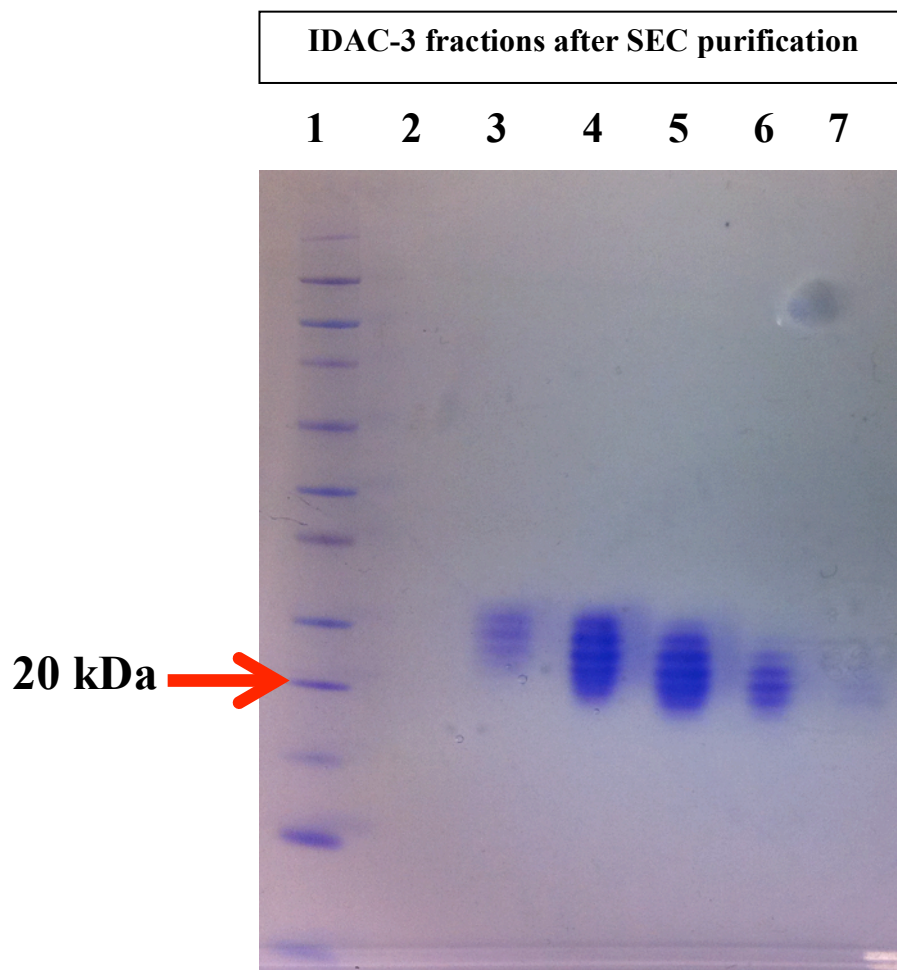


**Figure 2.1** Characterization of IDAC-1 and -3 were done by SDS-PAGE gel (A), CD (B), and mass spectrometry (C). **Figure 2.1A:** SDS-PAGE analysis of the conjugate following separation using SEC and after staining with Coomassie blue: molecular weight marker (lane 1), fractions of conjugated IDAC-3 in the order of elution from SEC (lanes 3–7).

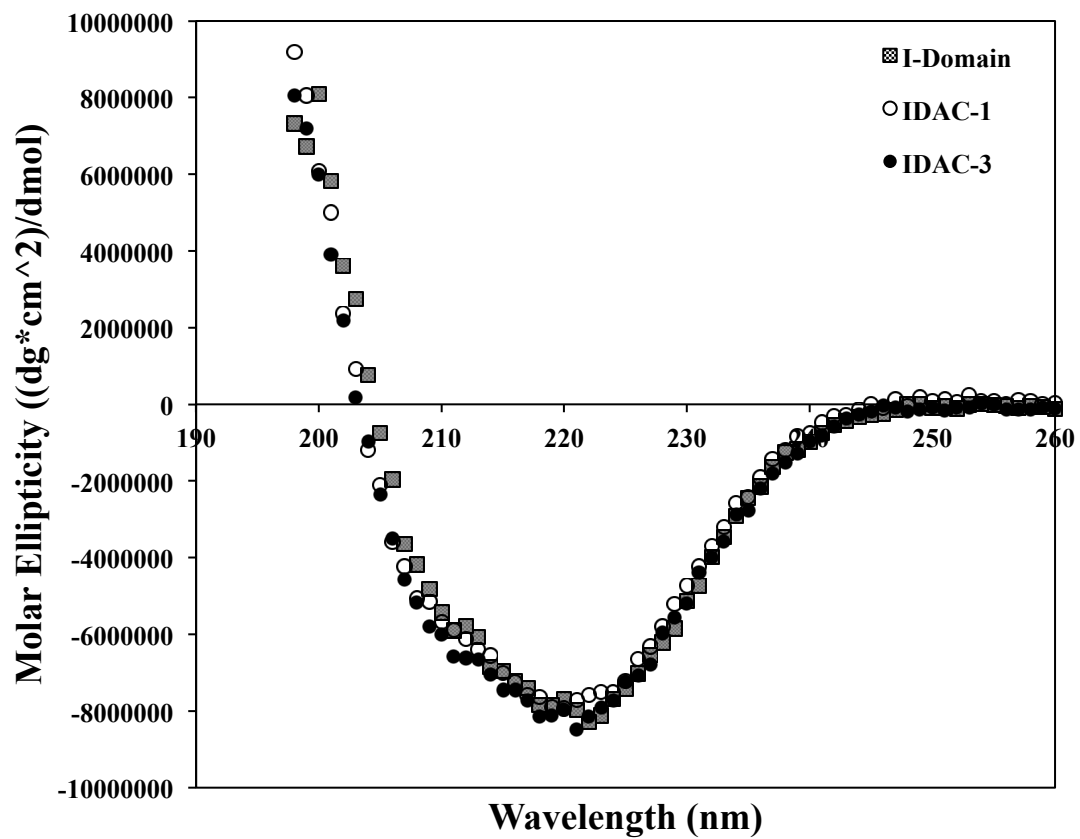


**Figure 2.1B:** CD spectra of the parent I-domain (square), IDAC-1 (open circle) and IDAC-3 (closed circle).

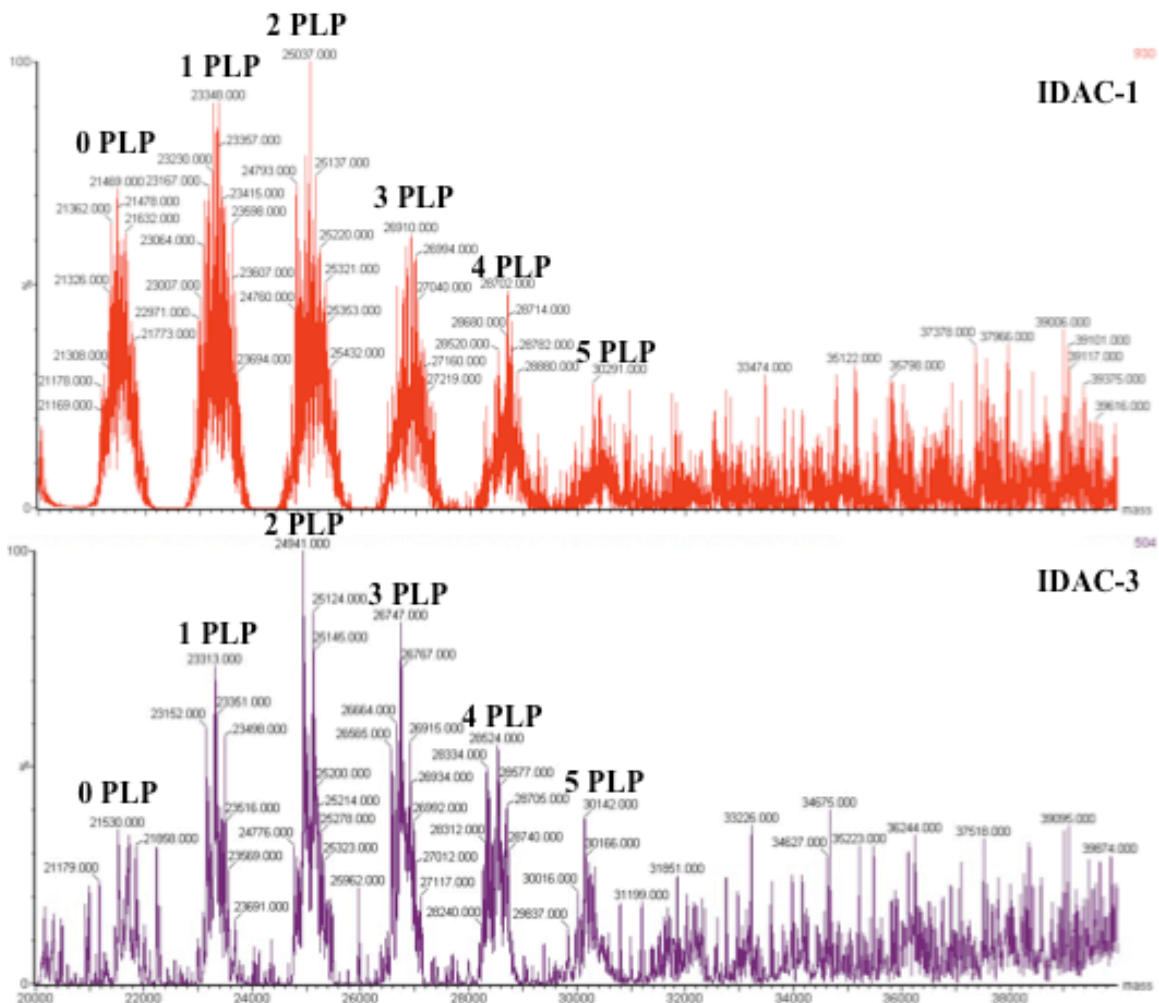


**Figure 2.1C:** Deconvoluted mass spectra of LC ESI-MS analysis of IDAC-1 and IDAC-3.

significantly suppressed the progress of EAE compared to the PBS-treated mice, as determined by the clinical score (**Fig. 2.2A**), change in body weight (**Fig. 2.2B**), and the incidence of disease (**Fig. 2.2C**).

In the second study, the efficacies of IDAC-1 and IDAC-3 with uncapped and capped PLP peptides, respectively, were compared upon intravenous injections of 26 nmol/injection on days 4 and 7; the control group was injected with PBS. Clinical scores (**Fig. 2.3A**) indicated that both proteins delayed the onset of disease and were significantly better at suppressing EAE than to PBS ( $p < 0.0005$ , through days 12–17). Furthermore, IDAC-3 was better than IDAC-1 in suppressing EAE ( $p < 0.005$ , through days 12–17), suggesting that capping the antigenic PLP peptide at both ends yields a more efficacious product. The body weight change for IDAC-1- and IDAC-3-treated animals supported the clinical score data; two injections of IDAC-1 and -3 were significantly more effective than PBS in suppressing disease (**Fig. 2.3B**,  $p < 0.05$  through days 12–24). In addition, there were delays in disease incidence in IDAC-1- and IDAC-3-treated animals (**Fig. 2.3C**).

After establishing that IDAC-3 was a better candidate to suppress EAE, the third study was aimed at evaluating an alternative route of injection (i.e., subcutaneous or s.c.), dose response to determine therapeutic index, and optimal timing of IDAC-3 injections (**Fig. 2.4**). First, IDAC-3 injected s.c. (26 nmol/injection) on days 4 and 7 was significantly more efficacious than PBS in suppressing EAE as shown by clinical scores ( $p < 0.005$ , through days 12–17; **Fig. 2.4A**), change in body weight of the mice ( $p < 0.005$ , through days 12–24; **Fig. 2.4B**), and disease incidence (**Fig. 2.4C**). It was difficult

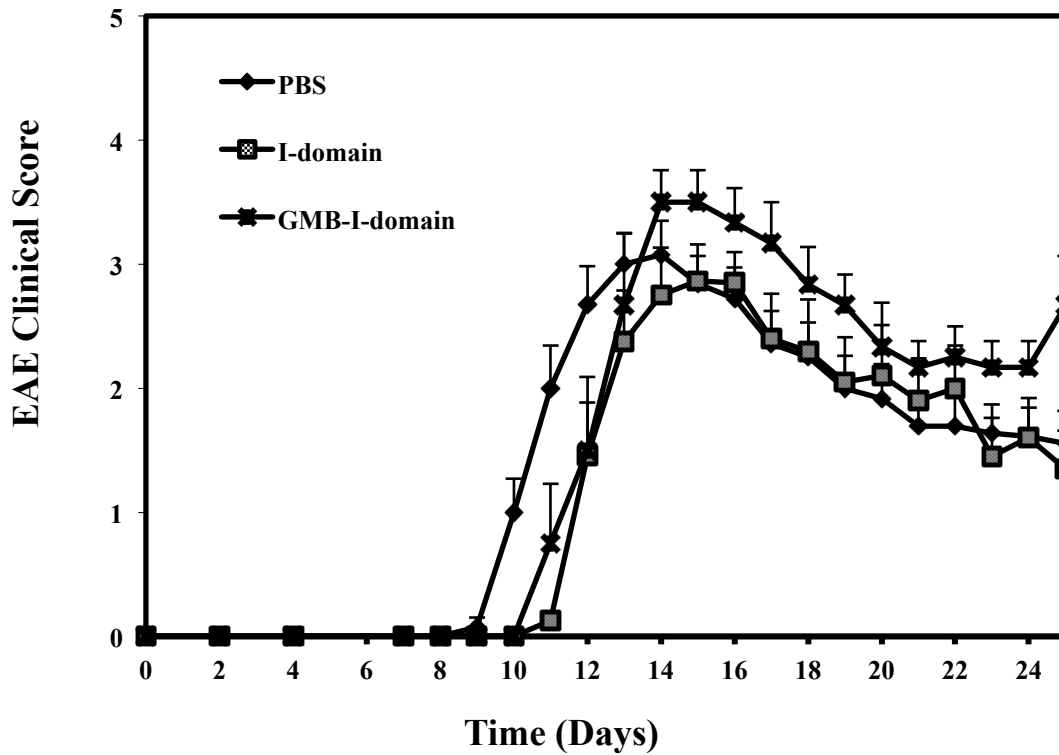
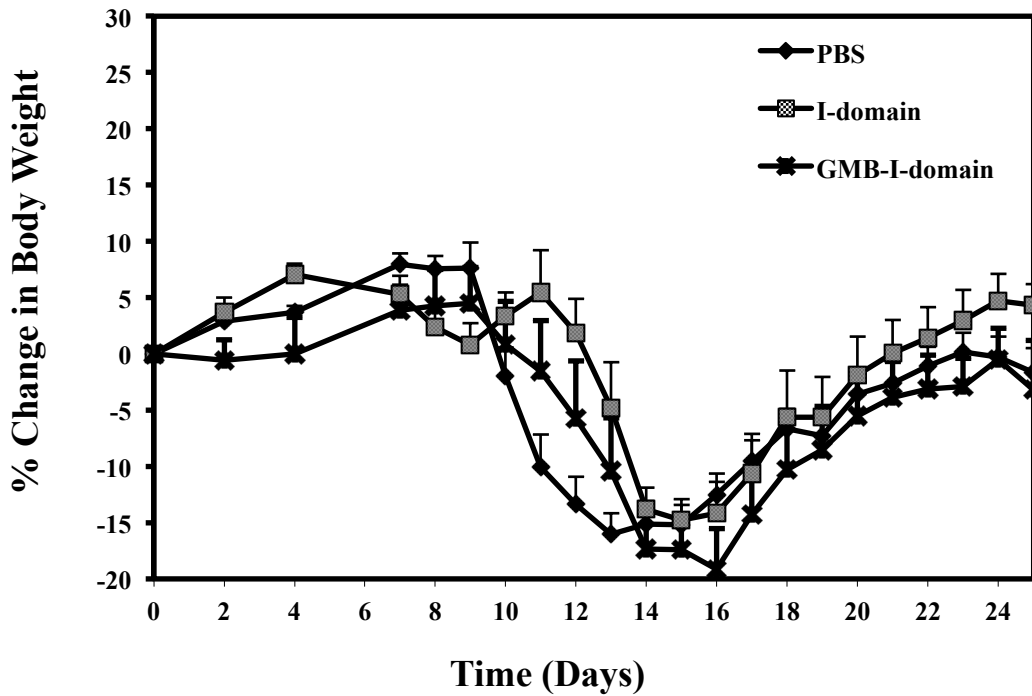


**Figure 2.2A** *In vivo* activity of I-domain, GMB-I-domain, and PBS in mouse EAE model evaluated by clinical scores. After immunization with PLP peptide in CFA, the mice received i.v. injections of 26 nmol/injection/day of I-domain or GMB-I-domain on days 4 and 7. Control mice were treated with PBS on days 4, 7, and 10. Disease progression was evaluated using (A) clinical disease scores, (B) change in body weight, and (C) incidence of disease. Although there was a slight delay in the onset of disease, neither protein significantly suppressed the progress of EAE compared to the PBS-treated mice. The results are expressed as the mean  $\pm$  S.E. ( $n \geq 6$ ).



to

**Figure 2.2B** *In vivo* activity of I-domain, GMB-I-domain, and PBS in mouse EAE model evaluated using change in body weight. After immunization with PLP peptide in CFA, the mice received i.v. injections of 26 nmol/injection/day of I-domain or GMB-I-domain on days 4 and 7. Control mice were treated with PBS on days 4, 7, and 10. There are no significant differences between I-domain and GMB-I-domain compared to the PBS-treated mice. The results are expressed as the mean  $\pm$  S.E. ( $n \geq 6$ ).

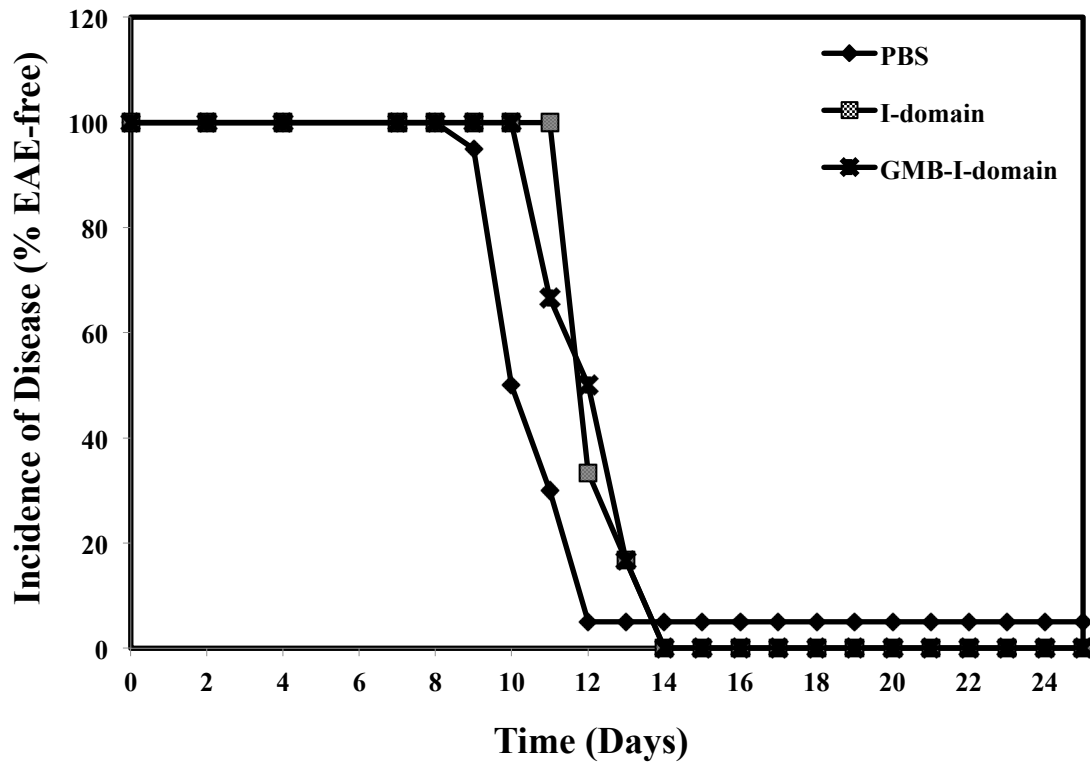


**Figure 2.2C** *In vivo* activity of I-domain, GMB-I-domain, and PBS in mouse EAE model evaluated using incidence of disease. After immunization with PLP peptide in CFA, the mice received i.v. injections of 26 nmol/injection/day of I-domain or GMB-I-domain on days 4 and 7. Control mice were treated with PBS on days 4, 7, and 10. I-domain and GMB-I-domain delayed the onset of disease compared to the PBS-treated mice, but did not fully suppress disease.



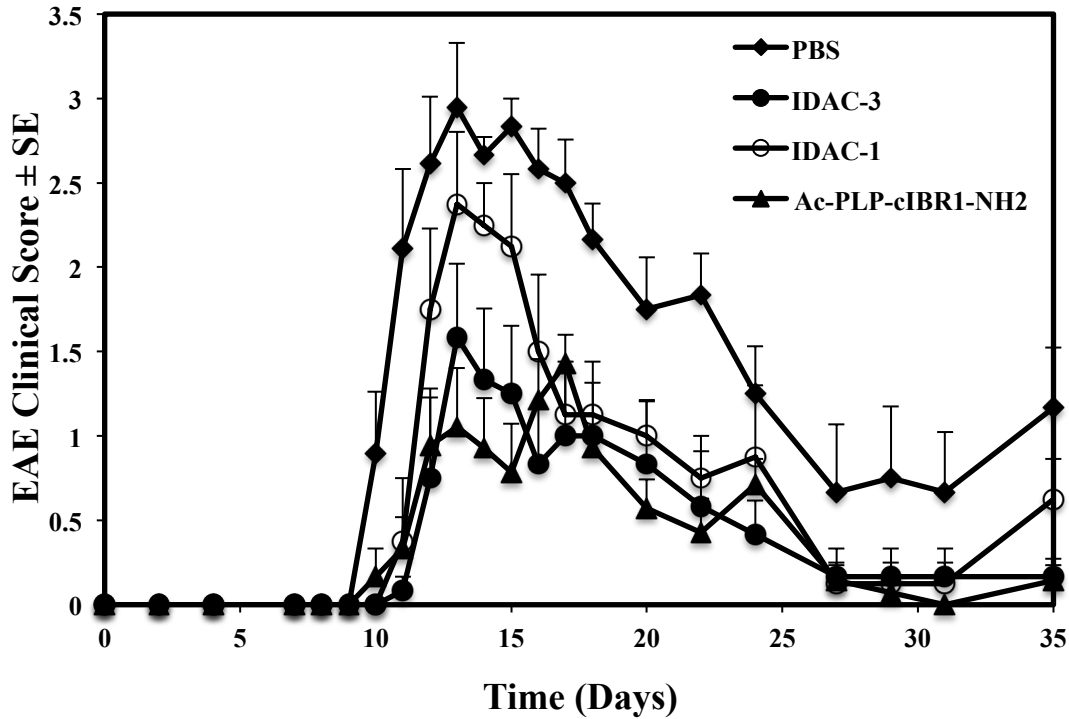


**Figure 2.3A** Comparison of the *in vivo* activity of IDAC-1, IDAC-3, Ac-PLP-cIBR1-NH<sub>2</sub>, and PBS in the mouse EAE model using clinical disease scores. After immunization with PLP peptide in CFA, the mice received i.v. injections of 26 nmol/injection/day of IDAC-1 or IDAC-3 on days 4 and 7. For the Ac-PLP-cIBR1-NH<sub>2</sub> treatment group, the mice received i.v. injections of 50 nmol/injection/day of the peptide on days 4, 7, and 10. Control mice were treated with PBS on days 4, 7, and 10. IDAC-1 and IDAC-3 delayed the onset of disease and were significantly better at suppressing EAE than to PBS ( $p < 0.0005$ , through days 12–17). IDAC-3 was better than IDAC-1 in suppressing EAE ( $p < 0.005$ , through days 12–17). The results are expressed as the mean  $\pm$  S.E. ( $n \geq 6$ ).

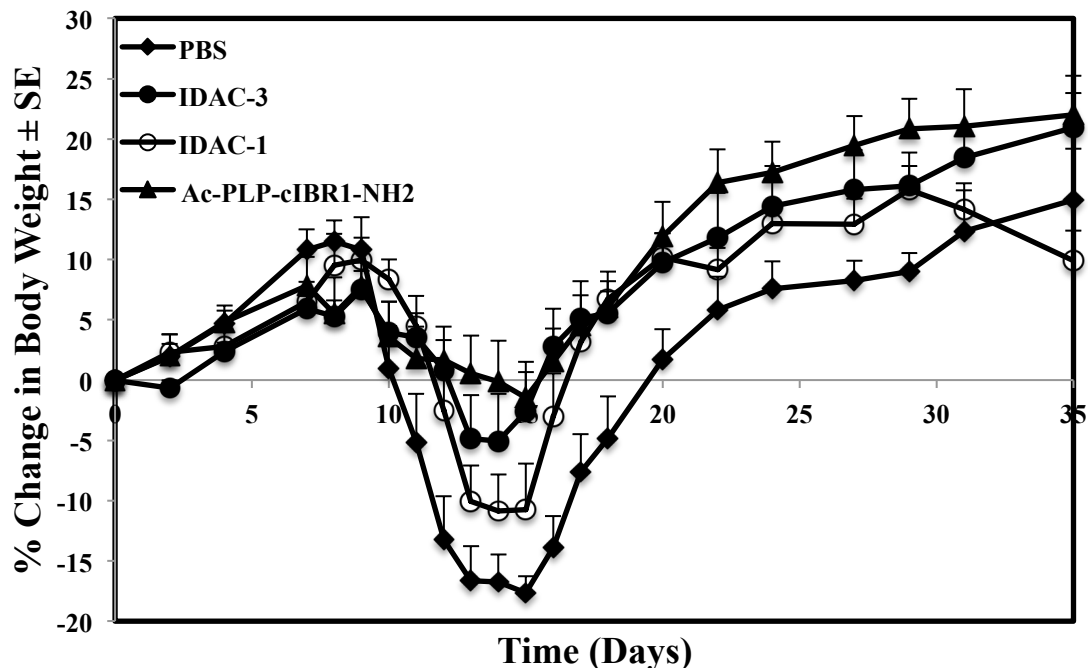


**Figure 2.3B** Comparison of the *in vivo* activity of IDAC-1, IDAC-3, Ac-PLP-cIBR1-NH<sub>2</sub>, and PBS in the mouse EAE model using change in body weight. After immunization with PLP peptide in CFA, the mice received i.v. injections of 26 nmol/injection/day of IDAC-1 or IDAC-3 on days 4 and 7. For the Ac-PLP-cIBR1-NH<sub>2</sub> treatment group, the mice received i.v. injections of 50 nmol/injection/day of the peptide on days 4, 7, and 10. For the control mice, they were treated with PBS on days 4, 7, and 10. Two injections of IDAC-1 and IDAC-3 were significantly more effective than PBS in suppressing disease ( $p < 0.05$  through days 12–24). The results are expressed as the mean  $\pm$  S.E. ( $n \geq 6$ ).

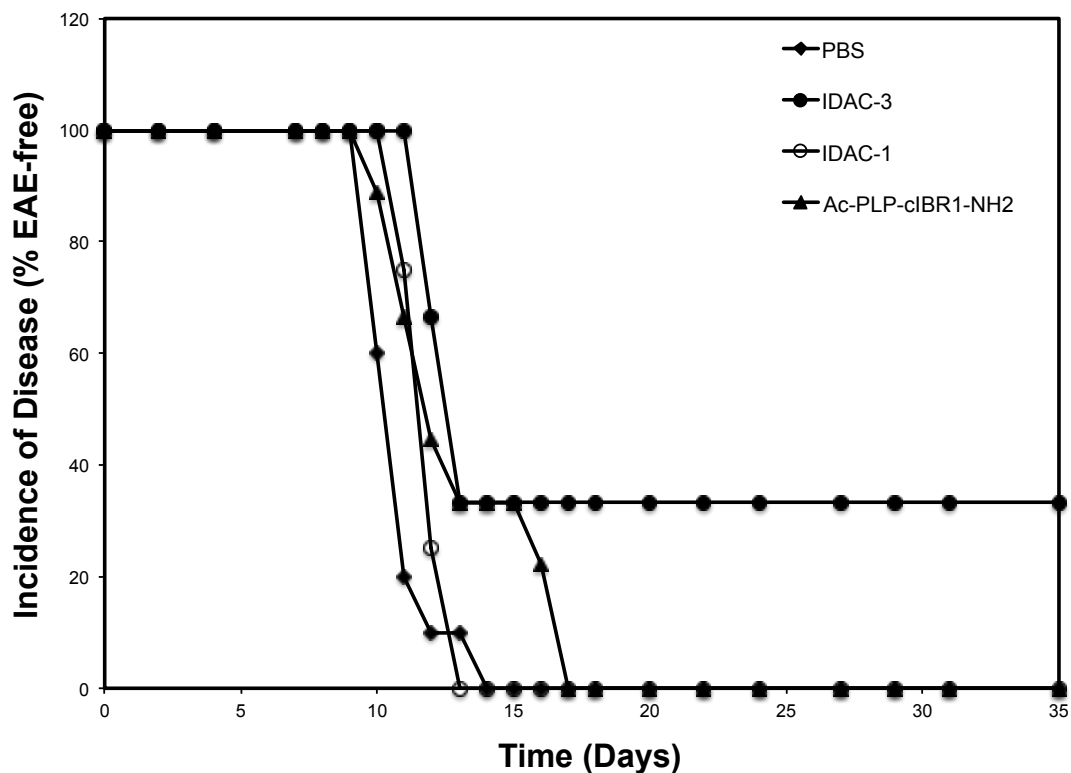


**Figure 2.3C** Comparison of the *in vivo* activity of IDAC-1, IDAC-3, Ac-PLP-cIBR1-NH<sub>2</sub>, and PBS in the mouse EAE model using incidence of disease. After immunization with PLP peptide in CFA, the mice received i.v. injections of 26 nmol/injection/day of IDAC-1 or IDAC-3 on days 4 and 7. For the Ac-PLP-cIBR1-NH<sub>2</sub> treatment group, the mice received i.v. injections of 50 nmol/injection/day of the peptide on days 4, 7, and 10. For the control mice, they were treated with PBS on days 4, 7, and 10. There were delays in disease incidence in IDAC-1- and IDAC-3-treated animals.

conclude whether s.c. administration is better than i.v. administration in the absence of a direct comparison. Our previous studies indicated that s.c. administration of BPI molecules was more effective than i.v. administration.<sup>13</sup> Second, the efficacy of IDAC-3 upon vaccine-like administrations was evaluated in different doses to determine the therapeutic index of the molecule. In this case, the mice received s.c. injections of two different doses of IDAC-3 (26 nmol/injection and 10 nmol/injection), Ac-PLP-BPI-NH<sub>2</sub>-2 (100 nmol/injection), and PBS at 11, 8, and 5 days prior to the induction of the disease at day 0. Ac-PLP-BPI-NH<sub>2</sub>-2, as positive control, significantly suppressed EAE compared to PBS as reflected in the clinical scores (**Fig. 2.4A**;  $p < 0.005$ , days 12–17) and change in body weight (**Fig. 2.4B**;  $p < 0.005$ , days 12–24). Although it was less potent than Ac-PLP-BPI-NH<sub>2</sub>-2, mice treated with a low dose of IDAC-3 (10 nmol/injection) had significantly better clinical scores (**Fig. 2.4A**,  $p < 0.005$ , days 12–17) and body weight changes (**Fig. 2.4B**;  $p < 0.005$  through days 12–24). At a high dose (26 nmol/injection), the third injection of IDAC-3 unfortunately caused a toxic effect in two of six mice; thus, the efficacy data were representative of four animals (**Fig. 2.4**). Although the statistical analysis was not carried out due to the lower number of animals, a high dose (26 nmol/injection) of IDAC-3 seemed to be better than the lower dose (10 nmol/injection) group and similar to the Ac-PLP-BPI-NH<sub>2</sub>-2-treated group. IDAC-3 effectively suppressed the disease when given in a vaccine-like schedule, and this study provided us with an estimated therapeutic window of IDAC-3 with a maximum toxic concentration of 3 injections of IDAC-3 at 26 nmol and a minimum effective concentration of 3 injections of 10 nmol. Finally, the best efficacy of IDAC-3 was found when using s.c. injections of IDAC-3 on days 4 and 7.

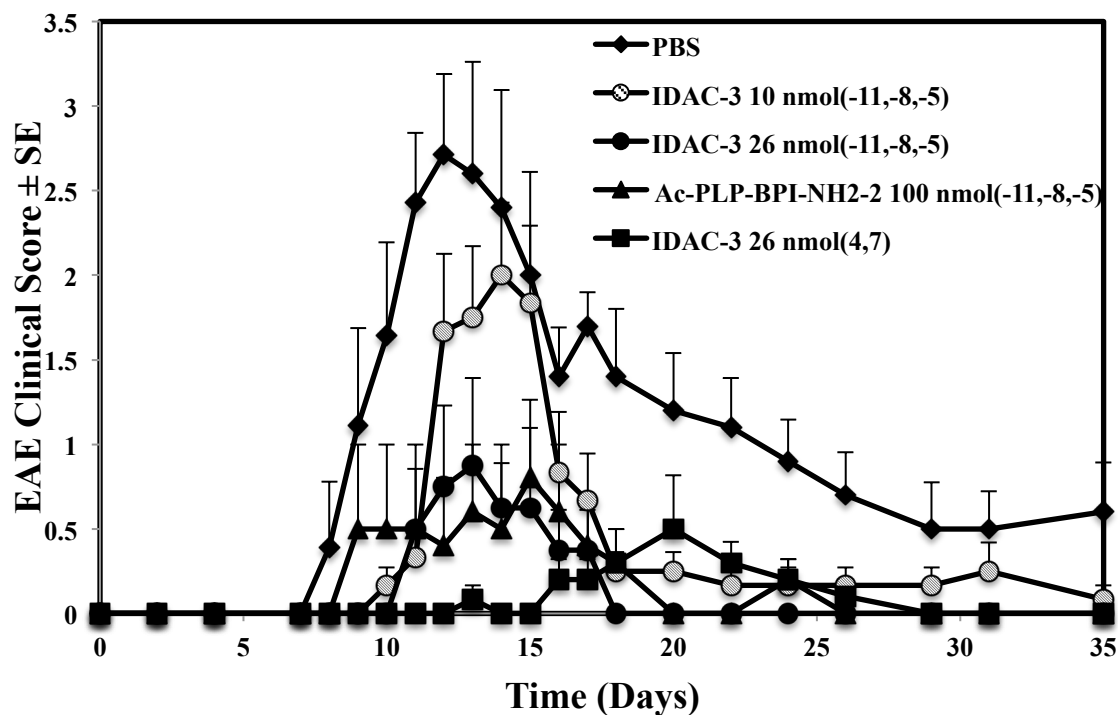


**Figure 2.4A** Comparison of the *in vivo* activity of IDAC-3, Ac-PLP-LABL-NH<sub>2</sub>-2, and PBS in the mouse EAE model using clinical disease scores. After immunization with PLP peptide in CFA, the mice received subcutaneous injections of either 10 nmol/injection/day or 26 nmol/injection/day of IDAC-3 on days -11, -8, and -5. Mice also received s.c. injections of 26 nmol/injection/day of IDAC-3 on days 4 and 7. For the Ac-PLP-LABL-NH<sub>2</sub>-2 treatment group, the mice received s.c. injections of 100 nmol/injection/day of the peptide on days -11, -8, and -5. The control mice were treated with s.c. injections of PBS on days -11, -8, and -5. IDAC-3 injected s.c. (26 nmol/injection) on days 4 and 7 was significantly more efficacious than PBS in suppressing EAE ( $p < 0.005$ , through days 12–17). Ac-PLP-BPI-NH<sub>2</sub>-2 significantly suppressed EAE compared to PBS ( $p < 0.005$ , days 12–17). Mice treated with a low dose of IDAC-3 (10 nmol/injection) had significantly better clinical scores than PBS ( $p < 0.005$ , days 12–17). The results are expressed as the mean  $\pm$  S.E. ( $n \geq 6$ ).

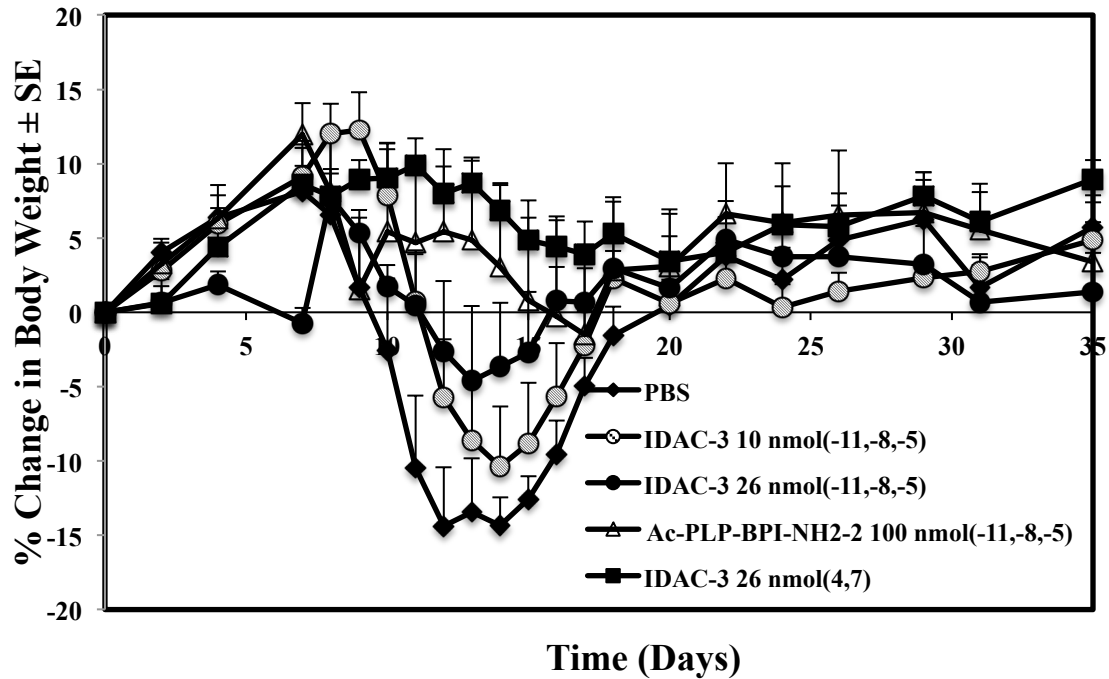


**Figure 2.4B** Comparison of the *in vivo* activity of IDAC-3, Ac-PLP-LABL-NH<sub>2</sub>-2, and PBS in the mouse EAE model using change in body weight. After immunization with PLP peptide in CFA, the mice received subcutaneous injections of either 10 nmol/injection/day or 26 nmol/injection/day of IDAC-3 on days -11, -8, and -5. Mice also received s.c. injections of 26 nmol/injection/day of IDAC-3 on days 4 and 7. For the Ac-PLP-LABL-NH<sub>2</sub>-2 treatment group, the mice received s.c. injections of 100 nmol/injection/day of the peptide on days -11, -8, and -5. The control mice were treated with s.c. injections of PBS on days -11, -8, and -5. IDAC-3 injected s.c. (26 nmol/injection) on days 4 and 7 was significantly more efficacious than PBS in suppressing EAE ( $p < 0.005$ , through days 12–24). Ac-PLP-BPI-NH<sub>2</sub>-2 significantly suppressed EAE compared to PBS ( $p < 0.005$ , days 12–24). Mice treated with a low dose of IDAC-3 (10 nmol/injection) lost significantly less weight than PBS ( $p < 0.005$  through days 12–24). The results are expressed as the mean  $\pm$  S.E. ( $n \geq 6$ ).

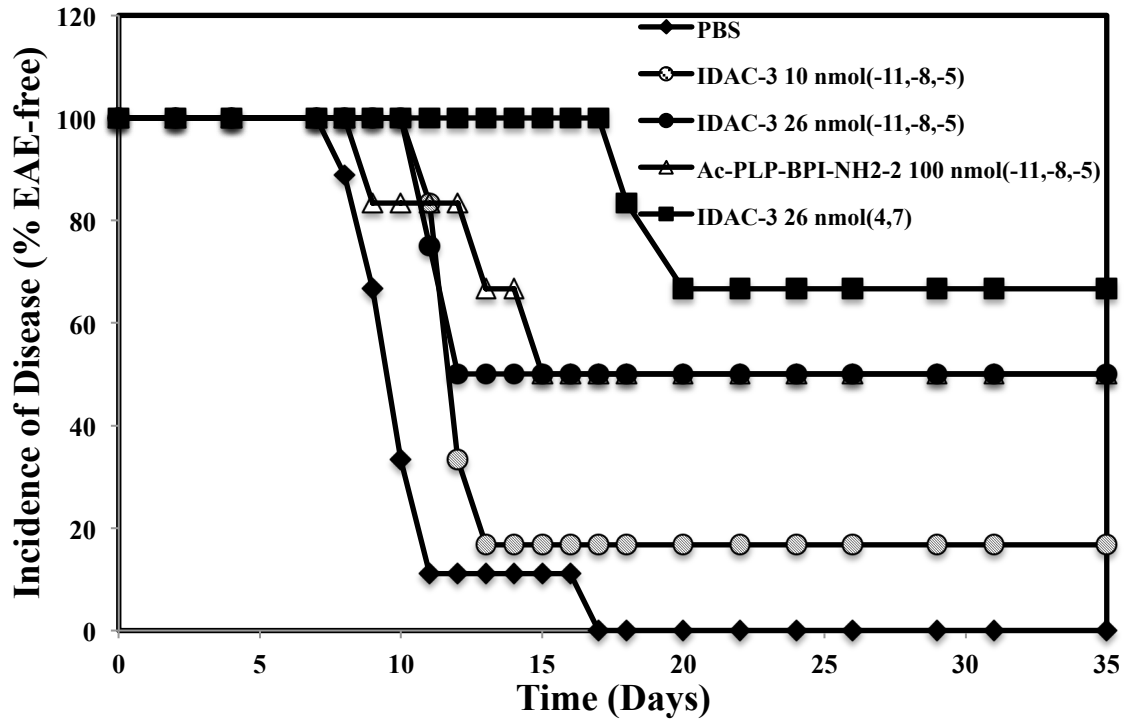


**Figure 2.4C** Comparison of the *in vivo* activity of IDAC-3, Ac-PLP-LABL-NH<sub>2</sub>-2, and PBS in the mouse EAE model using incidence of disease. After immunization with PLP peptide in CFA, the mice received subcutaneous injections of either 10 nmol/injection/day or 26 nmol/injection/day of IDAC-3 on days -11, -8, and -5. Mice also received s.c. injections of 26 nmol/injection/day of IDAC-3 on days 4 and 7. For the Ac-PLP-LABL-NH<sub>2</sub>-2 treatment group, the mice received s.c. injections of 100 nmol/injection/day of the peptide on days -11, -8, and -5. The control mice were treated with s.c. injections of PBS on days -11, -8, and -5. All treatment groups delayed the onset of disease. Compared to PBS, the percent of mice that were EAE-free were greater in the IDAC-treated groups.

To test the optimal concentration for vaccine-like delivery and its long-term effect in suppressing relapse, IDAC-3 was injected twice via the s.c. route (26 nmol/injection on days -11 and -8) and was compared to three s.c. injections of Ac-PLP-BPI-NH<sub>2</sub>-2 (100 nmol/injection; days -11, -8, and -5), and PBS (days -11, -8, -5). Two injections of IDAC-3 (26 nmol) clearly suppressed EAE significantly better than PBS and had a long-term effect in suppressing relapse of the disease as indicated in the clinical scores (**Fig. 2.5A**,  $p < 0.0001$ , days 12–17, and days 45–55) and change of body weight (**Fig. 2.5B**,  $p < 0.0001$ , days 12–24). Similarly, Ac-PLP-BPI-NH<sub>2</sub>-2 had a long-term effect to prevent relapse. Delay in the onset of disease was observed in both treatment groups (**Fig. 2.5C**).

### **2.3.3 Cytokine Levels in SJL/J Mice *In Vitro***

The potential mechanism of action of IDAC-3 was elucidated by comparing the cytokine levels (i.e., IL-2, IL-5, IL-10, IL-12, and IL-17) in splenocytes after two s.c. injections of IDAC-3 (26 nmol/injection) and PBS on days 4 and 7. The levels of cytokines were determined during the peak of disease on day 13 and after EAE went into remission and plateaued on day 35 (**Fig. 2.6**). Due to the low detection limit or the lack of statistical significance between IDAC-3 and PBS treatment, the levels of IL-4, IL-6, and IFN $\gamma$  were inconclusive. One of the most exciting findings was that the IDAC-3-treated animals had fourfold lower IL-17 during the disease remission on day 35 compared to the PBS-treated group (**Fig. 2.6A**,  $p < 0.0001$ ).

In the PBS-treated group, IL-2 cytokine levels were higher than in the IDAC-3-treated group on day 13 ( $p < 0.05$ ) whereas no significant difference was observed on day



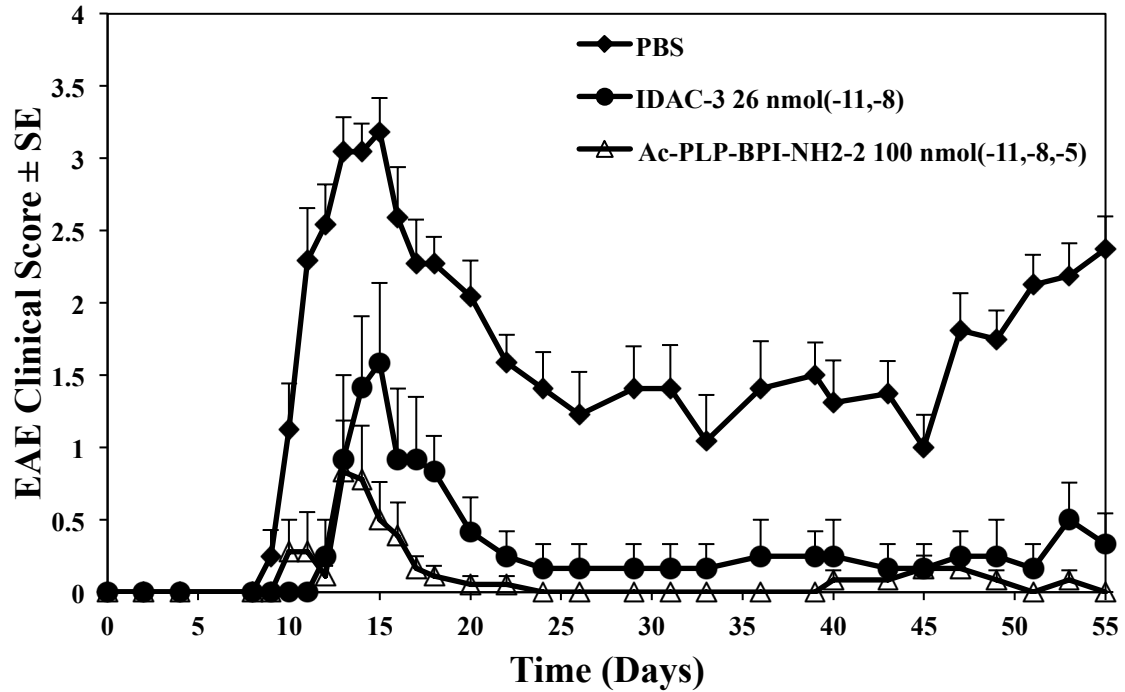


**Figure 2.5A** Comparison of the *in vivo* activity of IDAC-3, Ac-PLP-BPI-NH<sub>2</sub>-2, and PBS in the mouse EAE model using clinical disease scores. After immunization with PLP peptide in CFA, the mice received vaccine-like s.c. injections of 26 nmol/injection/day of IDAC-3 on days -11 and -8. For the Ac-PLP-BPI-NH<sub>2</sub>-2 treatment group, the mice received s.c. injections of 100 nmol/injection/day of the peptide on days -11, -8, and -5. The control mice were treated with PBS on days -11, -8, and -5. IDAC-3 suppressed EAE significantly better than PBS and had a long-term effect in suppressing relapse of the disease ( $p < 0.0001$ , days 12–17, and days 45–55). The results are expressed as the mean  $\pm$  S.E. ( $n \geq 6$ ).

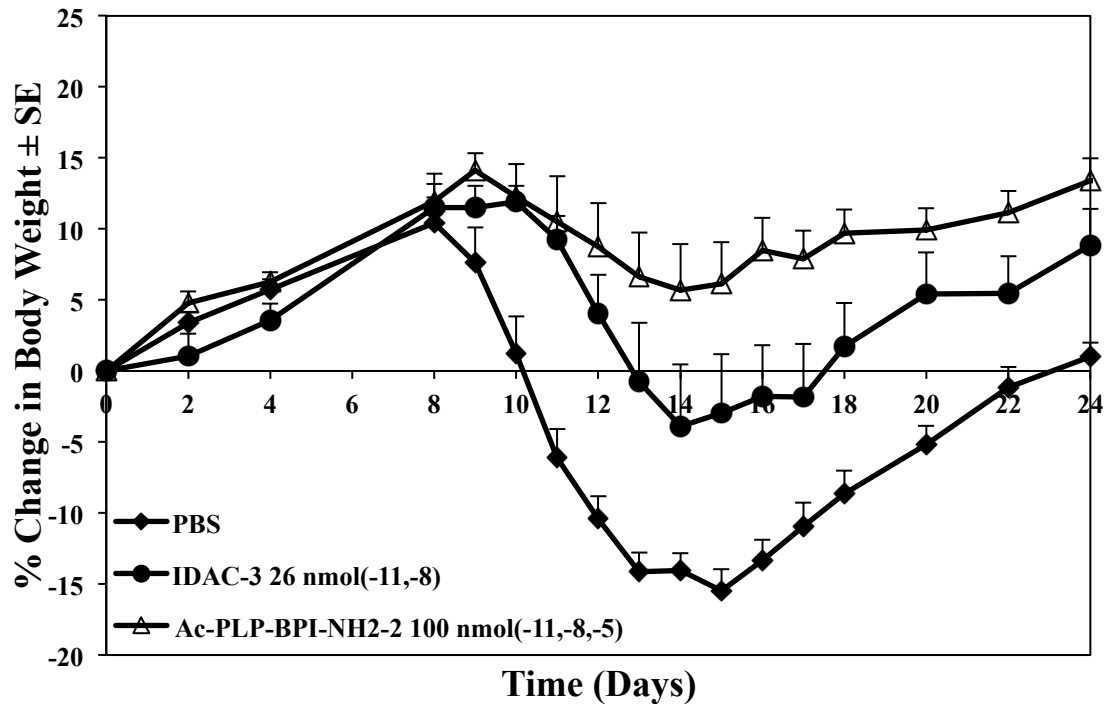


**Figure 2.5B** Comparison of the *in vivo* activity of IDAC-3, Ac-PLP-BPI-NH<sub>2</sub>-2, and PBS in the mouse EAE model using change in body weight. After immunization with PLP peptide in CFA, the mice received vaccine-like s.c. injections of 26 nmol/injection/day of IDAC-3 on days -11 and -8. For the Ac-PLP-BPI-NH<sub>2</sub>-2 treatment group, the mice received s.c. injections of 100 nmol/injection/day of the peptide on days -11, -8, and -5. The control mice were treated with PBS on days -11, -8, and -5. IDAC-3 suppressed EAE significantly better than PBS ( $p < 0.0001$ , days 12–24). The results are expressed as the mean  $\pm$  S.E. ( $n \geq 6$ ).

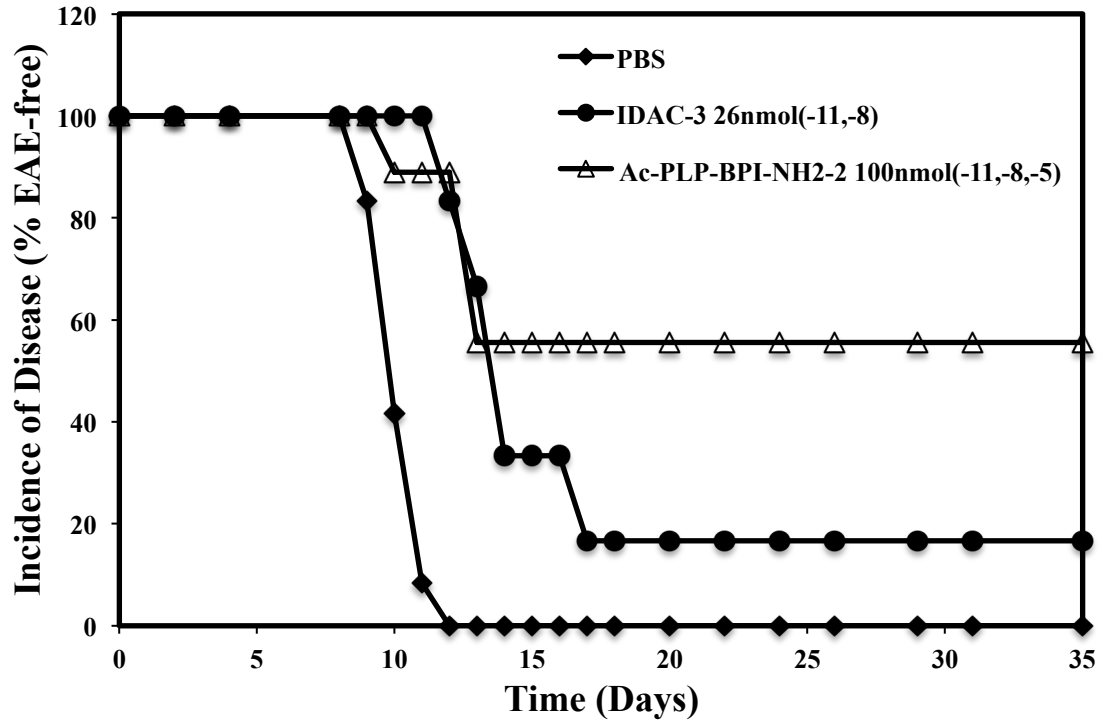


**Figure 2.5C** Comparison of the *in vivo* activity of IDAC-3, Ac-PLP-BPI-NH<sub>2</sub>-2, and PBS in the mouse EAE model by incidence of disease. After immunization with PLP peptide in CFA, the mice received vaccine-like s.c. injections of 26 nmol/injection/day of IDAC-3 on days -11 and -8. For the Ac-PLP-BPI-NH<sub>2</sub>-2 treatment group, the mice received s.c. injections of 100 nmol/injection/day of the peptide on days -11, -8, and -5. The control mice were treated with PBS on days -11, -8, and -5. Both treatment groups delayed the onset of disease compared to PBS. Compared to PBS, the percent of mice that were EAE-free were greater in both of the treatment groups.

35 (**Fig. 2.6B**). Although there was no significant difference in IL-5 levels on day 13, the IL-5 levels on day 35 were significantly higher in the IDAC-3-treated group than in the PBS-treated group (**Fig. 2.6C**,  $p < 0.0005$ ). The cytokine levels of IL-10 on day 13 could not be detected; however, once the disease remission plateaued on day 35, the IDAC-3-treated group had significantly higher levels of IL-10 compared to the PBS group (**Fig. 2.6D**,  $p < 0.05$ ). In the IDAC-3-treated group, the level of IL-12 was significantly lower than in the PBS-treated group on day 35 (**Fig. 2.6E**,  $p < 0.005$ ).

## 2.4 DISCUSSION

The I-domain emerged as a useful carrier protein to target antigenic peptides to suppress EAE. Previously, peptides derived from the I-domain, namely LABL (CD11a<sub>237-246</sub>), had been conjugated to immunodominant antigenic peptides to suppress various autoimmune diseases in animal models of EAE, type-1 diabetes, and rheumatoid arthritis.<sup>7,8,10</sup> In these studies, LABL was conjugated to a single antigenic peptide (i.e., PLP, collagen-II, or GAD peptide). In the current study, the I-domain lysine residues were conjugated with multiple peptides from a single epitope (PLP<sub>139-151</sub>). This approach would allow simultaneous delivery of multiple epitopes of PLP, as well as a mixture of epitopes from the proteolipid protein, myelin oligodendrocyte glycoprotein (MOG), and myelin basic protein (MBP). Another advantage of I-domain over LABL is that the I-domain contains the metal-ion dependent adhesion site (MIDAS) necessary for divalent cation coordination ( $\text{Ca}^{2+}$ ,  $\text{Mg}^{2+}$ , or  $\text{Mn}^{2+}$ ) to enhance binding

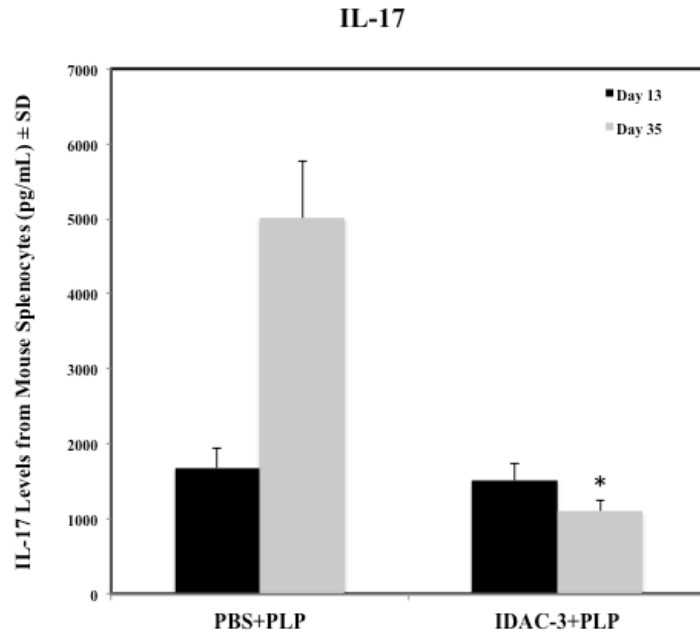


**Figure 2.6A** IL-17 levels (days 13 and 35) from splenocytes of mice treated subcutaneously with PBS and IDAC-3 (26 nmol on days 4 and 7). IDAC-3-treated animals had lower IL-17 during the disease remission on day 35 compared to the PBS-treated group ( $p < 0.0001$ ).

## IL-2

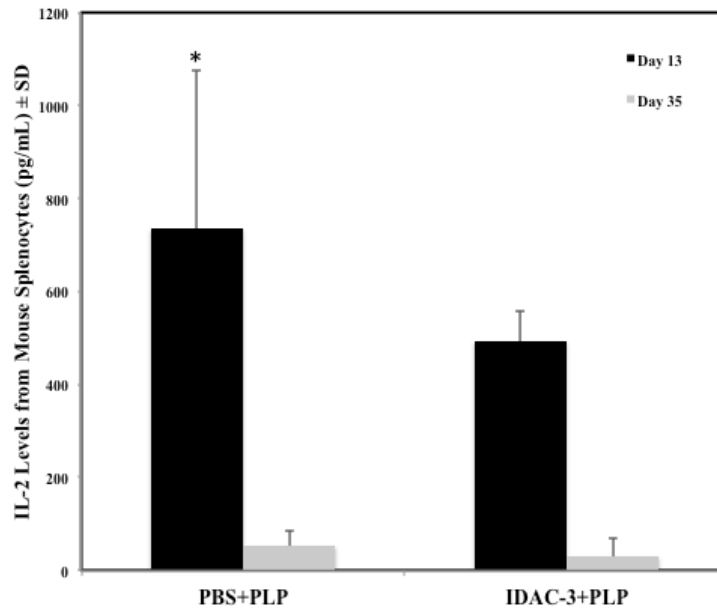


**Figure 2.6B** IL-2 levels (days 13 and 35) from splenocytes of mice treated subcutaneously with PBS and IDAC-3 (26 nmol on days 4 and 7). In the PBS-treated group, IL-2 cytokine levels were higher than in the IDAC-3-treated group on day 13 ( $p < 0.05$ ).

## IL-5

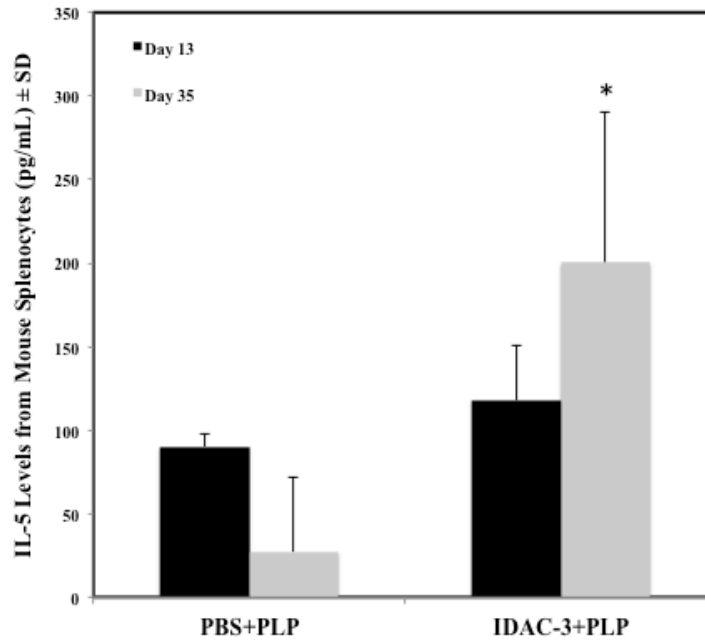


**Figure 2.6C** IL-5 levels (days 13 and 35) from splenocytes of mice treated subcutaneously with PBS and IDAC-3 (26 nmol on days 4 and 7). IL-5 levels on day 35 were significantly higher in the IDAC-3-treated group than in the PBS-treated group ( $p < 0.0005$ ).

## IL-10

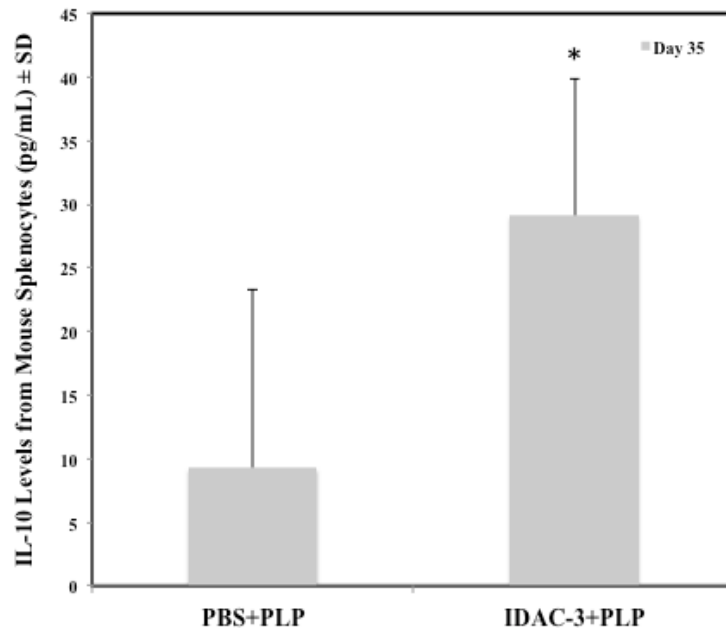


**Figure 2.6D** IL-10 levels (days 13 and 35) from splenocytes of mice treated subcutaneously with PBS and IDAC-3 (26 nmol on days 4 and 7). The IDAC-3-treated group had significantly higher levels of IL-10 compared to the PBS group ( $p < 0.05$ ).



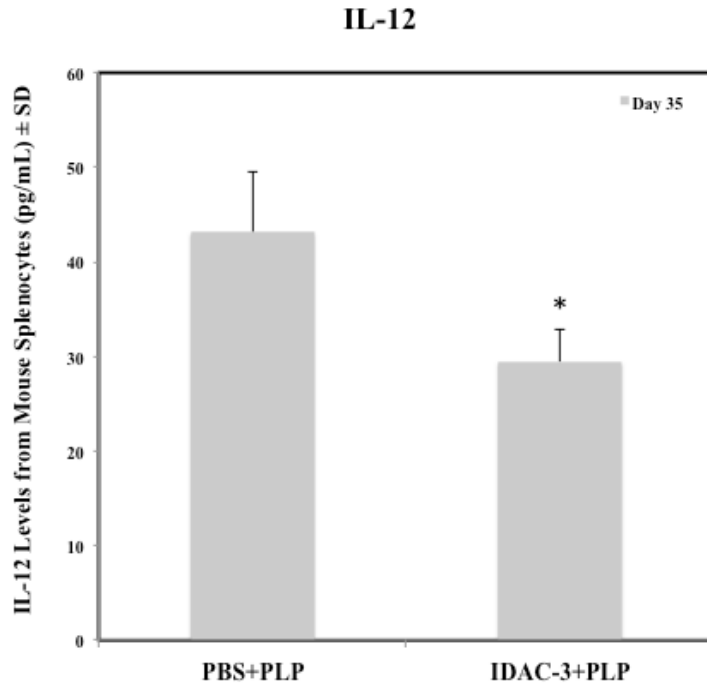


**Figure 2.6E** IL-12 levels (days 13 and 35) from splenocytes of mice treated subcutaneously with PBS and IDAC-3 (26 nmol on days 4 and 7). In the IDAC-3-treated group, the level of IL-12 was significantly lower than in the PBS-treated group on day 35 ( $p < 0.005$ ).

selectivity to ICAM-1 on the cell surface.<sup>14</sup> The expression of ICAM-1 is increased on cell surfaces in autoimmune diseases as well as in other diseases.<sup>15,16</sup>

Our current findings suggested that two injections (26 nmol/injection) of IDAC-3 with capped PLP peptide could suppress disease severity more efficiently than IDAC-1 with the uncapped PLP peptide. This corroborates a similar finding from our previous study in which capped Ac-PLP-BPI-NH<sub>2</sub>-2 peptide could suppress EAE better than its uncapped counterpart (PLP-BPI).<sup>7</sup> These results suggested that capped PLP peptide might have higher metabolic stability than the uncapped peptide; in other words, the uncapped peptide is prone to exopeptidases (i.e., amino- and carboxy-peptidases). Because SDS-PAGE, CD, and mass spectrometry analyses suggest that IDAC-1 and IDAC-3 are very similar, it is plausible that the major difference in their *in vivo* activity is due to the improved metabolic stability of the peptide and not due to the different conformation of the molecule.

IDAC-3 dosed subcutaneously on days 4 and 7 was very effective in suppressing EAE. One advantage of subcutaneous dosing is that IDAC molecules may drain into the lymph nodes to modulate immune cells.<sup>17,18</sup> The administration of IDAC-3 prior to the induction of disease had a significant long-term effect in suppressing disease relapse after 55 days compared to PBS, suggesting that IDAC-3 works by tipping the balance of the immune cells from inflammatory to regulatory phenotypes. It also suggested that vaccine-like delivery could alter the balance of the immune cells to regulatory cells prior to the stimulation of the disease. However, IDAC-3 had a narrow therapeutic index because the third injection of 26 nmol of IDAC-3 on day -5 in vaccine-like delivery caused adverse events in 2 of the 6 mice. A lower dose of vaccine-like subcutaneous injections of 10

nmol on days -11, -8, and -5 in a separate group did not result in anaphylaxis, but was not as effective as the 26 nmol dose. As controls, I-domain and the GMB-I-domain had slight delays of disease onset, but no significant suppression of disease; this activity was probably due to the general inhibition of LFA-1/ICAM-1-mediated leukocyte adhesion.<sup>11</sup> Thus, the effect of injections of IDAC-3 and I-domain on the differentiation of immune cells will be evaluated in the future. In addition, the effect of increasing the dose while maintaining the schedule of 2 injections as well as multiple injections (greater than 3 injections) at low doses (less than 10 nmol) by spreading the injection over a larger timespan will also be investigated.

During the peak severity of the disease on day 13, splenocytes isolated from the mice treated with PBS and IDAC-3 had similar levels of IL-17 production. However, on day 35, IDAC-3-treated mice were found to have significantly lower levels of IL-17 compared to the PBS group, indicating that IDAC-3 has long-term effects in suppressing EAE. Th17 is a major T cell found to play a large role in the pathogenesis of both EAE and MS.<sup>5,19-22</sup> Significant suppression of disease, coupled with lower levels of IL-17 on day 35, suggested that two injections of IDAC-3 suppressed the disease by modulating the immune system of the mice and shifting the response from an inflammatory to a regulatory phenotype. The higher level of IL-17 on day 35 in the mouse group treated with PBS may suggest an impending relapse of disease. This correlated with our previous observations in mice treated with Ac-PLP-BPI-NH<sub>2</sub>-2, suggesting the involvement of regulatory cells and the downregulation of Th17.<sup>7,9</sup>

While IL-10 levels were below detection limits on day 13, higher levels of IL-10 production were observed in mice treated with IDAC-3 compared to PBS on day 35,

indicating the potential involvement of T-reg cells. Previously, BPI-treated animals also produced IL-10 cytokine.<sup>8</sup> In addition, IDAC-3 induced IL-5, indicating the involvement of Th2 phenotype. A shift away from a Th1-response was observed from the involvement of lower levels of IL-2 in the IDAC-3-treated group compared to the PBS-treated mice. Furthermore, the lower levels of IL-12 in the IDAC-3-treated compared to PBS-treated mice imply that the IDAC-3 induced the differentiation away from a Th1-mediated response to a non-immunogenic response.

The potential mechanisms of action of IDAC-3 could be due to the delivery of the antigenic peptide to APC to alter the differentiation of naïve T cells to regulatory T cells and suppress the proliferation of inflammatory Th17 and Th1. As in BPI molecules, IDAC-3 could bind simultaneously to ICAM-1 and MHC-II to inhibit the formation of the immunological synapse at the interface between T cells and APC. By inhibiting the formation of the immunological synapse, the differentiation of T cells was shifted from inflammatory to immune-regulatory response. Previously, it was found that a BPI molecule (GAD-BPI) that suppressed type I diabetes could simultaneously bind to MHC-II and ICAM-1 and co-localize them on the surface of B cells isolated from the non-obese diabetic (NOD) mouse.<sup>10</sup>

Another possible mechanism by which IDAC could work is that the I-domain binds to ICAM-1 and the conjugate is internalized.<sup>11,23</sup> Previous studies had shown that the I-domain conjugated to fluorophores at the Lys residues could effectively bind to ICAM-1 and enter leukocytes by receptor-mediated endocytosis despite having a heterogeneous mixture.<sup>11,24</sup> The proposed mechanism is that IDAC-3 binds to ICAM-1 and suppresses the adequate leukocyte adhesion necessary to form a steady T cell:APC

contact. Once IDAC-3 is internalized into the APC cytoplasm, PLP is loaded onto the MHC-II in the Golgi apparatus and is transported to the cell surface for presentation, while the internalized ICAM-1 disappears from the cell surface.<sup>23</sup> Therefore, at the time the PLP-MHC-II-complex is presented at the surface of APC, the second signal (ICAM-1:LFA-1) necessary for T cell activation is absent, leading to T-reg differentiation.<sup>25,26</sup> However, the internalized ICAM-1 has been shown to recycle and resurface and, therefore, the absence of the second signal is transient.<sup>23</sup> Along the same line, another proposed mechanism is that IDAC-3, in the intracellular domain prior to recycling to the surface, could bind with empty MHC-II to form a complex of MHC-II/IDAC-3/ICAM-1 followed by presentation to the surface in a co-localized fashion. This co-localization prevents the formation of the immunological synapse. The efficacy of IDAC has been confirmed and now studies may be carried out to elucidate the potential mechanisms of action of IDAC molecules.

IDAC-3 is a mixture of conjugation products in which several lysine residues are conjugated with PLP peptide. The conditions of conjugation reaction have been optimized to maintain batch-to-batch reproducibility, as determined by mass spectrometry and CD. Using tryptic digest and mass spectrometry the sites of peptide conjugation were determined and the number of conjugations was found to be between one and five peptides per I-domain. Because IDAC-3 is a mixture, it is possible that not all of the conjugated products have biological activity to suppress EAE. In the future, several individual lysine residues will be mutated to cysteine residues (Cys-I-domain) for selective conjugation of peptides to a selected cysteine residue. It should be noted that the I-domain does not contain any cysteine residues. Thus, the resulting conjugate will be a

single conjugate instead of a mixture of conjugates. Then, the efficacy of each conjugated product may be evaluated in the EAE mouse model. This study will provide us with the important conjugation site(s) in the I-domain that produce biological activity.

## **2.5 CONCLUSIONS**

In conclusion, IDAC-3 effectively inhibited the onset and severity of EAE in mice. The conjugation of multiple copies of a single antigenic epitope to the I-domain of LFA-1 suppressed EAE by shifting the immune response to a regulatory phenotype. IDAC-3 also suppressed the relapse of EAE when delivered in a vaccine-like manner. Cytokine studies suggested that IDAC-3 suppressed disease by shifting the immune balance away from Th17-mediated pathology by increasing involvement of T-reg. Further studies using IDAC will involve optimizing the dose and the dosing strategy to lower toxicity and improve efficacy. Finally, the effect of epitope spreading will be addressed by conjugating other immunodominant epitopes, such as MOG and MBP, to the I-domain.

## 2.6 REFERENCES

- 1 Ascherio, A. & Munger, K. L. Environmental risk factors for multiple sclerosis. Part I: the role of infection. *Ann Neurol* **61**, 288-299 (2007).
- 2 Ascherio, A. *et al.* Epstein-Barr virus antibodies and risk of multiple sclerosis: a prospective study. *Jama* **286**, 3083-3088 (2001).
- 3 Bagert, B. A. Epstein-Barr virus in multiple sclerosis. *Curr Neurol Neurosci Rep* **9**, 405-410 (2009).
- 4 Brennan, R. M. *et al.* Strains of Epstein-Barr virus infecting multiple sclerosis patients. *Mult Scler* **16**, 643-651 (2010).
- 5 Fletcher, J. M., Lalor, S. J., Sweeney, C. M., Tubridy, N. & Mills, K. H. T cells in multiple sclerosis and experimental autoimmune encephalomyelitis. *Clin Exp Immunol* **162**, 1-11 (2010).
- 6 Manikwar, P., Kiptoo, P., Badawi, A. H., Buyuktimkin, B. & Siahhaan, T. J. Antigen-specific blocking of CD4-specific immunological synapse formation using BPI and current therapies for autoimmune diseases. *Med Res Rev* (2011).
- 7 Kobayashi, N. *et al.* Prophylactic and therapeutic suppression of experimental autoimmune encephalomyelitis by a novel bifunctional peptide inhibitor. *Clin Immunol* **129**, 69-79 (2008).
- 8 Kobayashi, N., Kobayashi, H., Gu, L., Malefyt, T. & Siahhaan, T. J. Antigen-specific suppression of experimental autoimmune encephalomyelitis by a novel bifunctional peptide inhibitor. *J Pharmacol Exp Ther* **322**, 879-886 (2007).

- 9      Ridwan, R. *et al.* Antigen-specific suppression of experimental autoimmune encephalomyelitis by a novel bifunctional peptide inhibitor: structure optimization and pharmacokinetics. *J Pharmacol Exp Ther* **332**, 1136-1145 (2010).
- 10     Murray, J. S. *et al.* Suppression of type 1 diabetes in NOD mice by bifunctional peptide inhibitor: modulation of the immunological synapse formation. *Chem Biol Drug Des* **70**, 227-236 (2007).
- 11     Manikwar, P. *et al.* Utilization of I-domain of LFA-1 to Target Drug and Marker Molecules to Leukocytes. *Theranostics* **1**, 277-289 (2011).
- 12     Zimmerman, T. *et al.* ICAM-1 peptide inhibitors of T-cell adhesion bind to the allosteric site of LFA-1. An NMR characterization. *Chem Biol Drug Des* **70**, 347-353 (2007).
- 13     Zhao, H., Kiptoo, P., Williams, T. D., Siahaan, T. J. & Topp, E. M. Immune response to controlled release of immunomodulating peptides in a murine experimental autoimmune encephalomyelitis (EAE) model. *J Control Release* **141**, 145-152 (2010).
- 14     Stanley, P. & Hogg, N. The I domain of integrin LFA-1 interacts with ICAM-1 domain 1 at residue Glu-34 but not Gln-73. *J Biol Chem* **273**, 3358-3362 (1998).
- 15     Lee, S. J. & Benveniste, E. N. Adhesion molecule expression and regulation on cells of the central nervous system. *J Neuroimmunol* **98**, 77-88 (1999).
- 16     Seidel, M. F., Keck, R. & Vetter, H. ICAM-1/LFA-1 expression in acute osteodestructive joint lesions in collagen-induced arthritis in rats. *J Histochem Cytochem* **45**, 1247-1253 (1997).



- 17 Supersaxo, A., Hein, W., Gallati, H. & Steffen, H. Recombinant human interferon alpha-2a: delivery to lymphoid tissue by selected modes of application. *Pharm Res* **5**, 472-476 (1988).
- 18 Supersaxo, A., Hein, W. R. & Steffen, H. Effect of molecular weight on the lymphatic absorption of water-soluble compounds following subcutaneous administration. *Pharm Res* **7**, 167-169 (1990).
- 19 Annunziato, F., Cosmi, L. & Romagnani, S. Human and murine Th17. *Curr Opin HIV AIDS* **5**, 114-119 (2010).
- 20 Bruno, V., Battaglia, G. & Nicoletti, F. The advent of monoclonal antibodies in the treatment of chronic autoimmune diseases. *Neurol Sci* **31 Suppl 3**, 283-288 (2011).
- 21 El-behi, M., Rostami, A. & Ciric, B. Current views on the roles of Th1 and Th17 cells in experimental autoimmune encephalomyelitis. *J Neuroimmune Pharmacol* **5**, 189-197 (2010).
- 22 Haak, S. *et al.* IL-17A and IL-17F do not contribute vitally to autoimmune neuroinflammation in mice. *J Clin Invest* **119**, 61-69 (2009).
- 23 Muro, S., Gajewski, C., Koval, M. & Muzykantov, V. R. ICAM-1 recycling in endothelial cells: a novel pathway for sustained intracellular delivery and prolonged effects of drugs. *Blood* **105**, 650-658 (2005).
- 24 Manikwar, P., Zimmerman, T., Blanco, F. J., Williams, T. D. & Siahaan, T. J. Rapid Identification of Fluorochrome Modification Sites in Proteins by LC ESI-Q-TOF Mass Spectrometry. *Bioconjug Chem* **22**, 1330-1336 (2011).

- 25 Larche, M. & Wraith, D. C. Peptide-based therapeutic vaccines for allergic and autoimmune diseases. *Nat Med* **11**, S69-76 (2005).
- 26 Wraith, D. C. Therapeutic peptide vaccines for treatment of autoimmune diseases. *Immunol Lett* **122**, 134-136 (2009).

## **CHAPTER 3**

**Vaccine-like controlled-release delivery of an immunomodulating peptide to treat  
experimental autoimmune encephalomyelitis**

### 3.1 INTRODUCTION

During the course of multiple sclerosis (MS), the myelin sheath surrounding the nerves becomes demyelinated, exposing multiple proteins that are processed and presented on the surface of antigen-presenting cells (APC).<sup>1</sup> The immunodominant epitopes from the myelin sheath that are presented on the surface of major histocompatibility complex class II (MHC-II) include the proteolipid protein (PLP), myelin oligodendrocyte glycoprotein (MOG), and myelin basic protein (MBP).<sup>2</sup> Modulating the immune response is the goal of many of the available therapies for MS.<sup>3</sup> Many of the current treatments fall short because they suppress the general immune system.<sup>4</sup> In contrast, bifunctional peptide inhibitors (BPI) are molecules that provide a more selective approach in modulating the immune response by modifying the response of a sub-population of T cells. BPI is a peptide complex in which two functional peptides are tethered together by a linker. The hypothesis is that the antigenic peptide and the adhesion peptide of the BPI simultaneously bind to MHC-II and ICAM-1 on the surface of antigen-presenting cells (APC) suppressing the translocation of signal-1 (MHC-II:T cell interaction) and signal-2 (ICAM-1:LFA-1 interaction) molecules necessary for the formation of the immunological synapse, thereby suppressing T cell activation.<sup>5,6</sup>

PLP-BPI molecule has been shown to suppress experimental autoimmune encephalomyelitis (EAE) in the mouse model when injected three times in solution in a vaccine-like manner 11, 8, and 5 days prior to disease stimulation. Although we have had success with this treatment in suppressing EAE, translating this into a human model must be simplified. Studies have shown that compliance is an important factor in achieving success in multi-dose vaccinations.<sup>7</sup> A one-time injection is ideal for achieving a higher

degree of compliance. Therefore, it will be beneficial if PLP-BPI can be delivered in a controlled-release manner using a one-time injection. Previously, there have been very few successful applications of protein and peptide controlled-release therapies.<sup>13,14</sup> Because nanoparticles containing alginate and chitosan have been shown to be effective for delivering protein antigen and can stabilize ovalbumin, we decided to utilize these polysaccharides to deliver a therapeutic peptide to suppress EAE.<sup>15</sup> Poly(D,L-lactic-co-glycolic acid) (PLGA) is a well-established biocompatible and biodegradable polymer.<sup>16</sup> Therefore, chitosan and alginate, along with PLGA, were used to deliver PLP-BPI for treating EAE in a vaccine-like manner.

Here, a PLP-BPI molecule called Ac-PLP-BPI-NH<sub>2</sub> was formulated into alginate-PLGA/chitosan-PLGA colloidal gels for the controlled-release delivery of peptide in a vaccine-like manner. In this study, the efficacy of Ac-PLP-BPI-NH<sub>2</sub> released from colloidal gel to suppress EAE after a single injection was evaluated, and its long-term effect in suppressing EAE was also monitored. The results indicated that vaccine-like injection of Ac-PLP-BPI-NH<sub>2</sub>-2 in colloidal gel was very effective in suppressing EAE as well as the relapse of EAE in the mouse model. The mechanism of suppression was due to the shift in the immune response away from Th17-mediated pathology of EAE.

## **3.2 MATERIALS AND METHODS**

### **3.2.1 Materials**

PLGA (50:50) (Polymer Type: 5050 DLG 2A, inherent viscosity: 0.15–0.25 dl/g) was purchased from Lakeshore Biomaterials (Birmingham, AL). Low molecular weight chitosan was purchased from Sigma Aldrich Co. (St. Louis, MO) (448869, degree of

deacetylation: 75%–85%, Brookfield viscosity: 20–200 cps). Sodium alginate ( $M_v = 1.6 \times 10^5$ , dynamic viscosity was 39 MPa·s in a 1.0% solution at 20 °C) was obtained from FMC BioPolymer (Philadelphia, PA).

### 3.2.2 Animals

The female SJL/J mice used in this study were purchased from Charles River Laboratories, Inc. (Wilmington, MA) and were housed under specific pathogen-free conditions at the animal facility at The University of Kansas approved by the Association for Assessment and Accreditation of Laboratory Animal Care (AAALAC). All experimental procedures used in this study were approved protocols reviewed by the Institutional Animal Care and Use Committee (IACUC) at The University of Kansas.

### 3.2.3 Peptide Synthesis

PLP (NH<sub>2</sub>-HSLGKWLGHDPKF-OH) and Ac-PLP-BPI-NH<sub>2</sub>-2 (Ac-HSLGKWLGHDPKF-(AcpGAcpGAcp)<sub>2</sub>-ITDGEATDSG-NH<sub>2</sub> (Ac = acetyl, Acp = aminocaproic acid)) were synthesized using a 9-fluorenylmethyloxycarbonyl- (Fmoc) protected solid-phase peptide chemistry on appropriate polyethylene glycol-polystyrene resins on an automated peptide synthesizer (Pioneer; Perceptive Biosystems, Framingham, MA). Trifluoroacetic acid (TFA) with scavengers was used to remove the amino acid protecting groups as well as the peptides from the resin. A semi-preparative reversed-phase high-performance liquid chromatography (RP-HPLC) with a C18 column was used to purify the crude peptides. A gradient method was used for purification with solvent A (94.9% water, 5% acetonitrile, and 0.1% trifluoroacetic acid) and solvent B (100%

acetonitrile). The purity of the peptide was analyzed by analytical RP-HPLC using a C18 column (purity > 96%). The identity of the peptides was confirmed using matrix-assisted laser desorption/ionization time-of-flight (MALDI-TOF) mass spectrometry.

### **3.2.4 Preparation of Charged PLGA Nanoparticles**

Oppositely charged blank PLGA nanoparticles were prepared by a solvent diffusion method. 150 mg of PLGA was dissolved in 10 ml of acetone and then the solution was added into 0.2% of either alginate or chitosan (150 ml) surfactant solution through a syringe pump at a constant rate of 30 ml/h under stirring at 200 rpm. The resulting solution was stirred overnight to evaporate the acetone. Nanoparticles were then centrifuged (10,000 rpm) for 30 min and the resulting PLGA pellet was resuspended in double-distilled water and washed three times to remove excess surfactant. The final resuspended product was then lyophilized for two days.

### **3.2.5 Preparation of Peptide-loaded Colloidal Gels**

Lyophilized nanoparticles (PLGA-alginate or PLGA-chitosan) were dispersed in deionized water at 20% weight/volume followed by mixing of the two dispersions in a 1:1 ratio; then, the mixture was sonicated for 3 minutes to prepare a homogenous colloid mixture. Immediately before injecting into mice, Ac-PLP-BPI-NH<sub>2</sub>-2 peptide was physically mixed for 2 min with the colloidal gel in a 1:10 ratio of peptide to PLGA.

### **3.2.6 Characterization of Nanoparticles and Colloidal Gels**

The zeta potentials and the sizes of PLGA-alginate and PLGA-chitosan nanoparticles were determined in triplicate using dynamic light scattering (Brookhaven, ZetaPALS). Scanning electron microscopy (SEM) was performed using a Leo 1550 field emission scanning electron microscope at an accelerating voltage of 5 kV.

### **3.2.7 *In Vitro* Peptide Release from Colloidal Gel**

Peptide release from colloidal gel formulation was measured fluorometrically at excitation  $\lambda=280$  nm and emission  $\lambda=350$  nm with a Shimadzu RF5000U spectrofluorophotometer (Shimadzu Co., Kyoto, Japan). Colloidal gel samples containing Ac-PLP-BPI-NH<sub>2</sub>-2 (n = 3) were placed in a sealed 1.5 ml buffered solution (PBS, pH 7.4) and stirred at 50 rpm at 37 °C. Samples containing the peptide were removed at different time points after centrifugation and replaced with fresh buffer. The concentrations of the peptide were determined using fluorescence spectroscopy as described above.

### **3.2.8 Induction of EAE and Efficacy Evaluations**

Six-to-eight week old mice were immunized subcutaneously (s.c.) on day 0 with 200  $\mu$ g PLP<sub>139-151</sub> peptide in a 0.2 ml emulsion consisting of equal volumes of PBS and complete Freund's adjuvant (CFA) containing killed *mycobacterium tuberculosis* strain H37RA (at a final concentration of 4 mg/ml, Difco, Detroit, MI) to induce disease. The emulsion of PLP/CFA was administered to the regions above the shoulder and the flanks (50  $\mu$ l at each injection site, for a total of 4 injections). Additionally, 200 ng of pertussis toxin was administered intraperitoneally on days 0 and 2.



As a positive control, mice received three s.c. injections of Ac-PLP-BPI-NH<sub>2</sub>-2 in PBS (100 nmol/injection) at 11, 8, and 5 days prior to stimulation of the disease on day 0. Then, Ac-PLP-BPI-NH<sub>2</sub>-2 (300 nmol) in colloidal gel (Ac-PLP-BPI-NH<sub>2</sub>-2-NP) was injected once via the s.c. route 5 days before induction of the disease on day 0. To determine the effects of the timing of the dose, a different group of mice was treated with one s.c. injection of Ac-PLP-BPI-NH<sub>2</sub>-2-NP at day 4 after disease stimulation on day 0. To determine the ability of the Ac-PLP-BPI-NH<sub>2</sub>-2-NP treatment to suppress the relapse of EAE, another group was treated on day 30, after the disease went into remission. As negative controls, two different groups of mice received either PBS on days -11, -8, and -5, or blank colloidal gel (blank-NP) on day -5 prior to disease induction.

Disease progression was evaluated by observing the change in body weight of the mice and clinical scoring: 0—no clinical symptoms of disease; 1—tail weakness or limp tail; 2—paraparesis (weakness or partial paralysis of one or two hind limbs); 3—paraplegia (complete paralysis of two hind limbs); 4—paraplegia with forelimb weakness or paralysis; 5—moribund. When the mice were found to be moribund, they were promptly euthanized.

### **3.2.9 Determination of Cytokine Levels *In Vitro***

Spleens from representative mice treated with Ac-PLP-BPI-NH<sub>2</sub>-2, Ac-PLP-BPI-NH<sub>2</sub>-2-NP, and blank-NP were isolated during the peak of the relapse, on day 55. The spleen was gently smashed using the coarse end of a 1 ml syringe in a petri dish containing RPMI 1640 medium (10% FBS, 0.05 M BME) to yield the splenocytes of interest. The splenocytes were then filtered through a nylon 40 micrometer strainer. After

centrifugation, “ACK lysis buffer” containing 0.15 M NH<sub>4</sub>Cl, 10 mM KHCO<sub>3</sub>, and 0.1 mM EDTA was used to lyse the red blood cells followed by washing of the remaining white blood cells with medium.  $5 \times 10^6$  splenocytes/ml were cultured in parallel in the presence of 20 μM PLP and blank RPMI medium. Supernatants were collected at a 72 h time-point for the measurement of cytokine levels and stored at -80 °C until analysis. The samples were then analyzed using a fully quantitative ELISA-based Q-Plex™ Mouse Cytokine-Screen (Quansys Biosciences, Logan, UT).

### **3.2.10 Statistical Analysis**

Statistical differences among the groups in clinical disease scores were determined by calculating the average score for each mouse from day 12 to day 17, or from day 45 to day 55 by one-way analysis of variance followed by Fisher’s least significant difference. Statistical differences in body weight among groups were also analyzed in the same fashion, but from day 12 to day 24. Comparison of cytokine concentrations was also performed by one-way analysis of variance. All analyses were performed using StatView (SAS Institute, Cary, NC).

## **3.3 RESULTS**

### **3.3.1 Characterization of Coated Nanoparticles and Colloidal Gel**

Coated nanoparticles were prepared by a solvent diffusion method where PLGA in acetone was titrated into an alginate- or chitosan-containing water phase. Once in the water phase, PLGA was precipitated and coated with either a negatively charged (alginate) or a positively charged (chitosan) polysaccharide. Mixing these two particle

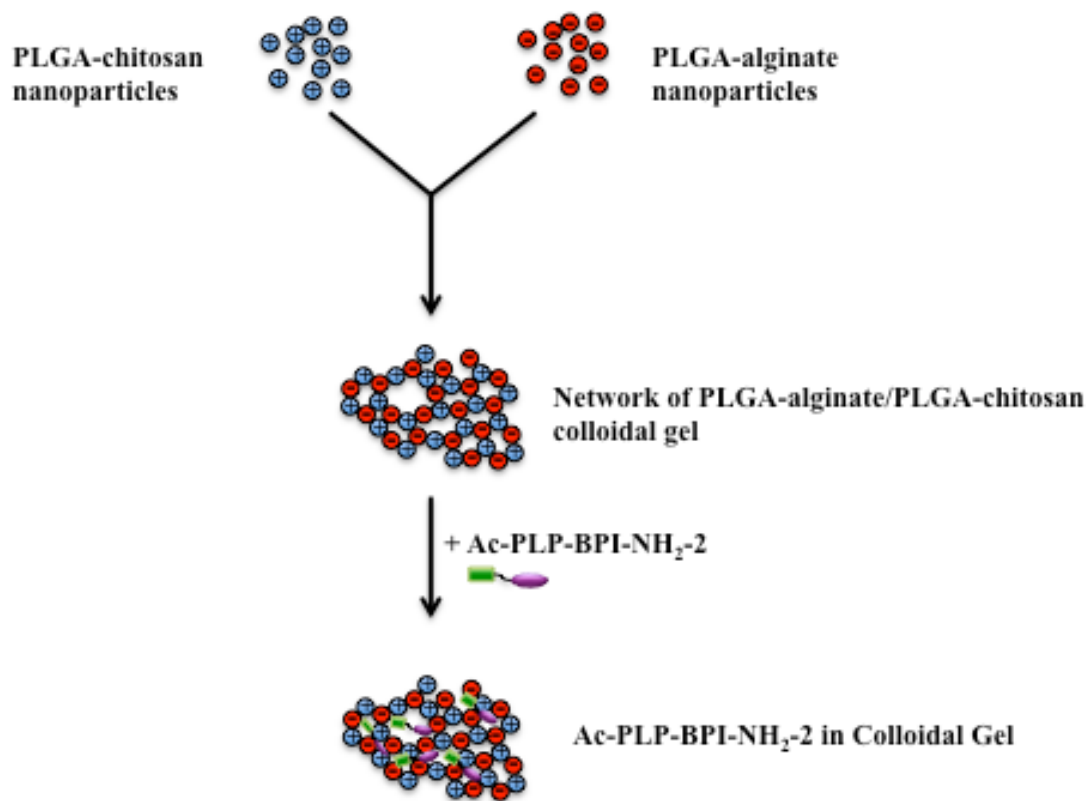
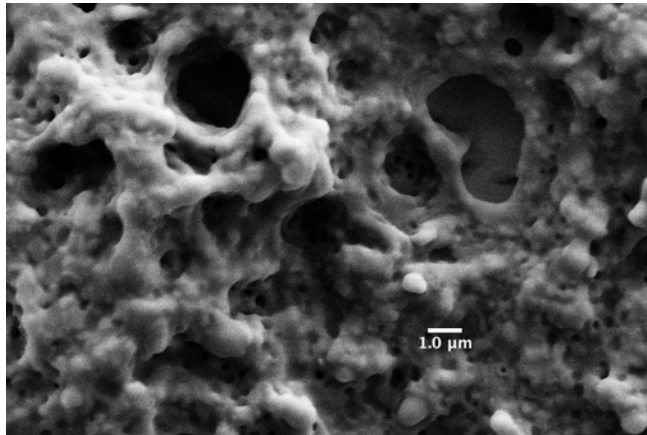


**Figure 3.1:** Scheme of positively and negatively charged PLGA nanoparticle fabrication to form peptide-loaded colloidal gel.

A)



B)

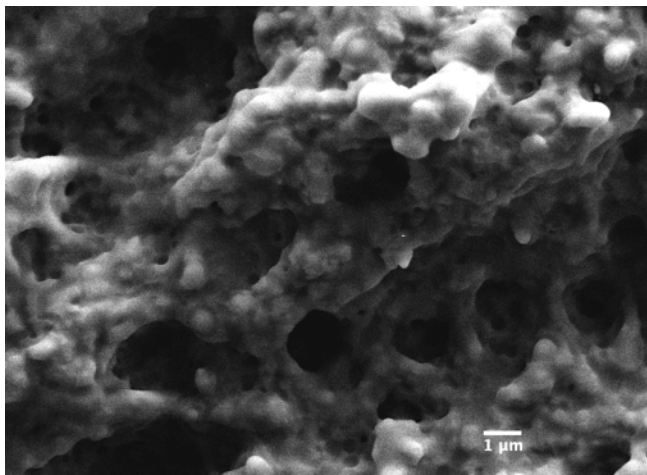


**Figure 3.2:** Scanning electron micrographs of (A) blank colloidal gel, and (B) Ac-PLP-BPI-NH<sub>2</sub>-2-loaded colloidal gel. Scale bar is 1 μm.

types together leads to the self-assembly of dense colloidal gels (**Fig. 3.1**). The size of the chitosan-PLGA was  $400.1 \pm 13.9$  nm (polydispersity = 0.092), whereas the alginate-PLGA size was  $208.1 \pm 7.6$  nm (polydispersity = 0.111). The zeta potentials of alginate-PLGA and chitosan-PLGA were found to be  $-38.85 \pm 1.54$  mV and  $23.79 \pm 2.16$  mV, respectively. Using scanning electron microscopy, no differences were observed between the structure of the dried blank colloidal gel and dried Ac-PLP-BPI-NH<sub>2</sub>-2-loaded colloidal gel (**Fig. 3.2A** and **3.2B**). Both images suggested a tightly packed colloidal gel formed by the interacting chitosan-alginate nanoparticles.

### **3.3.2 *In Vitro* Peptide Release from Colloidal Gel**

The *in vitro* peptide release into PBS medium from colloidal gels was measured by detection of fluorescence emission of the tryptophan and phenylalanine side chains in Ac-PLP-BPI-NH<sub>2</sub>-2 (**Fig. 3.3**). Initially, approximately 24% of the peptide was released within the first two hours; this was most likely due to the rapid release of peptide from the surface of the colloidal gel. It was followed by a relatively less pronounced release over a period of 24 hours (~ 64%). Eventually, the amount of peptide released plateaued after day 1, suggesting that the remaining peptide diffused through the gel network into the solution.

### **3.3.3 Efficacy of Ac-PLP-BPI-NH<sub>2</sub>-2 in Colloidal Gel for Suppression of EAE**

Previously, EAE could be suppressed in mice by administering Ac-PLP-BPI-NH<sub>2</sub>-2 in buffered solution (i.v. or s.c.) on days 4, 7, and 10, or a one-time injection of Ac-PLP-BPI-NH<sub>2</sub>-2-loaded microparticles (s.c.) on day 4. Here,

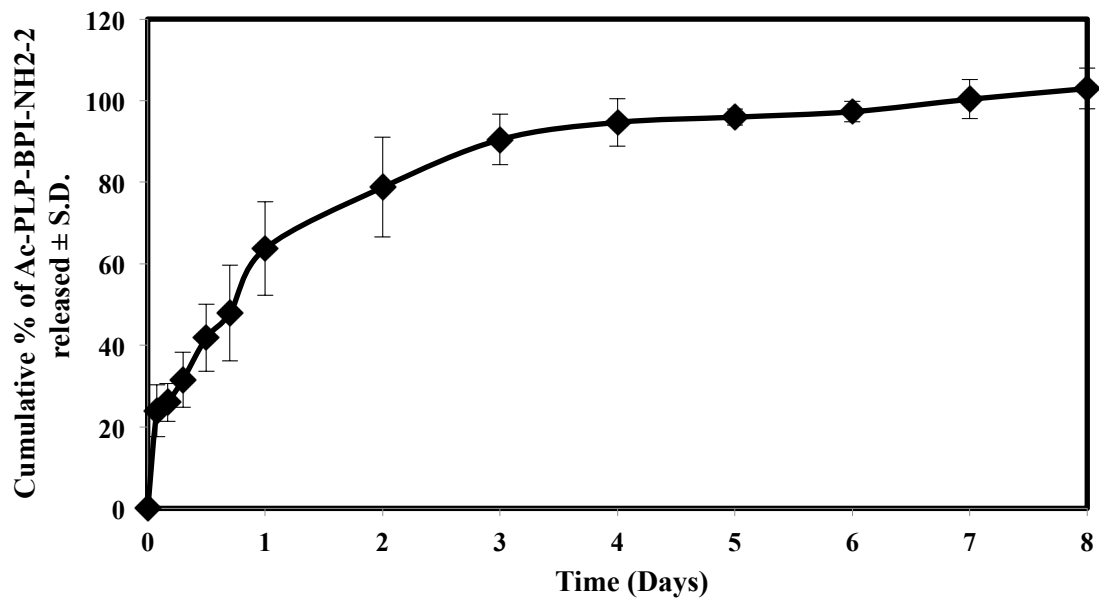


**Figure 3.3:** *In vitro* release of Ac-PLP-BPI-NH<sub>2</sub>-2 from colloidal gel (in PBS solution, 37 °C, 50 rpm stirring). n = 3 ± S.D.

Ac-PLP-BPI-NH<sub>2</sub>-2-NP was used for one-time delivery of the peptide to suppress EAE. Three groups of mice received subcutaneous injections of the peptide-loaded colloidal gel (300 nmol/injection) on day -5, day 4, or day 30 (**Fig. 3.4**). The mice treated with Ac-PLP-BPI-NH<sub>2</sub>-2-NP five days prior to (day -5) or four days after (day 4) the induction of disease had significantly lower clinical scores compared to control, PBS, or blank-NP ( $p < 0.01$ , through days 12–17) (**Fig. 3.4A**). Furthermore, the changes in body weight were significantly less than in the control groups, suggesting that treating mice with Ac-PLP-BPI-NH<sub>2</sub>-2-NP prior to the onset of disease is significantly more effective than treatment with PBS or blank-NP in suppressing disease ( $p < 0.01$ , through days 12–24) (**Fig. 3.4B**). Although the group that received the peptide-loaded gel formulation on day 4 got sick faster, their recovery was quicker than that of the control groups, and the amount of body weight lost was similar to that of the Ac-PLP-BPI-NH<sub>2</sub>-2-NP (-5) group by day 15 (**Fig. 3.4A and 3.4B**). Compared to PBS and the blank colloidal gel control groups, a delay in the onset of disease was apparent in the mice groups treated with Ac-PLP-BPI-NH<sub>2</sub>-2-NP on day -5 (**Fig. 3.4C**).

When observing the long-term effect of suppressing the relapse of disease, it was noted that Ac-PLP-BPI-NH<sub>2</sub>-2-NP (-5) could suppress disease significantly better than the controls and there was no significant difference when compared to the positive control ( $p > 0.05$ , through days 45–55) (**Fig. 3.4A**). Ac-PLP-BPI-NH<sub>2</sub>-2-NP, when administered 4 days after the induction of disease, could suppress disease significantly better than the controls ( $p < 0.0001$ , through days 45–55) (**Fig. 3.4A**).

To test the efficacy of Ac-PLP-BPI-NH<sub>2</sub>-2-NP to suppress relapse, another group of mice was administered the peptide-loaded colloidal gel on day 30. It was observed that

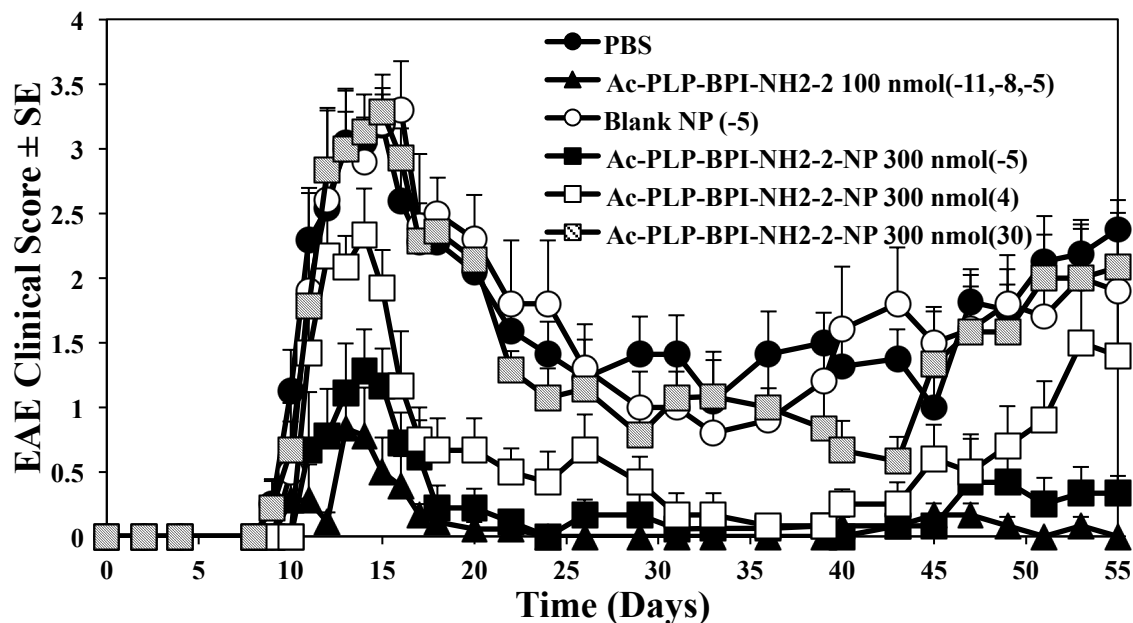


**Figure 3.4A:** Comparison of the *in vivo* activity of Ac-PLP-BPI-NH<sub>2</sub>-2 in solution, Ac-PLP-BPI-NH<sub>2</sub>-2-NP, blank colloidal gel, and PBS using clinical disease scores. In the controlled-release treatments, different groups of SJL/J mice received a one-time injection of 300 nmol peptide-gel formulation on days -5, 4, or 30. Mice were also treated with a one-time injection of blank colloidal gel 5 days prior to the induction of disease. The positive control group (Ac-PLP-BPI-NH<sub>2</sub>-2, 100 nmol/injection) was treated on days -11, -8, and -5. The mice group receiving PBS was also injected on days -11, -8, and -5. The mice treated with Ac-PLP-BPI-NH<sub>2</sub>-2-NP on day -5 and day 4 had significantly lower clinical scores compared to negative control, PBS, or blank-NP ( $p < 0.01$ , through days 12–17, and  $p < 0.0001$ , through days 45–55). No significant difference was observed between Ac-PLP-BPI-NH<sub>2</sub>-2-NP (-5) and the positive control ( $p > 0.05$ , through days 45–55). No significant difference in clinical scores was observed when comparing the mice treated with Ac-PLP-BPI-NH<sub>2</sub>-2-NP on day 30 to negative controls ( $p > 0.05$ , through days 45–55). The results are expressed as the mean  $\pm$  S.E. ( $n \geq 6$ ).



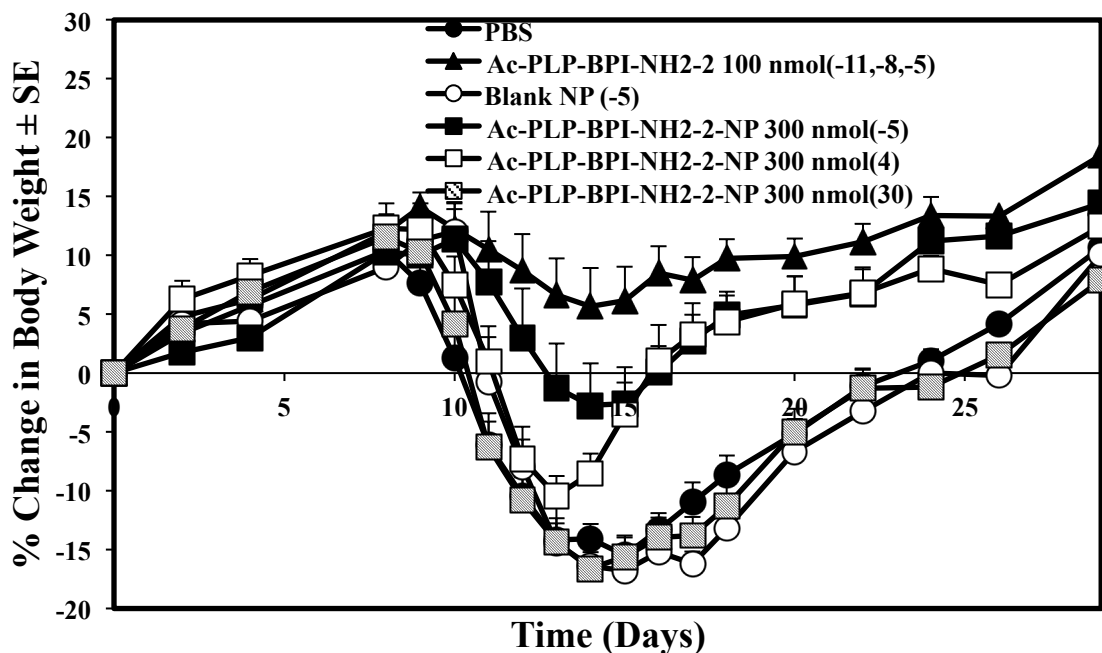


**Figure 3.4B:** Comparison of the *in vivo* activity of Ac-PLP-BPI-NH<sub>2</sub>-2 in solution, Ac-PLP-BPI-NH<sub>2</sub>-2-NP, blank colloidal gel, and PBS using change in body weight. In the controlled-release treatments, different groups of SJL/J mice received a one-time injection of 300 nmol peptide-gel formulation on days -5, 4, or 30. Mice were also treated with a one-time injection of blank colloidal gel 5 days prior to the induction of disease. The positive control group (Ac-PLP-BPI-NH<sub>2</sub>-2, 100 nmol/injection) was treated on days -11, -8, and -5. The mice group receiving PBS was also injected on days -11, -8, and -5. The mice treated with Ac-PLP-BPI-NH<sub>2</sub>-2-NP on day -5 and day 4 had significantly less changes in body weight compared to PBS, or blank-NP ( $p < 0.01$ , through days 12–24). The results are expressed as the mean  $\pm$  S.E. ( $n \geq 6$ ).

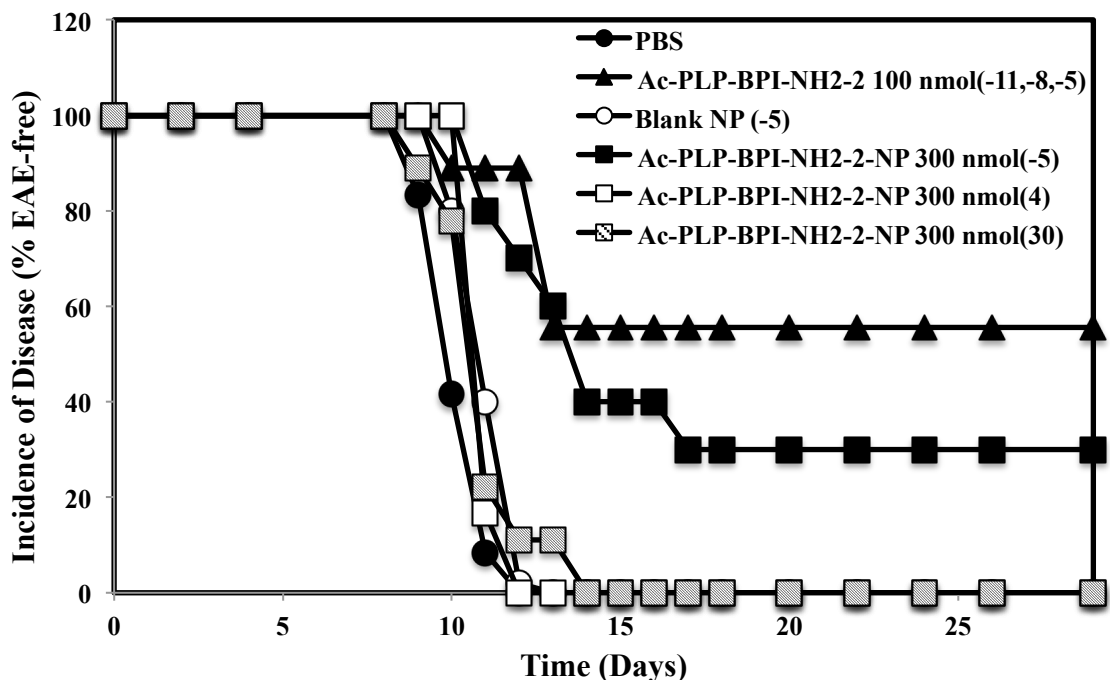


**Figure 3.4C:** Comparison of the *in vivo* activity of Ac-PLP-BPI-NH<sub>2</sub>-2 in solution, Ac-PLP-BPI-NH<sub>2</sub>-2-NP, blank colloidal gel, and PBS using incidence of disease. In the controlled-release treatments, different groups of SJL/J mice received a one-time injection of 300 nmol peptide-gel formulation on days -5, 4, or 30. Mice were also treated with a one-time injection of blank colloidal gel 5 days prior to the induction of disease. The positive control group (Ac-PLP-BPI-NH<sub>2</sub>-2, 100 nmol/injection) was treated on days -11, -8, and -5. The mice group receiving PBS was also injected on days -11, -8, and -5. Compared to PBS and the blank colloidal gel control groups, a delay in the onset of disease was apparent in the mice group treated with Ac-PLP-BPI-NH<sub>2</sub>-2-NP on day -5. The results are expressed as the mean  $\pm$  S.E. (n  $\geq$  6).

the mice showed signs of recovery with a decreasing clinical score but, upon the time of the relapse of disease (after day 43), no significant difference in clinical scores was observed when compared to the negative controls ( $p > 0.05$ , through days 45–55) (**Fig. 3.4A**).

### **3.3.4 *In Vitro* Cytokine Production**

To examine the cytokines produced in response to the different treatments, spleens from three different groups (Ac-PLP-BPI-NH<sub>2</sub>-2, Ac-PLP-BPI-NH<sub>2</sub>-2-NP, and blank-NP) were isolated on day 55 and observed for their response to PLP stimulation. The interactions of many different cytokines are complicated, and the ability to determine the role for an individual cytokine is not straightforward. However, one can generalize cytokines into different effector groups. The cytokines that are generally produced during an inflammatory response include IL-6, IL-17, and IFN $\gamma$  whereas the cytokines that induce suppressor and regulatory responses include IL-2, IL-4, and IL-5.

Mice treated with solution Ac-PLP-BPI-NH<sub>2</sub>-2 and Ac-PLP-BPI-NH<sub>2</sub>-2-NP were observed to have significantly lower levels of IL-6, IL-17, and IFN $\gamma$ , suggesting that both formulations were effectively suppressing disease by shifting the immune response away from Th17 production (**Fig. 3.5A-C**,  $p < 0.05$ ). It was interesting to observe that IL-6 and IFN $\gamma$  levels were significantly lower for the Ac-PLP-BPI-NH<sub>2</sub>-2-NP formulation group than the group treated with solution Ac-PLP-BPI-NH<sub>2</sub>-2 ( $p < 0.005$ ).

Compared to the blank-NP group, IL-2 levels were significantly higher for the Ac-PLP-BPI-NH<sub>2</sub>-2 treated mice ( $p < 0.05$ ) whereas no significant difference was observed between the peptide-loaded gel and the blank colloidal gel ( $p > 0.05$ ) (**Fig.**

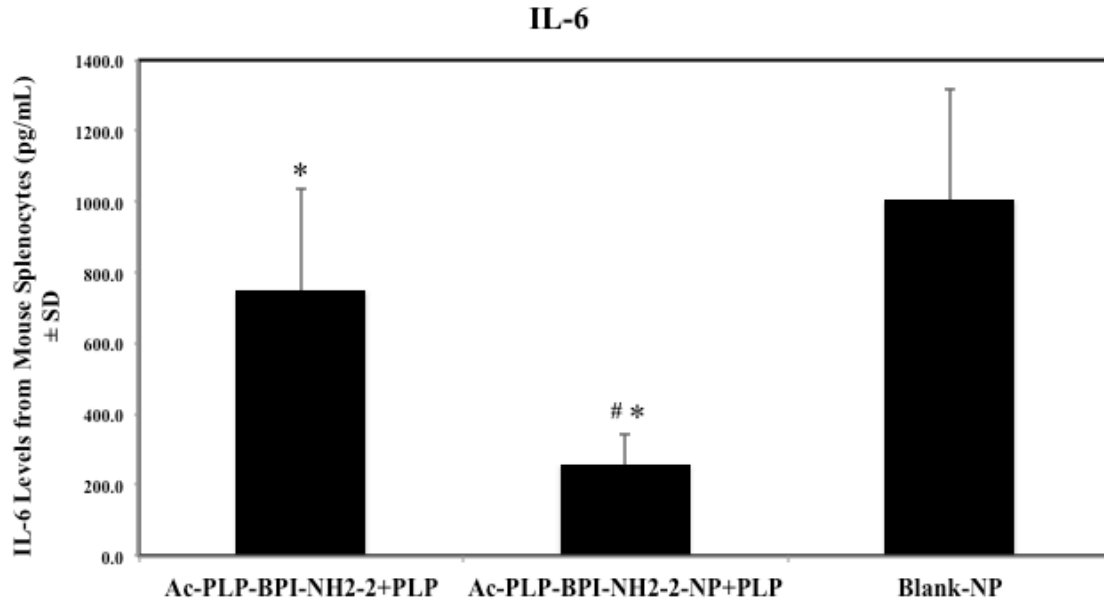


**Figure 3.5A:** Cytokine levels (day 55) from splenocytes of mice treated subcutaneously with solution Ac-PLP-BPI-NH<sub>2</sub>-2, Ac-PLP-BPI-NH<sub>2</sub>-2-NP, or PBS. In the Ac-PLP-BPI-NH<sub>2</sub>-2-NP-treated group, IL-6 cytokine levels were significantly lower than in the groups treated with Ac-PLP-BPI-NH<sub>2</sub>-2 (#,  $p < 0.005$ ) and PBS (\*,  $p < 0.05$ ).

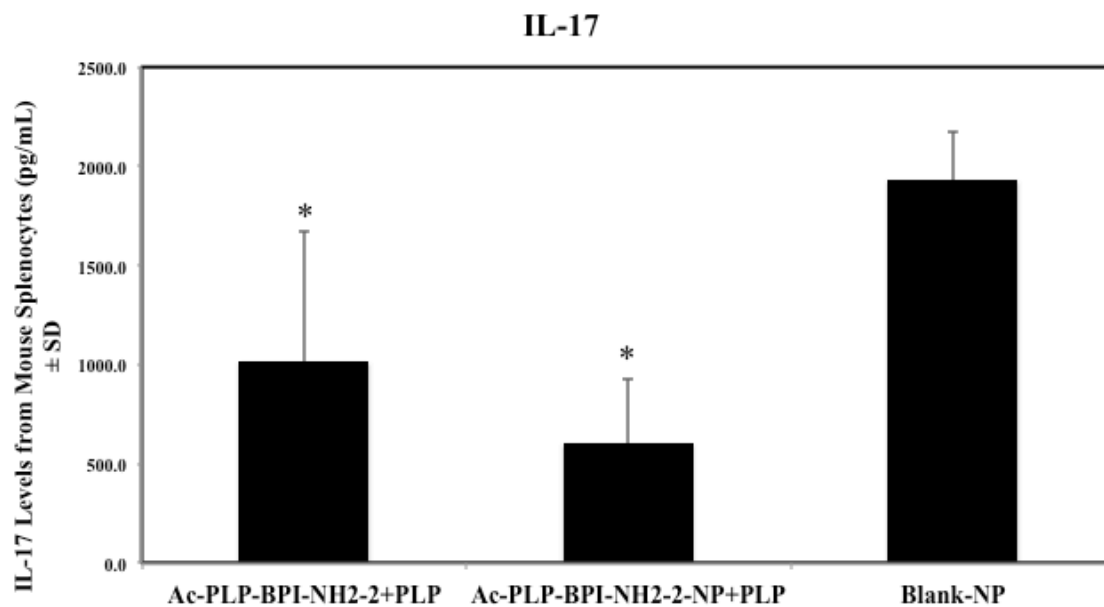


**Figure 3.5B:** Cytokine levels (day 55) from splenocytes of mice treated subcutaneously with solution Ac-PLP-BPI-NH<sub>2</sub>-2, Ac-PLP-BPI-NH<sub>2</sub>-2-NP, or PBS. In the Ac-PLP-BPI-NH<sub>2</sub>-2- and Ac-PLP-BPI-NH<sub>2</sub>-2-NP-treated groups, IL-17 cytokine levels were significantly lower than in the group treated PBS (\*,  $p < 0.05$ ).

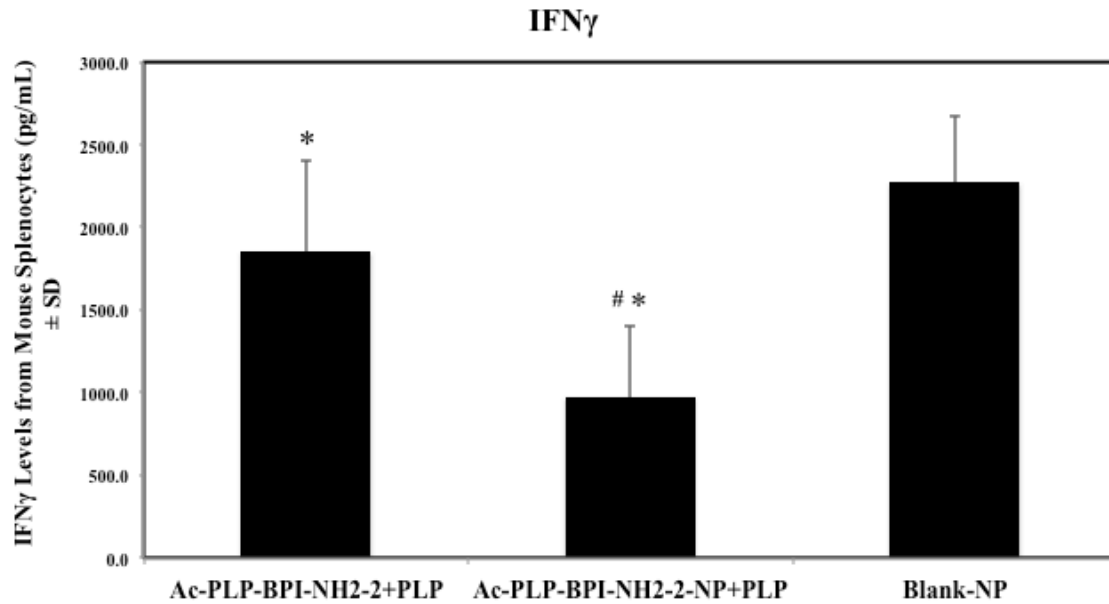


**Figure 3.5C:** Cytokine levels (day 55) from splenocytes of mice treated subcutaneously with solution Ac-PLP-BPI-NH<sub>2</sub>-2, Ac-PLP-BPI-NH<sub>2</sub>-2-NP, or PBS. In the Ac-PLP-BPI-NH<sub>2</sub>-2-NP-treated group, IFN $\gamma$  cytokine levels were significantly lower than in the groups treated with Ac-PLP-BPI-NH<sub>2</sub>-2 (#,  $p < 0.005$ ) and PBS (\*,  $p < 0.05$ ).

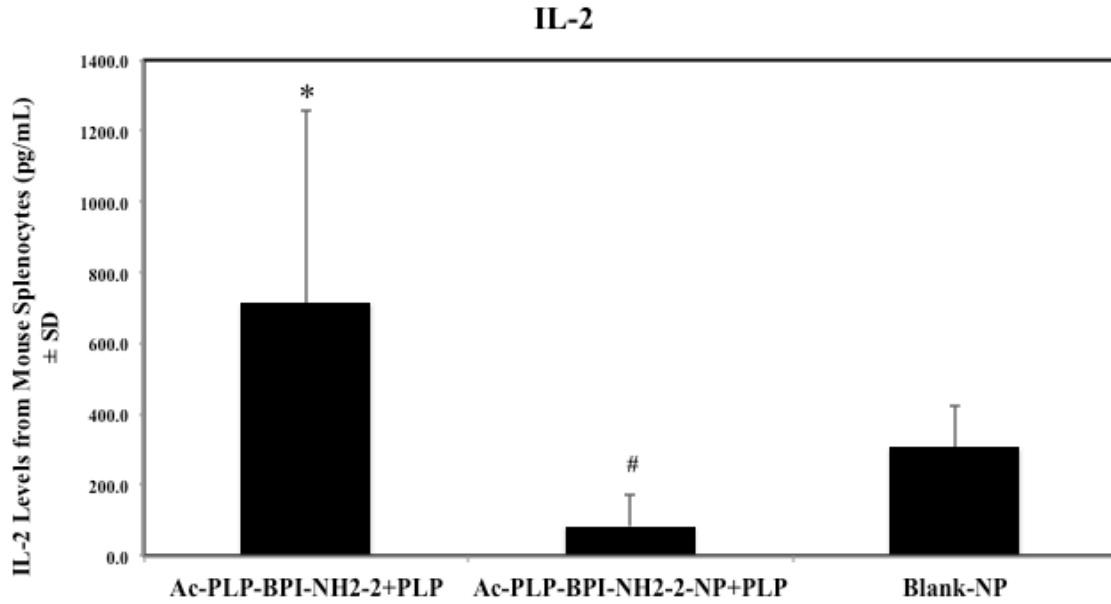


**Figure 3.5D:** Cytokine levels (day 55) from splenocytes of mice treated subcutaneously with solution Ac-PLP-BPI-NH<sub>2</sub>-2, Ac-PLP-BPI-NH<sub>2</sub>-2-NP, or PBS. In the Ac-PLP-BPI-NH<sub>2</sub>-2-NP-treated group, IL-2 cytokine levels were significantly lower than in the group treated with Ac-PLP-BPI-NH<sub>2</sub>-2 (#,  $p < 0.0005$ ). On the other hand, IL-2 production was higher in the Ac-PLP-BPI-NH<sub>2</sub>-2-treated group than in the negative control ( $p < 0.05$ ).

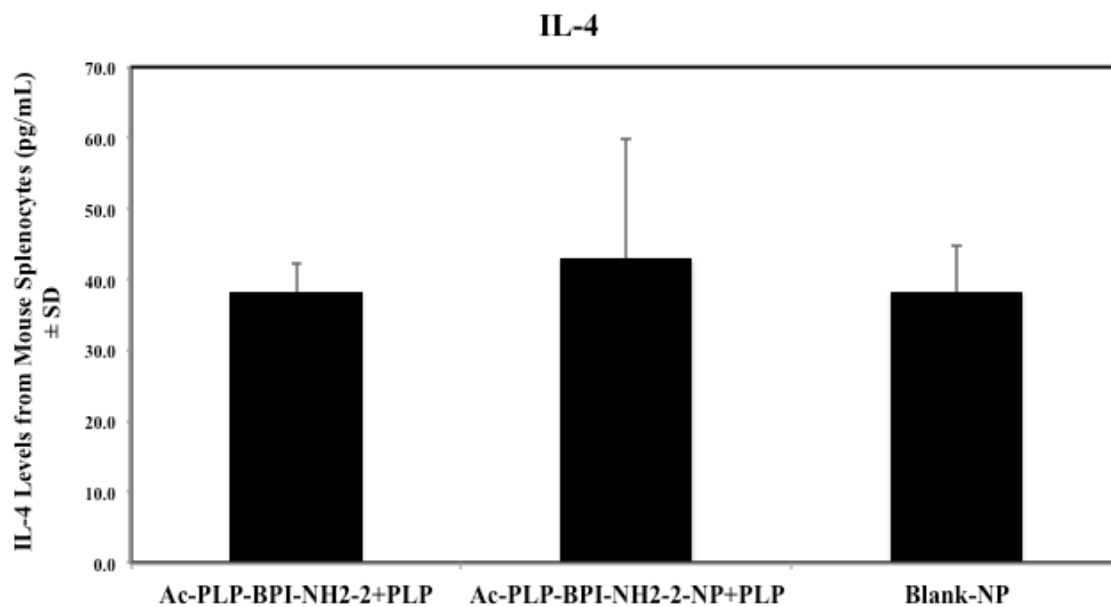


**Figure 3.5E:** Cytokine levels (day 55) from splenocytes of mice treated subcutaneously with solution Ac-PLP-BPI-NH<sub>2</sub>-2, Ac-PLP-BPI-NH<sub>2</sub>-2-NP, or PBS. No significant difference in IL-4 production was observed between any of the groups ( $p > 0.05$ ).



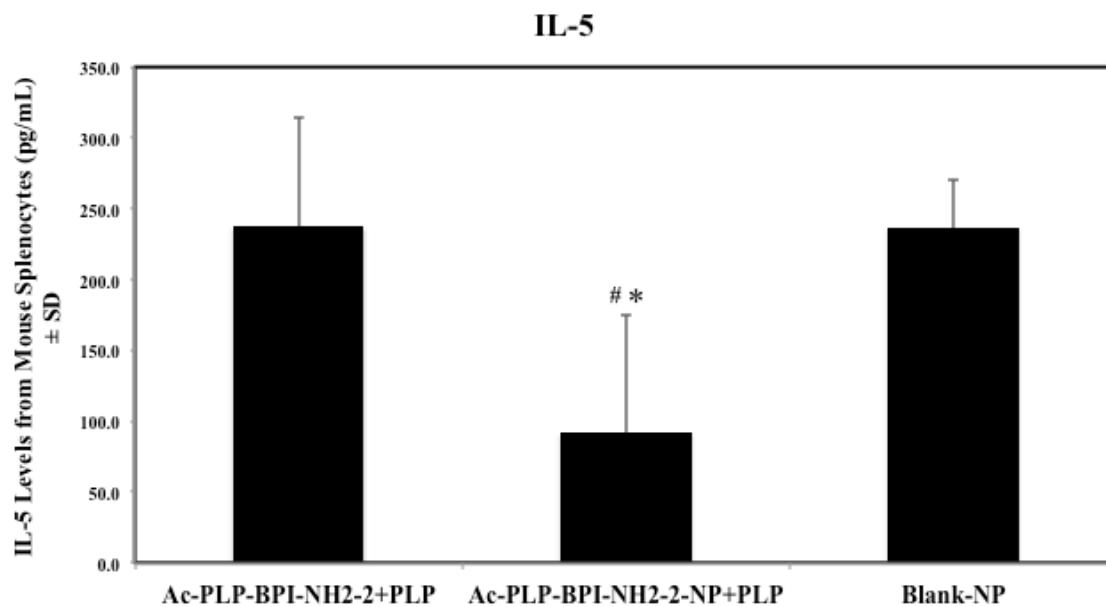


**Figure 3.5F:** Cytokine levels (day 55) from splenocytes of mice treated subcutaneously with solution Ac-PLP-BPI-NH<sub>2</sub>-2, Ac-PLP-BPI-NH<sub>2</sub>-2-NP, or PBS. In the Ac-PLP-BPI-NH<sub>2</sub>-2-NP-treated group, IL-5 cytokine levels were significantly lower than in the groups treated with Ac-PLP-BPI-NH<sub>2</sub>-2 (#,  $p < 0.0005$ ) and PBS (\*,  $p < 0.0005$ ).

**3.5D**). When comparing the two treatment groups, significant differences in IL-2 production were observed ( $p < 0.0005$ ) (**Fig. 3.5D**). No significant difference in IL-4 production was observed between any of the groups on day 55 (**Fig. 3.5E**). Whereas no significant difference between Ac-PLP-BPI-NH<sub>2</sub>-2 and blank-NP control groups was observed, IL-5 levels were significantly lower for the Ac-PLP-BPI-NH<sub>2</sub>-2-NP group ( $p < 0.0005$ ) (**Fig. 3.5F**).

### 3.4 DISCUSSION

Previously, BPI molecules such as PLP-BPI, GAD-BPI, and CII-BPI have been shown to suppress the progression of autoimmune diseases in the animal models of diseases such as MS, type 1 diabetes, and rheumatoid arthritis, respectively.<sup>6,17-20</sup> Furthermore, GAD-BPI was found to simultaneously bind to MHC-II and ICAM-1, co-localizing them on the surface of B cells that were isolated from a non-obese diabetic (NOD) mouse.<sup>6</sup> It is proposed that blocking the formation of the immunological synapse that is necessary for T-cell activation will alter the immune response toward a regulatory and suppressor phenotype and away from a Th17 and/or Th1 inflammatory response.

There are two parameters of colloidal gel to consider in delivering Ac-PLP-BPI-NH<sub>2</sub>-2 in a controlled-release manner; these parameters are the particle size and zeta potential.<sup>21</sup> The particles were manufactured to a size of approximately 200–400 nm because the small size allowed a stronger cohesiveness of the colloidal gel.<sup>21</sup> For larger particles (in the  $\mu\text{m}$  range), the number of particle-particle contacts decreases, thus leading to a less stable colloidal gel. The large zeta potential of the coated nanoparticles also yields stronger electrostatic interactions, leading to tighter packing of the colloidal

gel. Using SEM, the formation of a tight network structure of the colloidal gel was observed, which suggested that oppositely charged particles are interacting and forming ring-like structures.<sup>22</sup> Grooves and pores are also observed, which further suggested that there is also a repulsive force among similarly charged nanoparticles.<sup>22</sup>

*In vitro* studies showed that Ac-PLP-BPI-NH<sub>2</sub>-2 could be delivered in a controlled-release manner, where the full dose was delivered in a period of a little over a week. One advantage of using a controlled-release system over the traditional dosing method is that Ac-PLP-BPI-NH<sub>2</sub>-2 was being continually released, permitting a persistent exposure of the peptide to APC, whereas the control method required three separate injections, delivering bolus doses at every injection. In another study, a hepatitis B vaccine that required three injections was delivered effectively using one injection in an alginate-chitosan microsphere formulation to produce a robust immune response.<sup>23</sup>

Another advantage of using the colloidal gel system was the ease of formulating the peptide by simple mixing without losing peptide. To improve the release profile, such as slowing the release of the peptide, future studies will be done where the colloidal gel will be formulated to have higher amounts of positively charged PLGA nanoparticles to improve electrostatic adsorption,<sup>24</sup> due to the net charge of -2 for Ac-PLP-BPI-NH<sub>2</sub>-2. Peptide release may also be delayed or increased by adjusting the loading.

Vaccine-like delivery of Ac-PLP-BPI-NH<sub>2</sub>-2 (day -5) from the colloidal gel was shown to be effective in suppressing disease throughout the study, including relapse. Administration of Ac-PLP-BPI-NH<sub>2</sub>-2 after the induction of disease on day 4 was able to suppress disease better than the controls during both the initial phase of the disease and the relapse. However, administration of Ac-PLP-BPI-NH<sub>2</sub>-2-NP on day 4 did not

suppress disease as well as when given on day -5. This is possibly due to the timing of the delivery of the Ac-PLP-BPI-NH<sub>2</sub>-2-NP, which is too close to the time of disease onset (day ~10). In this case, the peptide may not be completely released by the onset of the disease. *In vitro* release studies suggest that it takes approximately eight days for the peptide to completely release for the mice to receive the full dose. Therefore, for the peptide to be fully effective, Ac-PLP-BPI-NH<sub>2</sub>-2-NP would need to be administered anywhere between day -5 and day 4. It is also plausible that the difference in the efficacy of the two treatments was due to the production of regulatory and suppressor cells that shift the balance of the immune system to a non-immunogenic phenotype in the group treated on day -5. Cytokine studies need to be done in the future to confirm this proposal.

Most of the initial cases of MS are characterized as relapsing-remitting.<sup>25</sup> To test for the ability to suppress relapse after remission, Ac-PLP-BPI-NH<sub>2</sub>-2-NP was administered on day 30. We observed that while the group initially showed clinical signs of improvement, the treatment was not able to fully suppress relapse. Because MS is an autoimmune disease that generally involves multiple epitopes from different myelin sheath proteins, it is possible that the peptide is suppressing a subpopulation of T cells that are responsible for the recognition of PLP; however, the MOG- and MBP-specific T cells may be responsible for the relapse in disease.<sup>2,26</sup> The reason a relapse was not observed in the Ac-PLP-BPI-NH<sub>2</sub>-2-NP (day -5) group was possibly because the peptide completely suppressed any immunogenic T cells in the early stage, and this resulted in a shift in the immune balance towards a regulatory response before any epitope spreading occurred.<sup>26</sup>

Th17 is thought to play a large role in the pathogenesis of both EAE and MS.<sup>27</sup> Through cytokine studies, it was revealed that IL-6, a proinflammatory marker that is a precursor for Th17 production, was significantly lower in both Ac-PLP-BPI-NH<sub>2</sub>-2 and Ac-PLP-BPI-NH<sub>2</sub>-2-NP treatment groups.<sup>27</sup> Furthermore, IL-6 is important in the breakdown of the blood brain barrier (BBB), a hallmark of MS and EAE.<sup>28</sup> Our previous work had shown that Ac-PLP-BPI-NH<sub>2</sub>-2 prevented the destruction of the BBB (unpublished data). The lower IL-6 production by the Ac-PLP-BPI-NH<sub>2</sub>-2-NP group compared to the Ac-PLP-BPI-NH<sub>2</sub>-2 group suggested that continual exposure to the peptide dose may be better at suppressing Th17 production. It could also be that the higher initial dose followed by a more sustained release provided by the colloidal gel formulation might be a more optimal way to deliver this peptide. Lower levels of IL-17 by both treatments compared to blank-NP on day 55 corroborate the IL-6 findings, suggesting that suppression of Th17 production was the major mechanism of the peptide. The other inflammatory marker, IFN $\gamma$ , was also significantly lower in the treated groups than in the blank-NP group. Just as in IL-6, IFN $\gamma$  was significantly lower in the Ac-PLP-BPI-NH<sub>2</sub>-2-NP group compared to the mice group treated with bolus injections of Ac-PLP-BPI-NH<sub>2</sub>-2, suggesting that delivering the peptide using a colloidal gel formulation is more advantageous at suppressing the Th1 immunogenic response.

Th2 cells generally function as suppressor cells and usually develop in the presence of IL-4.<sup>29</sup> IL-4 production was not significantly different in the treatment groups compared to the negative control. This suggests that Th2 involvement, especially during the peak of the relapse (day 55), may not be as important as Th17. IL-5, also considered to be a Th2 marker, was significantly lower in the group treated with

Ac-PLP-BPI-NH<sub>2</sub>-2-NP compared to the controls. IL-2 levels in the Ac-PLP-BPI-NH<sub>2</sub>-2 treatment group were also significantly higher. These results suggested that, although the peptide used for treatment is the same, the dosing schedule and dose availability play vital roles in developing an immunotolerant state.

### **3.5 CONCLUSIONS**

In conclusion, a one-time injection given in a vaccine-like manner with the colloidal gel formulation loaded with Ac-PLP-BPI-NH<sub>2</sub>-2 suppressed EAE as well as the three-times injection of the positive control, Ac-PLP-BPI-NH<sub>2</sub>-2. Even though treatment with Ac-PLP-BPI-NH<sub>2</sub>-2-NP on day 4 could suppress EAE, the timing of the dose was found to be an important factor in suppressing disease. Ac-PLP-BPI-NH<sub>2</sub>-2-NP was also found to suppress disease by downregulating production of IL-6 and IL-17, cytokines associated with Th17 production. Future studies using Ac-PLP-BPI-NH<sub>2</sub>-2-NP will aim to further elucidate its mechanism of action. The effect of epitope spreading will be studied by co-administering other immunodominant epitopes, such as MOG-BPI.<sup>26</sup> Finally, a colloidal gel was found to be an effective way of delivering Ac-PLP-BPI-NH<sub>2</sub>-2 in a controlled-release manner without the loss of peptide during formulation.

### 3.6 REFERENCES

- 1 Lassmann, H. Classification of demyelinating diseases at the interface between etiology and pathogenesis. *Curr Opin Neurol* **14**, 253-258 (2001).
- 2 Wu, G. F. & Alvarez, E. The immunopathophysiology of multiple sclerosis. *Neurol Clin* **29**, 257-278 (2011).
- 3 Markowitz, C. E. The current landscape and unmet needs in multiple sclerosis. *Am J Manag Care* **16**, S211-218 (2010).
- 4 Manikwar, P., Kiptoo, P., Badawi, A. H., Buyuktimkin, B. & Siahaan, T. J. Antigen-specific blocking of CD4-specific immunological synapse formation using BPI and current therapies for autoimmune diseases. *Med Res Rev* (2011).
- 5 Lee, K. H. *et al.* T cell receptor signaling precedes immunological synapse formation. *Science* **295**, 1539-1542 (2002).
- 6 Murray, J. S. *et al.* Suppression of type 1 diabetes in NOD mice by bifunctional peptide inhibitor: modulation of the immunological synapse formation. *Chem Biol Drug Des* **70**, 227-236 (2007).
- 7 Heron, L. *et al.* Immunogenicity, reactogenicity and safety of two-dose versus three-dose (standard care) hepatitis B immunisation of healthy adolescents aged 11-15 years: a randomised controlled trial. *Vaccine* **25**, 2817-2822 (2007).
- 8 Peek, L. J., Middaugh, C. R. & Berkland, C. Nanotechnology in vaccine delivery. *Adv Drug Deliv Rev* **60**, 915-928 (2008).
- 9 Mata, E., Igartua, M., Patarroyo, M. E., Pedraz, J. L. & Hernandez, R. M. Enhancing immunogenicity to PLGA microparticulate systems by incorporation of alginate and RGD-modified alginate. *Eur J Pharm Sci* **44**, 32-40 (2011).

- 10 Zhu, B. *et al.* Chitosan microspheres enhance the immunogenicity of an Ag85B-based fusion protein containing multiple T-cell epitopes of *Mycobacterium tuberculosis*. *Eur J Pharm Biopharm* **66**, 318-326 (2007).
- 11 Nishimura, K. *et al.* Adjuvant activity of chitin derivatives in mice and guinea-pigs. *Vaccine* **3**, 379-384 (1985).
- 12 Otterlei, M. *et al.* Induction of cytokine production from human monocytes stimulated with alginate. *J Immunother (1991)* **10**, 286-291 (1991).
- 13 Brodbeck, K. J., Pushpala, S. & McHugh, A. J. Sustained release of human growth hormone from PLGA solution depots. *Pharm Res* **16**, 1825-1829 (1999).
- 14 Jiang, W., Gupta, R. K., Deshpande, M. C. & Schwendeman, S. P. Biodegradable poly(lactic-co-glycolic acid) microparticles for injectable delivery of vaccine antigens. *Adv Drug Deliv Rev* **57**, 391-410 (2005).
- 15 Borges, O., Borchard, G., Verhoef, J. C., de Sousa, A. & Junginger, H. E. Preparation of coated nanoparticles for a new mucosal vaccine delivery system. *Int J Pharm* **299**, 155-166 (2005).
- 16 Shive, M. S. & Anderson, J. M. Biodegradation and biocompatibility of PLA and PLGA microspheres. *Adv Drug Deliv Rev* **28**, 5-24 (1997).
- 17 Kobayashi, N. *et al.* Prophylactic and therapeutic suppression of experimental autoimmune encephalomyelitis by a novel bifunctional peptide inhibitor. *Clin Immunol* **129**, 69-79 (2008).
- 18 Kobayashi, N., Kobayashi, H., Gu, L., Malefyt, T. & Siahaan, T. J. Antigen-specific suppression of experimental autoimmune encephalomyelitis by a novel bifunctional peptide inhibitor. *J Pharmacol Exp Ther* **322**, 879-886 (2007).



- 19 Ridwan, R. *et al.* Antigen-specific suppression of experimental autoimmune encephalomyelitis by a novel bifunctional peptide inhibitor: structure optimization and pharmacokinetics. *J Pharmacol Exp Ther* **332**, 1136-1145 (2010).
- 20 Zhao, H., Kiptoo, P., Williams, T. D., Siahaan, T. J. & Topp, E. M. Immune response to controlled release of immunomodulating peptides in a murine experimental autoimmune encephalomyelitis (EAE) model. *J Control Release* **141**, 145-152 (2010).
- 21 Wang, Q., Wang, J., Lu, Q., Detamore, M. S. & Berklund, C. Injectable PLGA based colloidal gels for zero-order dexamethasone release in cranial defects. *Biomaterials* **31**, 4980-4986 (2010).
- 22 Wang, Q., Jamal, S., Detamore, M. S. & Berklund, C. PLGA-chitosan/PLGA-alginate nanoparticle blends as biodegradable colloidal gels for seeding human umbilical cord mesenchymal stem cells. *J Biomed Mater Res A* **96**, 520-527 (2011).
- 23 Zheng, X., Huang, Y., Zheng, C., Dong, S. & Liang, W. Alginate-chitosan-PLGA composite microspheres enabling single-shot hepatitis B vaccination. *Aaps J* **12**, 519-524 (2010).
- 24 Wang, Y. & Irvine, D. J. Engineering chemoattractant gradients using chemokine-releasing polysaccharide microspheres. *Biomaterials* **32**, 4903-4913 (2011).
- 25 Fox, E. J. Alemtuzumab in the treatment of relapsing-remitting multiple sclerosis. *Expert Rev Neurother* **10**, 1789-1797 (2010).

- 26 Vanderlugt, C. L. *et al.* Pathologic role and temporal appearance of newly emerging autoepitopes in relapsing experimental autoimmune encephalomyelitis. *J Immunol* **164**, 670-678 (2000).
- 27 Strzepa, A. & Szczepanik, M. IL-17-expressing cells as a potential therapeutic target for treatment of immunological disorders. *Pharmacol Rep* **63**, 30-44 (2011).
- 28 Abbott, N. J., Ronnback, L. & Hansson, E. Astrocyte-endothelial interactions at the blood-brain barrier. *Nat Rev Neurosci* **7**, 41-53 (2006).
- 29 Harrington, L. E. *et al.* Interleukin 17-producing CD4<sup>+</sup> effector T cells develop via a lineage distinct from the T helper type 1 and 2 lineages. *Nat Immunol* **6**, 1123-1132 (2005).

## **CHAPTER 4**

### **The effects of bifunctional peptide inhibitors in suppressing rheumatoid arthritis in an animal model**

## 4.1 INTRODUCTION

Rheumatoid arthritis (RA) is an autoimmune disease that causes pain, stiffness, chronic inflammation, and deformity due to cartilage, bone, and ligament destruction in the joints.<sup>1</sup> Although the etiology of RA is not fully understood, it has been suggested that the cause of the disease is the attack of the host joints by immune cells along with the generation of lymphocytes that release inflammatory cytokines such as tumor necrosis factor (TNF)- $\alpha$ , interferon (IFN) $\gamma$ , interleukin (IL)-1, and IL-6.<sup>2-5</sup> T helper-1 (Th1) cells infiltrate the synovium where they release proinflammatory cytokines and chemokines that promote macrophage and neutrophil infiltration and activation.<sup>1,4,6</sup> Th17, a subset of T-helper (Th) cells, have also been implicated in autoimmune diseases such as rheumatoid arthritis.<sup>3,7</sup> Another possible cause is that the body fails to activate regulatory T cells (T-reg); thus, enhancing the functions of T-reg may be one therapeutic strategy to suppress RA and other autoimmune diseases.<sup>8-12</sup>

Because there is no known cure for RA, current treatments are aimed at decreasing joint inflammation and pain, maximizing joint function, and preventing joint destruction. RA medications can be divided into “first-line” and “second-line” drugs. The first-line drugs include various non-steroidal anti-inflammatory drugs (NSAIDs) (i.e., aspirin, naproxen, ibuprofen, etodolac, and celecoxib) and corticosteroids.<sup>13,14</sup> NSAIDs normally act quickly to ameliorate pain and decrease tissue inflammation and swelling; however, they have side effects that can cause upset stomach, abdominal pain, ulcers, and GI bleeding.<sup>15</sup>

The second-line drugs are disease-modifying antirheumatic drugs (DMARDs), which include immunosuppressive drugs such as methotrexate (Rheumatrex<sup>®</sup>, Trexall<sup>™</sup>),

azathioprine (Imuran<sup>®</sup>), cyclophosphamide (Cytosan<sup>®</sup>), Chlorambucil (Leukeran<sup>®</sup>), and cyclosporine (Sandimmune<sup>®</sup>). These slower acting drugs promote RA remission and prevent progressive joint destruction (i.e., cartilage, bone, and adjacent soft tissues). These drugs may take up to a few months to become effective. With the exception of methotrexate, immunosuppressive drugs are generally reserved for patients with very aggressive disease or serious rheumatoid inflammation complications, such as vasculitis.<sup>13</sup> These can have side effects that suppress bone marrow function, causing anemia, decreased white blood cell and platelet counts, and increased risk of infection and bleeding.

Newer second-line drugs, called biologic response modifiers (i.e., Enbrel<sup>®</sup> (etanercept), Remicade<sup>®</sup> (infliximab), Humira<sup>®</sup> (adalimumab), Rituxan<sup>®</sup> (rituximab), and Orencia<sup>®</sup> (abatacept)), are more specific and have a quicker onset of action to prevent progressive joint destruction in RA. For example, golimumab, etanercept, infliximab, and adalimumab act to lower TNF $\alpha$  levels in the systemic circulation, whereas Orencia<sup>®</sup> blocks T-cell activation.<sup>13,14,16,17</sup> Their use is recommended after initial second-line medications have been shown to be ineffective, and they are often more effective in combination with DMARDs.<sup>13,14</sup>

Although the current biologic response modifiers have been effective in treating patients, they can suppress the general immune system and ultimately increase the risk of infections. Therefore, there is a need to develop a new immune modulator that can selectively suppress the activity of a sub-population of the immune cells that cause joint damage in RA and that decrease the likelihood of a totally immune-compromised host. In this study, a novel type of bifunctional peptide inhibitor (BPI) molecule called CII-BPI

(i.e., CII-BPI-1, CII-BPI-2, and CII-BPI-3; **Table 1**) that selectively suppresses the activation of a subpopulation of T cells that respond to collagen II antigen was developed. These molecules are composed of antigenic peptides from collagen II (i.e., CII<sub>256-270</sub>, and CII<sub>1237-1249</sub>, CII<sub>707-721</sub>) linked via a spacer to a cell adhesion peptide called LABL. The LABL peptide is derived from the I-domain of  $\alpha_L$ -integrin (CD11a<sub>237-246</sub>), which binds to ICAM-1. The hypothesis of how BPI molecules suppress RA is that CII-BPI binds simultaneously to MHC-II and ICAM-1 on the surface of antigen-presenting cells (APC) and alters the differentiation of naïve T cells to T-reg upon interaction of these APC with naïve T cells to halt the progression of the disease. At the molecular level, because BPI molecules bind simultaneously to MHC-II and ICAM-1, they may block the formation of the immunological synapse necessary for T-cell activation.<sup>18</sup> The ability of CII-BPI molecules to suppress the progression of RA were evaluated and compared to those of the respective parent antigenic peptides from collagen II in the CIA mouse model. The effect of CII-BPI molecules in altering cytokine production was also determined.

## **4.2 MATERIALS AND METHODS**

### **4.2.1 Animals**

The DBA1BO-M male mice utilized in study-I were purchased from Taconic Farms (Germantown, NY). For study-II and -III, DBA/1J male mice were purchased from Jackson Laboratory (Bar Harbor, ME). All mice were housed under specific pathogen-free conditions at the animal facility at The University of Kansas approved by the Association for Assessment and Accreditation of Laboratory Animal Care. All

<b>Table 1. The sequences of peptides used in the present study</b>		
<b>CII Sequence Source</b>	<b>Peptide</b>	<b>Sequence</b>
CII <sub>256-270</sub>	CII-1	Ac-GEPGIAGFKGEQGPK-NH <sub>2</sub>
CII <sub>256-270</sub>	CII-BPI-1	Ac-GEPGIAGFKGEQGPK-(AcpGAcpGAcp) <sub>2</sub> -ITDGEATDSG-NH <sub>2</sub>
CII <sub>1237-1249</sub>	CII-2	Ac-QYMRADSTLR-NH <sub>2</sub>
CII <sub>1237-1249</sub>	CII-BPI-2	Ac-QYMRADSTLR-(AcpGAcpGAcp) <sub>2</sub> -ITDGEATDSG-NH <sub>2</sub>
CII <sub>707-721</sub>	CII-3	PPGANGNPGPAGPPG
CII <sub>707-721</sub>	CII-BPI-3	Ac-PPGANGNPGPAGPPG-(AcpGAcpGAcp) <sub>2</sub> -ITDGEATDSG-NH <sub>2</sub>
Ac = Acetyl Group; Acp = ε-aminocaproic acid; G = Glycine		

experimental procedures using live mice were approved by the Institutional Animal Care and Use Committee at The University of Kansas.

#### **4.2.2 Peptide synthesis**

The peptides used in this study (Table 4.1) were synthesized using a solid phase peptide synthesizer (Pioneer; Perceptive Biosystems, Framingham, MA) on a polyethylene glycol-polystyrene resin (Applied Biosystems, Foster City, CA) with 9-fluorenylmethyloxycarbonyl-protected amino acid chemistry. Cleavage of the peptides from the resin and removal of the protecting groups were carried out using trifluoroacetic acid in the presence of scavengers. The crude peptides were purified by reversed-phase high-performance liquid chromatography (HPLC) using a C18 column with a gradient of solvent A (94.9% H<sub>2</sub>O with 0.1% trifluoroacetic acid and 5% acetonitrile) and solvent B (100% acetonitrile). The purity of the peptide was analyzed by analytical HPLC using an analytical C18 column. The peptide identity was confirmed by matrix-assisted laser desorption/ionization time-of-flight (MALDI-TOF) mass spectrometry.

#### **4.2.3 Induction of CIA and therapeutic study**

For study-I, a readily prepared chicken collagen/CFA emulsion, containing 1.0 mg/ml of type II chicken collagen and 2.0 mg/ml of *mycobacterium tuberculosis*, was injected intradermally (Hooke Laboratories, Lawrence, MA). This was followed by an intradermal IFA emulsion injection, containing 1 mg/ml of chicken type-II collagen, on day 21. The mice were given intravenous (i.v.) injections of CII-1 and CII-BPI-1 peptides (100 nmol/injection) on days 17, 22, 25, and 28.



For study-II and -III, bovine type II collagen (CII, Elastin Products, Owensville, MO) was dissolved in 0.05 M acetic acid overnight at 4°C at a concentration of 6 mg/ml. CFA was prepared by addition of killed *Mycobacterium tuberculosis* H37RA (Difco, Detroit, MI) to IFA (Difco) at a concentration of 8 mg/ml. The solution of CII (6 mg/ml) was emulsified in an equal volume of CFA. Six- to eight-week-old DBA/1J mice were immunized with 100 µl of emulsion containing 300 µg CII and 400 µg mycobacteria injected intradermally at the tail base. After 21 days, all mice received a booster dose of 100 µl of emulsion containing 300 µg CII injected intradermally at the tail base. For study-II, the mice received i.v. injections of CII-BPI-1, CII-BPI-2, CII-1, and CII-2 (100 nmol/injection) on days 19, 22, and 25. For study-III, the same disease induction protocol was followed, with the mice receiving i.v. injections of CII-BPI-3 and CII-3 peptides (100 nmol/injection) on days 19, 22, and 25. In another group, mice were injected with 5 mg/kg in 100 µl of MTX-cIBR for 10 days from day 19. MTX-cIBR is a conjugate of methotrexate and a cIBR adhesion peptide derived from ICAM-1.

Initially, disease progression was evaluated by using a clinical scoring scale for each paw ranging from 0 to 4 as follows: 0–no clinical symptoms, 1–paws with swelling of finger joints or redness; 2–paws with mild swelling of wrist or ankle joints; 3–paws with severe swelling of entire paw; 4–paws with deformity or ankylosis. Disease progression was also evaluated throughout the study by measuring the increase in paw swelling of the fore limbs as well as hind limbs.

#### **4.2.4 Determination of IL-6 levels in serum *in vivo***

Cytokine production in the peptide-treated and untreated mice was measured by obtaining blood samples on days 31 and 44 from study-I without sacrificing the mice. Blood samples were allowed to clot overnight at 4 °C before centrifuging at 5,000 rpm for 10 minutes the next day. Serum was collected and stored at -80 °C until analysis. Serum IL-6 analysis was performed using a fully quantitative ELISA-based Q-Plex™ Mouse Cytokine-Screen (Quansys Biosciences, Logan, UT). Serum IL-1, IL-4, IL-5, IL-10, IL-17, TNF $\alpha$ , and IFN $\gamma$  were below the detection limit.

#### **4.2.5 Histopathology of the joints**

Development of CIA in DBA mice was also assessed histologically. In study-II, both hind limbs were removed 30 days after the second immunization and fixed in formalin prior to analysis. Arthritic changes and joint damage were individually scored (articular cartilage damage, pannus formation, synovial membrane thickening, synovial capsule thickening, inflammatory cell infiltrate) and totaled as: 0, no lesions; 1, mild changes; 2, moderate changes; 3 and 4, severe changes. The histopathology evaluation was done by Dr. Stan Kosanke at the University of Oklahoma Health Sciences Center.

#### **4.2.6 Statistical analysis**

Statistical differences among the groups in clinical scoring, volume displacement, serum IL-6 levels, and histopathological score were determined by one-way analysis of variance followed by Fisher's least significant difference. All analyses were performed using StatView (SAS Institute, Cary, NC).

## 4.3 RESULTS

### 4.3.1 Suppression of CIA by CII-BPI

In study-I, DBA1BO-M male mice were used and disease was stimulated using chicken collagen in CFA. DBA1BO-M mice developed more severe clinical arthritis than the DBA/1J mice utilized in study-II and -III. Two different injection schedules (3 and 4 injections) were carried out to compare the efficacy of CII-BPI-1 and CII-1 peptides. The clinical scores indicated that both CII-1 and CII-BPI-1 peptides were significantly better in suppressing the arthritis compared to PBS ( $p < 0.0001$ , through days 28-44)(**Fig. 4.1A**). Using clinical scores, it was difficult to differentiate the efficacy of CII-1 and CII-BPI-1; however, the differences were clear when comparing paw swelling measurements because this method is more objective and quantitative.

According to the percent changes in paw swelling of all four limbs (**Fig. 4.1B**), it was clear that 3 and 4 injections of CII-BPI-1 and 4 injections of CII-1 peptides were significantly more effective than PBS and 3 injections of CII-1 peptide ( $p < 0.001$ , through days 34-44). It was difficult to differentiate the efficacy of 3 and 4 injections of CII-BPI-1 peptide. However, 3 injections of CII-BPI-1 were significantly better than 3 injections of CII-1 peptide ( $p < 0.001$ , through days 34-44), suggesting that CII-BPI-1 is more potent than CII-1 peptide. Evaluating the changes in paw volume of both hind limbs only (**Fig. 4.1C**), there was a trend to suggest that 4 injections of CII-BPI-1 were more effective than 3 injections of CII-BPI-1 ( $p$ -value of 0.0575, through days 34-44) and 4 injections of CII-1 peptide ( $p$ -value of 0.0893, through days 34-44). In this animal model, three injections of CII-1 peptide did not show any efficacy in suppressing the changes in

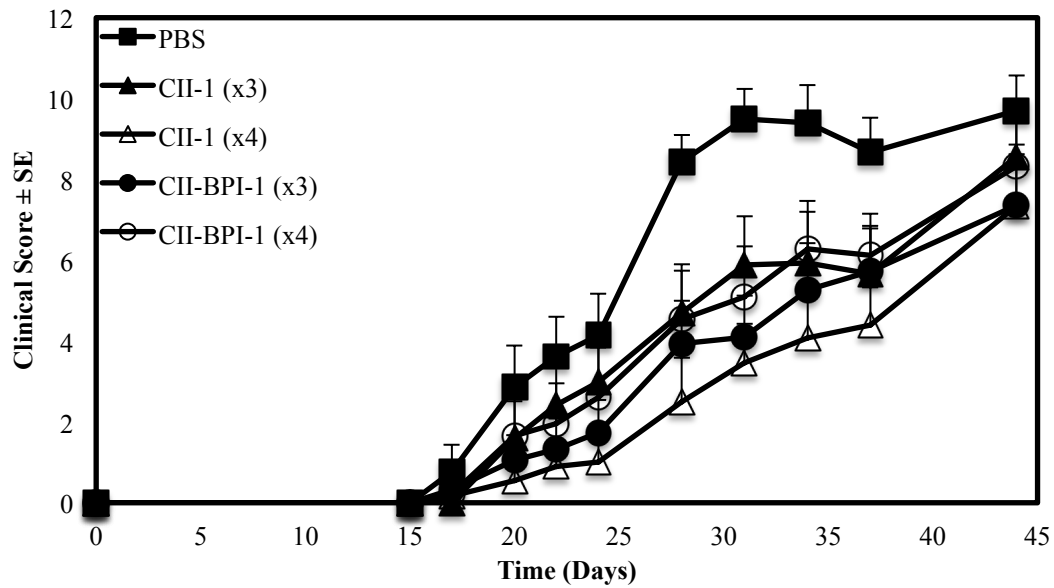


**Figure 4.1** *In vivo* activity of the CII-1 and CII-BPI-1 peptides in the mouse CIA model with varying injections. In study-I, DBA1BO male mice were immunized with CII/CFA intradermally and given a booster dose on day 21. The mice were then given four i.v. injections of peptides (100 nmol/injection) on days 17, 22, 25, and 28 or only three injections on days 17, 22, and 25. The disease progression was observed by (A) clinical scoring, (B) monitoring the changes in the volume of all four paws, or (C) by measuring just the hind paws. The results are expressed as the mean  $\pm$  standard error ( $n = 7-9$ ). **Figure 4.1A:** All peptides groups are significantly better than PBS ( $p < 0.0001$ , through days 28–44).

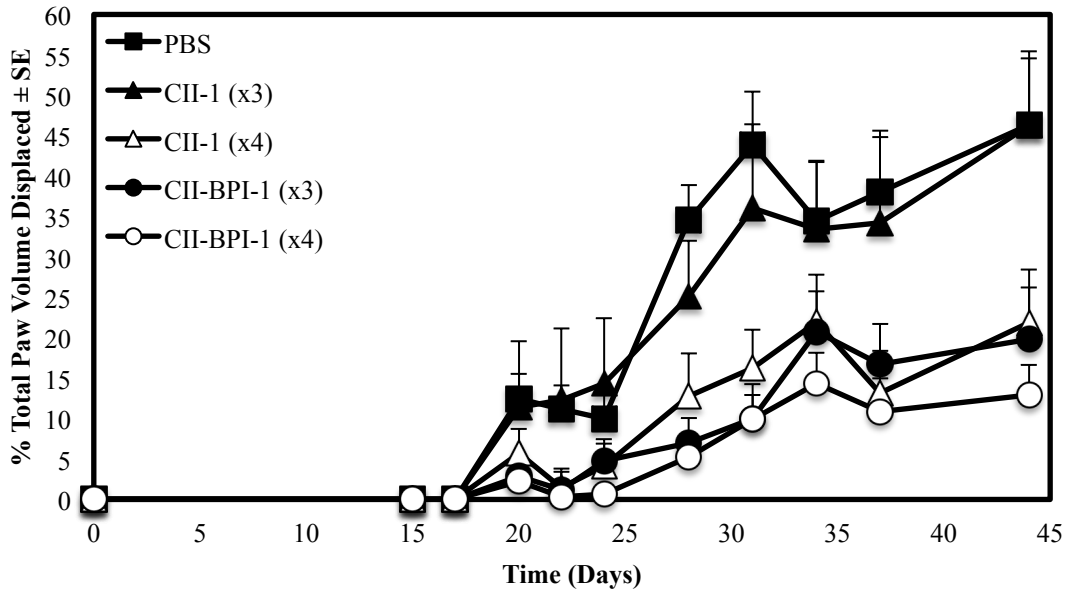


**Figure 4.1B** There were significant differences in the volume displaced by all four paws between four injections of CII-BPI-1 and PBS ( $p < 0.0001$ , through days 34–44), and three injections of CII-1 ( $p < 0.0001$ , through days 34–44). Three injections of CII-BPI-1 were significantly better than PBS ( $p < 0.001$ , through days 34–44) and three injections of CII-1 ( $p < 0.001$ , through days 34–44).

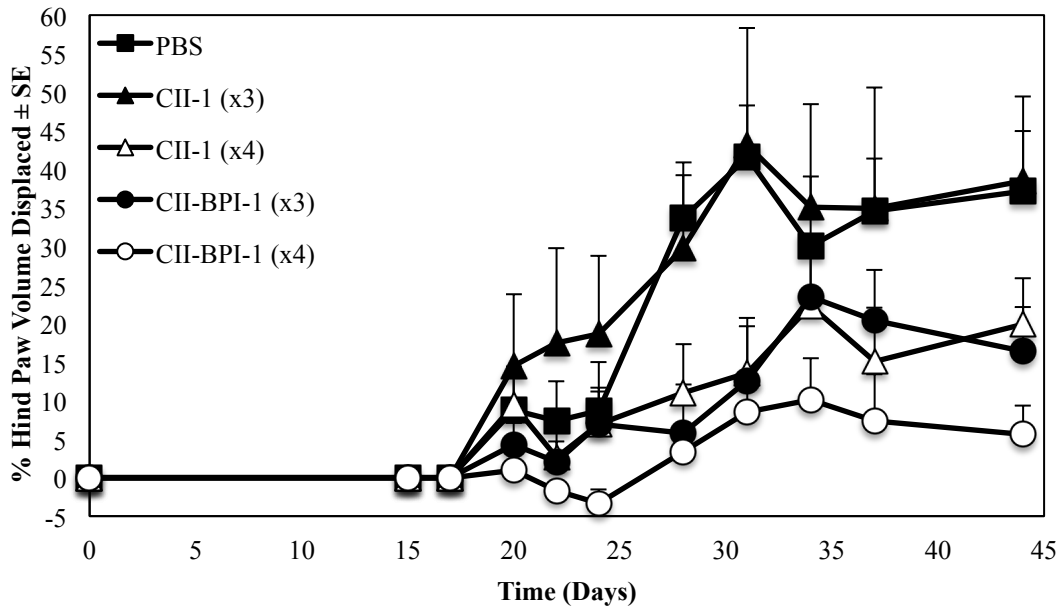


**Figure 4.1C** There were significant differences in the volume displaced by the hind paws between four injections of CII-BPI-1 and PBS ( $p < 0.0001$ , through days 34–44), and three injections of CII-1 ( $p < 0.0001$ , through days 34–44). The  $p$ -value for the difference between four injections of CII-BPI-1 and four injections of CII-1 is 0.0893. A  $p$ -value of 0.0575 suggests that four injections of CII-BPI-1 are better than three injections of CII-BPI-1.

paw volume. These results suggested that CII-BPI-1 was more potent than CII-1 peptide and that the activity of these peptides was dose-dependent.

In study-II, disease was induced using bovine collagen, and the efficacies of CII-BPI-1 and CII-BPI-2 were compared to those of their respective antigenic peptides, CII-1 and CII-2, in suppressing CIA (**Fig. 4.2**). The changes in paw volume suggested that CII-BPI-1 had the best activity in suppressing arthritis in mice compared to the other peptides, as well as PBS (**Fig. 4.2**). Although there was a trend indicating that CII-BPI-2 was better than CII-2 peptide, the difference was not statistically significant. It was clear that CII-BPI-1 had better efficacy than CII-BPI-2 and CII-2 peptide ( $p < 0.05$ , through days 40–44) and there was a trend to suggest that CII-2 could aggravate the disease compared to PBS.

In study-III, four groups of DBA/1J male mice were induced with disease. Then, two groups were injected three times intravenously with 100 nmol/injection of CII-BPI-3 and CII-3 peptides on days 19, 22, and 25; one group was injected with PBS. Another group was treated with MTX-cIBR with a daily dosing schedule of 5 mg/kg starting from day 19 for 10 consecutive days. The changes in paw volume due to swelling were significantly lower in CII-BPI-3-treated mice than in those treated with PBS (**Fig. 4.3**;  $p < 0.05$  from days 40 to 44). There was significant suppression of arthritis in CII-3 peptide-treated mice compared to the PBS-treated control group ( $p < 0.05$  from days 40 to 44). CII-BPI-3 peptide had a better CIA suppressive activity than CII-3 peptide ( $p < 0.01$ , through days 40–44), suggesting that forming BPI-type molecules improved the biological activity of the peptide. The positive control treatment, MTX-cIBR (5 mg/kg),

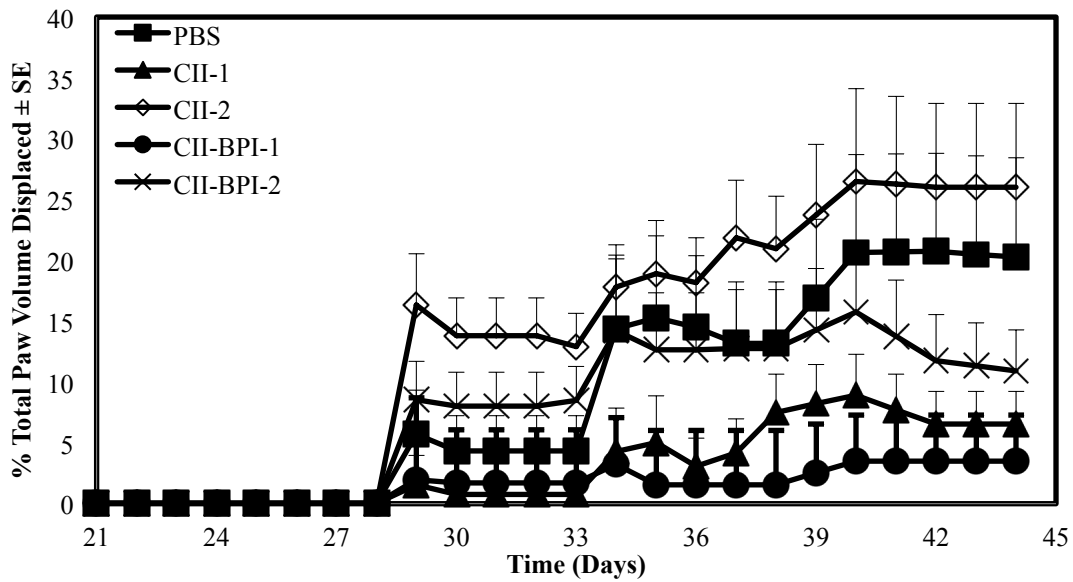


**Figure 4.2** Comparing the *in vivo* efficacies of CII-BPI-1 and CII-BPI-2 with those of their respective antigenic derivatives, CII-1 and CII-2, in the mouse CIA model. The negative control was mice treated with PBS. In the second study, mice immunized with CII/CFA received i.v. injections of the shown peptides (100 nmol/injection) on days 19, 22, and 25. There were significant differences in the changes in paw volume between CII-BPI-1- and PBS-treated ( $p < 0.0001$ , through days 40–44) and between CII-BPI-2- and PBS-treated groups ( $p < 0.05$ , through days 40–44). There was also a significant difference in mice treated with CII-1 and PBS ( $p < 0.0005$ , through days 40–44). In addition, a significant difference between the CII-BPI-1 and CII-BPI-2 groups was observed ( $p < 0.05$ , through days 40–44). The results are expressed as the mean  $\pm$  standard error ( $n = 7-9$ ).



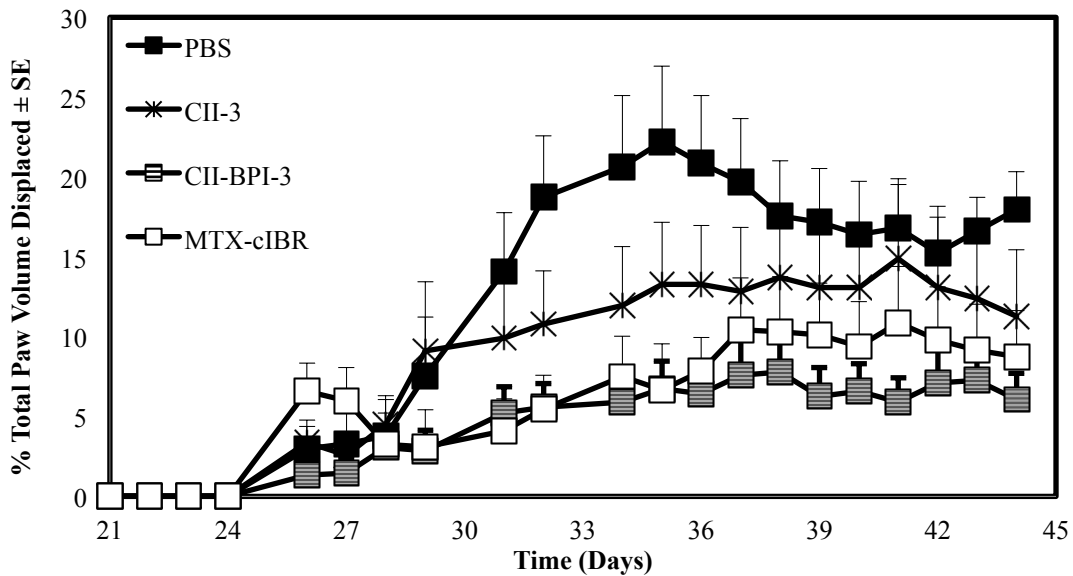


**Figure 4.3** The efficacies of CII-BPI-3, CII-3 and MTX-cIBR in suppressing rheumatoid arthritis were compared to those of PBS using the CIA mouse model. DBA/1J mice were immunized intradermally at the tail base with CII/CFA on day 0 followed by a booster dose at day 21. In study-III, three groups of mice were injected with 100 nmol of CII-BPI-3, CII-3, and PBS intravenously on days 19, 22, and 25. In another group, mice were injected with 5 mg/kg in 100 uL of MTX-cIBR for 10 days from day 19. The changes in paw volume were measured daily. There were significant differences in paw volume between CII-BPI-3- and PBS-treated and between CII-3- and PBS-treated groups ( $p < 0.01$ , through days 40–44). There was a significant difference in the changes in paw volume in mice treated with CII-BPI-3 and CII-3 ( $p < 0.01$ , through days 40–44). The results are expressed as the mean  $\pm$  standard error (n = 7–9).

suppressed arthritis better than PBS ( $p < 0.01$ , through days 40–44) and with almost the same potency as that of the CII-BPI-3 peptide ( $p > 0.10$ , through days 40–44).

#### 4.3.2 IL-6 serum levels in DBA mice *in vivo*

To determine the effect of the CII-BPI treatment in study-I on cytokine levels (**Fig. 4.4**), the levels of different cytokines in the serum were quantified using ELISA on day 31 at around the disease peak and on day 44 when the arthritis swelling was at the plateau region. Unfortunately, the levels for IL-1, IL-4, IL-5, IL-10, IL-17, TNF $\alpha$ , and IFN $\gamma$  were below the detection limit in serum and only IL-6 could be detected in the serum. On day 31, the IL-6 levels were significantly lower in mice injected 3 times with CII-BPI-1 than in those treated with PBS ( $p < 0.0001$ ) and CII-1 ( $p < 0.0001$ )(**Fig. 4.4A**). Furthermore, the CII-1-treated group had higher serum IL-6 levels than the PBS group ( $p < 0.0001$ ). Once the arthritic swelling reached a plateau on day 44 (**Fig. 4.4B**), the serum IL-6 concentration of the CII-1 group significantly decreased compared to the PBS-treated group ( $p < 0.0001$ ), and no significant difference was observed when compared to the group receiving CII-BPI-1. These results suggested that CII-BPI-1 and CII-1 might have had different mechanisms of suppressing arthritis.

In the groups injected four times with treatment peptides, the serum level of IL-6 in the CII-1 group was nearly three times higher than in the PBS-treated group at the peak of the disease on day 31 ( $p < 0.0001$ )(**Fig. 4.4C**). No significant difference between IL-6 concentrations of CII-BPI-1 and PBS on day 31 was observed. Analysis of the mouse cytokine levels at the end of the study (day 44) showed that IL-6 levels were lower in both the CII-1 and CII-BPI-1 groups when compared to the PBS group ( $p < 0.0001$ ). As

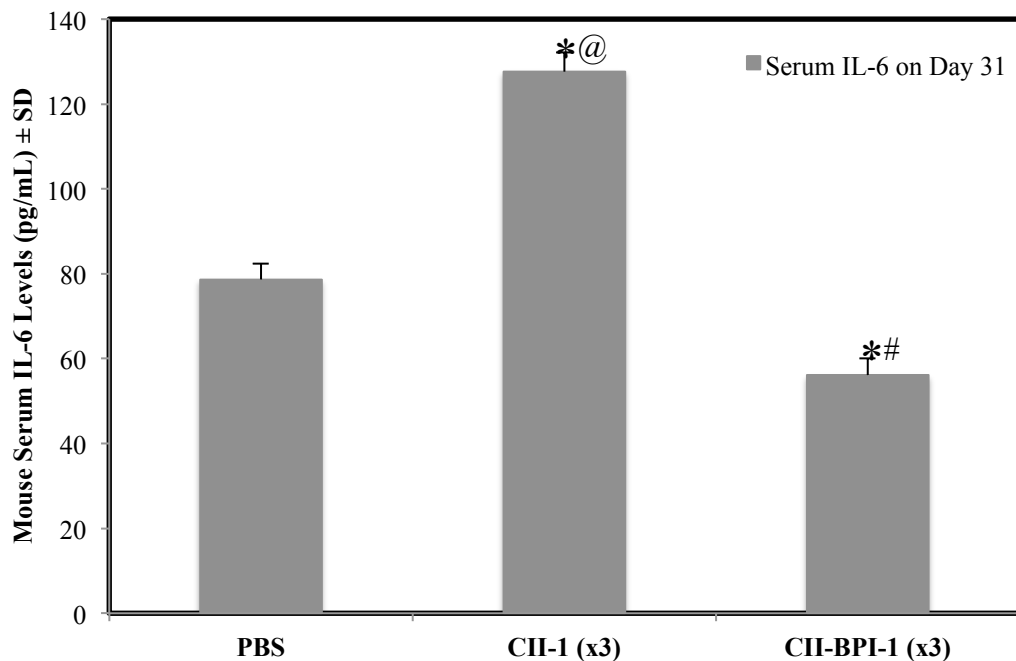


**Figure 4.4** The serum cytokine levels of IL-6 of mice treated with PBS, CII-1 and CII-BPI-1 on days 31 and 44. **Figure 4.4A:** Mice treated with three injections of CII-BPI-1 had significantly lower levels of IL-6 in the serum than those injected with PBS (\*,  $p < 0.0001$ ) and three injections of CII-1 (#,  $p < 0.0001$ ). Serum IL-6 levels were significantly higher in the mouse group treated with CII-1 than in the PBS-treated group (@,  $p < 0.0001$ ).

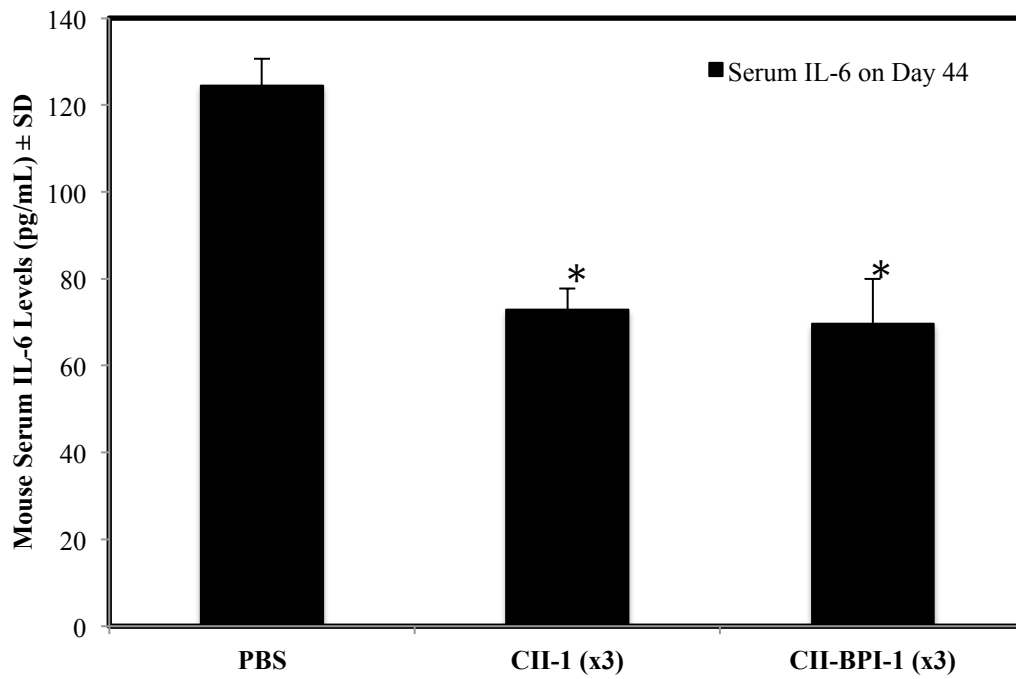


**Figure 4.4B** Serum levels of the cytokine IL-6 were significantly lower on day 44 after three-times injections of CII-1 (\*,  $p < 0.0001$ ) and CII-BPI-1 (\*,  $p < 0.0001$ ) compared to PBS. A significant difference between IL-6 levels of CII-1 and CII-BPI-1 on day 44 was not observed.

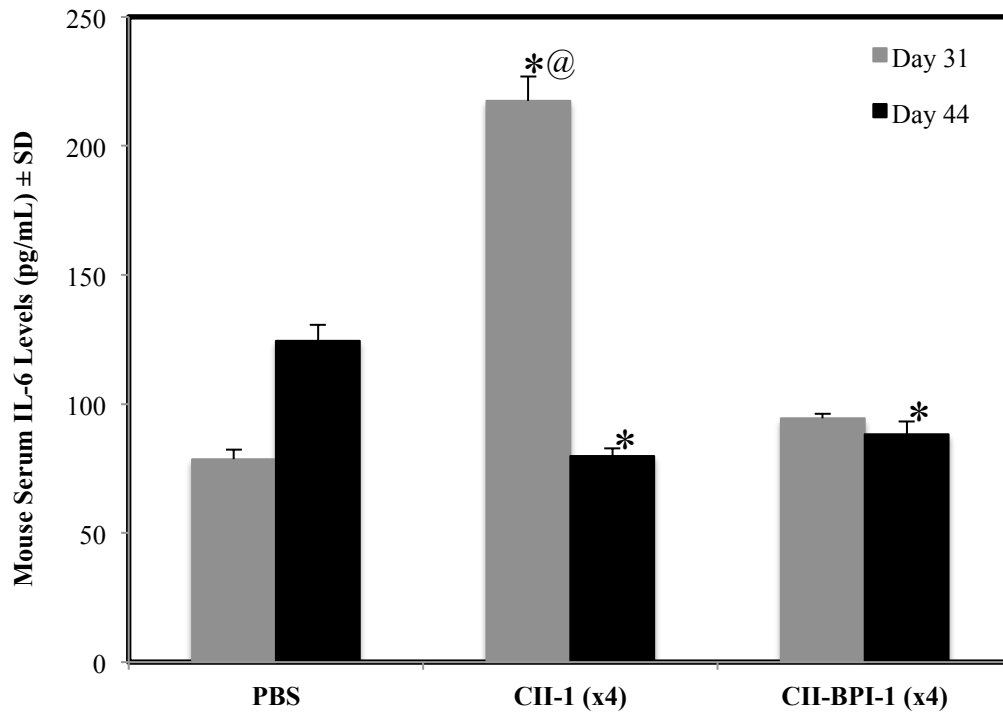


**Figure 4.4C** Comparison of serum IL-6 levels of mice treated with four injections of PBS, CII-1, and CII-BPI-1 on days 31 and 44. Serum IL-6 levels were significantly higher in the CII-1 group compared to PBS (<sup>@</sup>,  $p < 0.0001$ ) and CII-BPI-1 (\*,  $p < 0.0001$ ). Significant differences between IL-6 levels of CII-BPI-1 and PBS were not observed. On day 44, serum IL-6 levels were significantly higher in the PBS-treated group compared to CII-1 (\*,  $p < 0.0001$ ) and CII-BPI-1 (\*,  $p < 0.0001$ ). No significant difference in IL-6 levels was observed between CII-1 and CII-BPI-1 treatments on day 44.

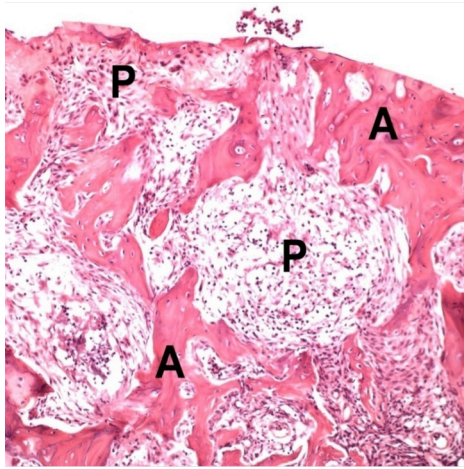
with day 31, the results of the IL-6 levels obtained from mouse serum on day 44 suggest that tethering an adhesion molecule to the antigenic peptide in CII-BPI-1 may induce a different immune response than that of CII-1 peptide.

### **4.3.3 Histopathological analysis**

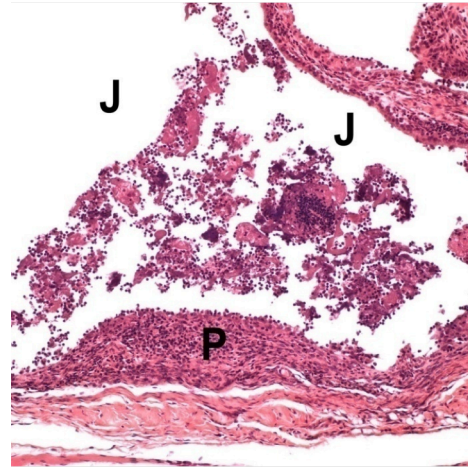
To evaluate the effect of CII-BPI molecules in suppressing the progress of arthritis in the joints, the histopathology of the joints of three representative animals from study-II were examined for cartilage erosion and cell infiltration in the joint space. For the untreated arthritic mice, the knee joints had moderate evidence of articular cartilage damage with pannus formation (**Fig. 4.5A**). The synovial membrane and capsule were both markedly thickened as a result of pannus formation and had inflammatory cell infiltration. The synovial linings were hyperplastic with sloughing of synoviocytes into the joint space. The inflammatory cellular infiltrate consisted of a mixture of mostly synovial macrophages, neutrophils, and lymphoplasmacytic cells. In the untreated arthritic group, the chronic inflammation destroyed the joint lining, including the cartilage and other nearby supporting structures, such as bone (**Fig. 4.5B**). The formation of pannus is a result of overgrowth of the synoviocytes and the observed accumulation of inflammatory cells that led to deformed cartilage and bone, which agreed with the observed clinical scores.

For mice treated with CII-1 peptide, four out of six knee joints appeared normal (**Fig. 4.5C**) and the two remaining joints had very mild evidence of synovial membrane thickening with pannus formation, which falls within normal limits. Minimal evidence of chronic inflammation and articular cartilage damage were observed in the mice group

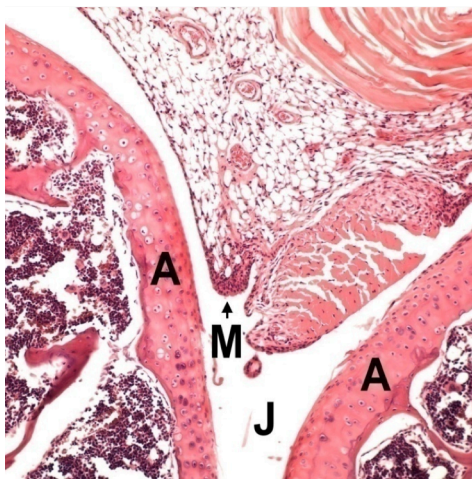
4.5A)



4.5B)



4.5C)



4.5D)

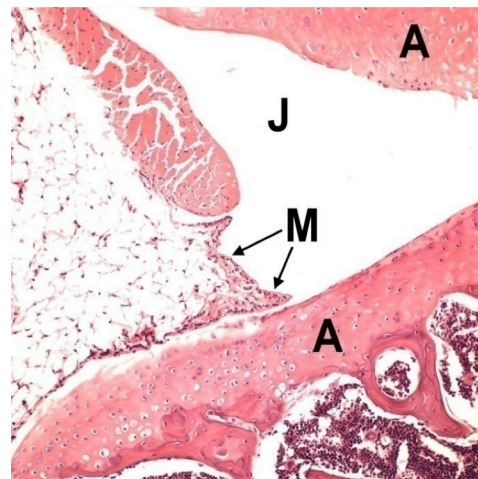


**Figure 4.5** Representative images of histological analysis of knee joints of peptide-treated and PBS-treated mice. **Figures 4.5A and 4.5B** are images of the joints of PBS-treated mice with articular cartilage damage as well as a collection of cellular exudates within the joint spaces. **Figure 4.5C** is the image of mouse joint treated with CII-1 peptide, which appears essentially normal. **Figure 4.5D** is the image of the joint of a mouse treated with CII-BPI-1 showing minimal inflammation. **J**=joint space **M**=synovial membrane **P**=pannus formation **A**=articular cartilage.

treated with CII-BPI-1 (**Fig. 4.5D**). Two of the six knee joints from the mice treated with CII-BPI-1 had very mild evidence of synovial membrane thickening. Mice treated with CII-1 and CII-BPI-1 had a lower incidence of inflammation and cell infiltration into the joint space as well as cartilage damage. Overall, mice treated with CII-1 and CII-BPI-1 peptides had significantly lower joint histopathological scores than the PBS-treated group ( $p < 0.0001$ )(**Fig. 4.6**). The CII-1-treated and CII-BPI-1-treated mice had significantly lower cartilage erosion and inflammatory infiltrates in the joint space compared to those treated with PBS.

#### 4.4 DISCUSSION

BPI molecules were developed by conjugating antigenic peptides to cell adhesion peptides (i.e., LABL peptide) derived from the I-domain of LFA-1 that binds to ICAM-1.<sup>19</sup> The hypothesis is that BPI molecules target and bind to the molecular components (Signal-1 and Signal-2) of the immunological synapse; thus, they inhibit the translocation of Signal-1 and Signal-2 for the final formation of the immunological synapse at the interface of T cell and antigen-presenting cell.<sup>18,20</sup> The current studies showed a proof-of-concept that BPI molecules such CII-BPI-1 and CII-BPI-3 have greater efficacies to suppress arthritis in CIA mice than their respective parent antigenic peptides (CII-1 and CII-3) and PBS (**Fig. 4.7**). It was also found that neither CII-BPI-2 nor CII-2 peptides were effective in preventing the progress of arthritis, suggesting that the sequence of the antigen was not appropriate for inducing tolerance in this model. This finding was consistent with our previous results in which another type of BPI molecule (proteolipid protein (PLP)-BPI derivatives) can suppress experimental autoimmune encephalomyelitis



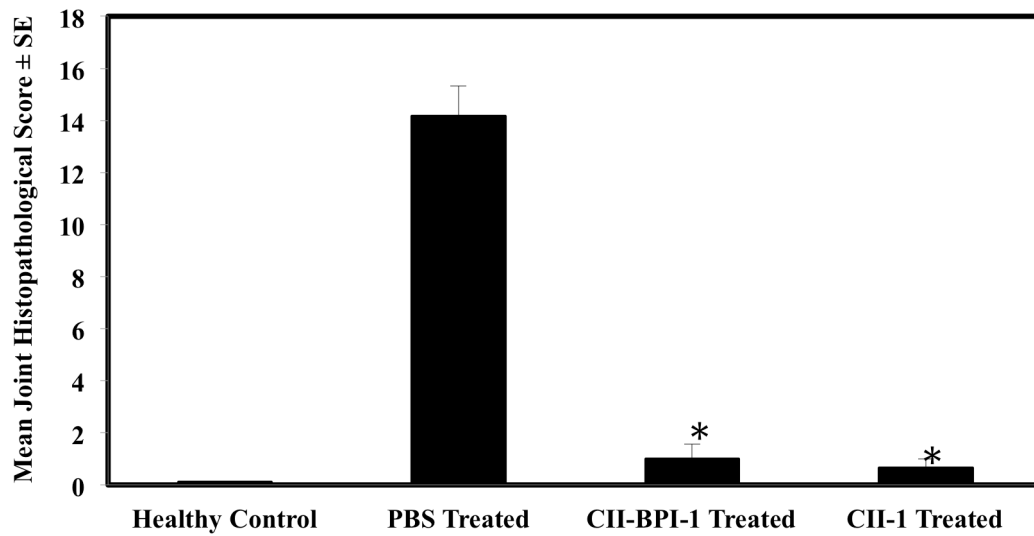


**Figure 4.6** Comparison of the mean scores of joint histopathology of normal untreated mice and diseased mice treated with PBS, CII-BPI-1, and CII-1 peptides in the mouse CIA model. There were significant differences between groups treated with PBS and CII-BPI-1 ( $p < 0.0001$ ) and CII-1 ( $p < 0.0001$ ).

4.7A)



4.7B)



**Figure 4.7** Representative images of the hind paws of mice treated with either PBS (**Figure 4.7A**) or CII-BPI-1 (**Figure 4.7B**).

(EAE) in the mouse model (a model for multiple sclerosis) more effectively than the parent PLP antigenic peptide.<sup>21-23</sup> In addition, GAD-BPI peptide could also suppress type-1 diabetes (T1D) in non-obese diabetic (NOD) mice.<sup>18</sup> These results suggested that BPI molecules have proven effective in suppressing three different autoimmune diseases (RA, MS, and T1D). Because BPI molecules are usually more effective than the parent antigenic peptides in suppressing autoimmune disease in animal models, this suggested that the cell adhesion peptide (i.e., LABL portion) in BPI has an important role in the in vivo activities of BPI molecules.

Although the mechanisms of action of the CII-BPI peptide remain to be fully elucidated, our previous work with PLP-BPI in EAE mouse model showed that the PLP-BPI treatment increased TGF- $\beta$  and IL-10 production, suggesting the involvement of T-reg.<sup>18</sup> Both PLP-BPI and GAD-BPI enhanced the production of IL-4, indicating the involvement of Th2 differentiation and proliferation. The PLP-BPI-treated animals had lower IL-17 than those treated with PBS, indicating the suppression of Th17 proliferation.<sup>21</sup> Researchers have recently confirmed the importance of the IL-17-producing Th17 in CIA.<sup>24</sup> In two separate experiments, the absence of Th17 lymphocytes in mice deficient in IL-17 and the administration of anti-IL-17 antibodies were shown to significantly reduce the severity of CIA.<sup>25,26</sup> Altered peptide ligands (APL) derived from collagen II also suppressed arthritis by the expansion of T-reg and lowering of Th1 and Th17.<sup>27,28</sup> IL-17 has been reported to activate osteoclasts and induce the production of various cytokines (IL-6, IL-8, IL-1, and TNF $\alpha$ ) by macrophages, monocytes, and synoviocytes.<sup>11,29,30</sup>

Studies support the importance of IL-17, showing that IL-17-deficient mice could mitigate CIA development by curbing the activation of autoantigen-specific T cells and B cells in the sensitization phase of CIA.<sup>31</sup> Although IL-23 is important in the differentiation of Th17, cytokines such as IL-6 and IL-21 have been directly implicated in the induction of Th17.<sup>30,32,33</sup> IL-6 has been shown to induce Th17 differentiation in both humans and mice. A study by Kelchtermans *et al.* showed that a transfer of T-reg significantly improved CIA and also lowered TNF $\alpha$  as well as IL-6 levels in mouse sera.<sup>11</sup> The decreased levels of mouse IL-6 cytokine in mouse sera that was observed on day 44 in the current study would suggest that CII-1 and CII-BPI-1 induced similar mechanisms to suppress CIA, by regulating the immune cells responsible for arthritis.<sup>8</sup> In the EAE mouse model, it was also shown that a deficiency of IL-6 shifted the immune response away from an immunogenic role to a protective one.<sup>34</sup> Given our results, a similar mechanism is possible when CIA mice are treated with CII-BPI.

It is interesting to note that even though our results show that CII<sub>256-270</sub> antigenic peptide eventually lowered IL-6 levels, IL-6 is higher than in the control group during the peak of the disease. In contrast, CII<sub>256-270</sub>-BPI (CII-BPI-1) had significantly lower levels of the inflammatory IL-6 cytokine in the thrice-injected mice and also significantly lower IL-6 levels at the peak of disease (day 31 – 4x injected) when compared to CII-1. The lower levels of IL-6 for CII-BPI-1 also corresponded well with our clinical paw swelling data. The cytokine results in our study suggested that the CII-BPI-1 peptide suppressed disease by decreasing IL-6 response. This can, in turn, suppress the downstream Th17 proliferation and perhaps enable a shift in the balance toward T-reg proliferation. Similarly, an anti-IL-6 receptor antibody, called tocilizumab, has been used to treat

rheumatoid arthritis. We also propose that, by decreasing the serum levels of IL-6, we are also inhibiting osteoclastogenesis.<sup>11</sup> In arthritis, osteoclasts are present in the inflamed synovium and greatly contribute to the destruction of bone. Histopathology of the mice treated with CII-BPI-1 confirmed the absence of osteoclasts.

The extracellular matrix of cartilage contains mainly type II (CII) collagen. CII, like myelin basic protein, can elicit tissue-specific autoimmune disease.<sup>35-37</sup> Currently, there are peptides that have been investigated for suppressing a subpopulation of T cells that can induce immunotolerance. These include peptide sequences that are derived from CII and have been shown to hinder the progression of CIA: CII<sub>256-270</sub>, CII<sub>707-721</sub>, or CII<sub>1237-1249</sub>.<sup>38,39</sup> The selection of CII peptides in this study was based on previous studies showing that certain epitopes such as CII<sub>256-270</sub> can bind to I-A<sup>q</sup> MHC class II molecules.<sup>37,40</sup> Previous experiments with CII<sub>256-270</sub> have also shown that this peptide sequence can inhibit the progression of CIA.<sup>37</sup> It has been suggested that CII<sub>260-267</sub> is the immunodominant core.<sup>37,41</sup> As a result of crystallographic analysis and alanine scanning, in rheumatoid arthritis, 267Q and 270K have been determined to be T-cell receptor (TCR) contact residues, while 263F and 266E are mainly responsible for binding with HLA-DR.<sup>42-44</sup> Another major immunodominant epitope (CII<sub>707-721</sub>, CII-3) that we studied has previously been found to elicit a significant proliferative T-cell response.<sup>38</sup> This peptide contains a combination of two overlapping core sequences of CII<sub>704-712</sub> and CII<sub>710-718</sub>.<sup>38</sup> CII<sub>707-721</sub> acetylated at the N-terminus and amidated at the C-terminus was shown to further enhance T cell proliferation. It has been observed that IFN- $\gamma$  release correlates well with the proliferative responses induced by CII<sub>707-721</sub>.<sup>38</sup> CII<sub>1237-1249</sub> (CII-2) peptide was selected based on its ability to selectively bind to the RA-associated DR4 MHC

molecule.<sup>45-47</sup> Because CII<sub>1237-1249</sub> and CII<sub>707-721</sub> have not been studied as extensively as CII<sub>256-270</sub>, their potential mechanisms have not been clearly elucidated. The susceptibility of mice to CIA is confined mostly to MHC type I-A<sup>q</sup>.<sup>40</sup>

These and other peptide molecules have been developed for treating CIA. As was reported here, small molecules that can block LFA-1/ICAM-1 interaction (LABL) can be attached to CII peptides and may facilitate a more specific suppression of T-cell activation. Here, it may be expected that the CII-BPI peptide will selectively block the activation of a subpopulation of T cells that recognizes the collagen peptide-MHC-II complex without eliminating the ability of the host to activate subpopulations of T cells that could fight pathogenic infections.

#### **4.5 CONCLUSIONS**

In conclusion, CII-BPI-1 and CII-BPI-3 can suppress CIA more effectively than CII antigens alone. Tethering of the LABL adhesion peptide to the CII peptide better suppressed CIA by perhaps shifting the immune balance from a pro-inflammatory to a regulatory response. This was supported by an observed deficiency in levels of mouse IL-6 cytokine in mouse sera. To better elucidate the mechanism of the BPI peptide, splenocytes will be isolated to study other cytokine markers in the future. The effect of CII-BPI in altering immunological synapse formation will also be evaluated. Furthermore, optimization of the dose, dosing schedule, and utilization of a different route of delivery may yield better suppression of CIA.

#### 4.6 REFERENCES

- 1 Smolen, J. S. & Steiner, G. Therapeutic strategies for rheumatoid arthritis. *Nat Rev Drug Discov* **2**, 473-488 (2003).
- 2 Joosten, L. A., Helsen, M. M., van de Loo, F. A. & van den Berg, W. B. Anticytokine treatment of established type II collagen-induced arthritis in DBA/1 mice. A comparative study using anti-TNF alpha, anti-IL-1 alpha/beta, and IL-1Ra. *Arthritis Rheum* **39**, 797-809 (1996).
- 3 Lindstrom, T. M. & Robinson, W. H. Rheumatoid arthritis: a role for immunosenescence? *J Am Geriatr Soc* **58**, 1565-1575 (2010).
- 4 Williams, R. O. Collagen-induced arthritis in mice. *Methods Mol Med* **136**, 191-199 (2007).
- 5 Yamamoto, S., Sugahara, S., Ikeda, K. & Shimizu, Y. Amelioration of collagen-induced arthritis in mice by a novel phosphodiesterase 7 and 4 dual inhibitor, YM-393059. *Eur J Pharmacol* **559**, 219-226 (2007).
- 6 Nandakumar, K. S. & Holmdahl, R. Antibody-induced arthritis: disease mechanisms and genes involved at the effector phase of arthritis. *Arthritis Res Ther* **8**, 223 (2006).
- 7 Annunziato, F., Cosmi, L. & Romagnani, S. Human and murine Th17. *Curr Opin HIV AIDS* **5**, 114-119 (2010).
- 8 Assier, E., Boissier, M. C. & Dayer, J. M. Interleukin-6: from identification of the cytokine to development of targeted treatments. *Joint Bone Spine* **77**, 532-536 (2010).

- 9 Augello, A., Tasso, R., Negrini, S. M., Cancedda, R. & Pennesi, G. Cell therapy using allogeneic bone marrow mesenchymal stem cells prevents tissue damage in collagen-induced arthritis. *Arthritis Rheum* **56**, 1175-1186 (2007).
- 10 Huan, J. *et al.* MHC class II derived recombinant T cell receptor ligands protect DBA/1LacJ mice from collagen-induced arthritis. *J Immunol* **180** (2008).
- 11 Kelchtermans, H. *et al.* Activated CD4+CD25+ regulatory T cells inhibit osteoclastogenesis and collagen-induced arthritis. *Ann Rheum Dis* **68**, 744-750, (2009).
- 12 Nakatsukasa, H., Tsukimoto, M., Tokunaga, A. & Kojima, S. Repeated gamma irradiation attenuates collagen-induced arthritis via up-regulation of regulatory T cells but not by damaging lymphocytes directly. *Radiat Res* **174**, 313-324 (2010).
- 13 Huizinga, T. W. & Pincus, T. In the clinic. Rheumatoid arthritis. *Ann Intern Med* **153**, ITC1-1-ITC1-15; quiz ITC11-16 (2010).
- 14 Scott, D. L., Wolfe, F. & Huizinga, T. W. Rheumatoid arthritis. *Lancet* **376**, 1094-1108 (2010).
- 15 Soubrier, M., Mathieu, S., Payet, S., Dubost, J. J. & Ristori, J. M. Elderly-onset rheumatoid arthritis. *Joint Bone Spine* **77**, 290-296 (2010).
- 16 Rubbert-Roth, A. & Finckh, A. Treatment options in patients with rheumatoid arthritis failing initial TNF inhibitor therapy: a critical review. *Arthritis Res Ther* **11 Suppl 1**, S1 (2009).
- 17 Zidi, I. *et al.* Golimumab therapy of rheumatoid arthritis: an overview. *Scand J Immunol* **72**, 75-85 (2010).



- 18 Murray, J. S. *et al.* Suppression of type 1 diabetes in NOD mice by bifunctional peptide inhibitor: modulation of the immunological synapse formation. *Chem Biol Drug Des* **70**, 227-236 (2007).
- 19 Manikwar, P., Kiptoo, P., Badawi, A. H., Buyuktimkin, B. & Siahaan, T. J. Antigen-specific blocking of CD4-specific immunological synapse formation using BPI and current therapies for autoimmune diseases. *Med Res Rev* (2011).
- 20 Yusuf-Makagiansar, H. *et al.* Sequence recognition of alpha-LFA-1-derived peptides by ICAM-1 cell receptors: inhibitors of T-cell adhesion. *Chem Biol Drug Des* **70**, 237-246 (2007).
- 21 Kobayashi, N. *et al.* Prophylactic and therapeutic suppression of experimental autoimmune encephalomyelitis by a novel bifunctional peptide inhibitor. *Clin Immunol* **129**, 69-79 (2008).
- 22 Kobayashi, N., Kobayashi, H., Gu, L., Malefyt, T. & Siahaan, T. J. Antigen-specific suppression of experimental autoimmune encephalomyelitis by a novel bifunctional peptide inhibitor. *J Pharmacol Exp Ther* **322**, 879-886 (2007).
- 23 Ridwan, R. *et al.* Antigen-specific suppression of experimental autoimmune encephalomyelitis by a novel bifunctional peptide inhibitor: structure optimization and pharmacokinetics. *J Pharmacol Exp Ther* **332**, 1136-1145 (2010).
- 24 Cho, Y. G., Cho, M. L., Min, S. Y. & Kim, H. Y. Type II collagen autoimmunity in a mouse model of human rheumatoid arthritis. *Autoimmun Rev* **7**, 65-70 (2007).
- 25 Lubberts, E. IL-17/Th17 targeting: on the road to prevent chronic destructive arthritis? *Cytokine* **41**, 84-91 (2008).

- 26 Lubberts, E. *et al.* IL-17 promotes bone erosion in murine collagen-induced arthritis through loss of the receptor activator of NF-kappa B ligand/osteoprotegerin balance. *J Immunol* **170**, 2655-2662 (2003).
- 27 Wakamatsu, E. *et al.* Altered peptide ligands regulate type II collagen-induced arthritis in mice. *Mod Rheumatol* **19**, 366-371 (2009).
- 28 Zhao, J. *et al.* Mucosal administration of an altered CII263-272 peptide inhibits collagen-induced arthritis by suppression of Th1/Th17 cells and expansion of regulatory T cells. *Rheumatol Int* **29**, 9-16 (2008).
- 29 Awasthi, A. & Kuchroo, V. K. Th17 cells: from precursors to players in inflammation and infection. *Int Immunol* **21**, 489-498 (2009).
- 30 Lubberts, E., Koenders, M. I. & van den Berg, W. B. The role of T-cell interleukin-17 in conducting destructive arthritis: lessons from animal models. *Arthritis Res Ther* **7**, 29-37 (2005).
- 31 Nakae, S., Nambu, A., Sudo, K. & Iwakura, Y. Suppression of immune induction of collagen-induced arthritis in IL-17-deficient mice. *J Immunol* **171**, 6173-6177 (2003).
- 32 Hirahara, K. *et al.* Signal transduction pathways and transcriptional regulation in Th17 cell differentiation. *Cytokine Growth Factor Rev* **21**, 425-434 (2010).
- 33 Korn, T., Bettelli, E., Oukka, M. & Kuchroo, V. K. IL-17 and Th17 Cells. *Annu Rev Immunol* **27**, 485-517 (2009).
- 34 Chitnis, T. & Houry, S. J. Cytokine shifts and tolerance in experimental autoimmune encephalomyelitis. *Immunol Res* **28**, 223-239 (2003).

- 35 Corthay, A., Backlund, J. & Holmdahl, R. Role of glycopeptide-specific T cells in collagen-induced arthritis: an example how post-translational modification of proteins may be involved in autoimmune disease. *Ann Med* **33**, 456-465 (2001).
- 36 Dzhambazov, B. *et al.* Therapeutic vaccination of active arthritis with a glycosylated collagen type II peptide in complex with MHC class II molecules. *J Immunol* **176**, 1525-1533 (2006).
- 37 Myers, L. K. *et al.* Peptide-induced suppression of collagen-induced arthritis in HLA-DR1 transgenic mice. *Arthritis Rheum* **46**, 3369-3377 (2002).
- 38 Bayrak, S. *et al.* T cell response of I-A<sub>q</sub> mice to self type II collagen: meshing of the binding motif of the I-A<sub>q</sub> molecule with repetitive sequences results in autoreactivity to multiple epitopes. *Int Immunol* **9**, 1687-1699 (1997).
- 39 Bayrak, S. & Mitchison, N. A. Bystander suppression of murine collagen-induced arthritis by long-term nasal administration of a self type II collagen peptide. *Clin Exp Immunol* **113**, 92-95 (1998).
- 40 Huang, J. C., Vestberg, M., Minguela, A., Holmdahl, R. & Ward, E. S. Analysis of autoreactive T cells associated with murine collagen-induced arthritis using peptide-MHC multimers. *Int Immunol* **16**, 283-293 (2004).
- 41 Holm, L., Kjellen, P., Holmdahl, R. & Kihlberg, J. Identification of the minimal glycopeptide core recognized by T cells in a model for rheumatoid arthritis. *Bioorg Med Chem* **13**, 473-482 (2005).
- 42 Malmstrom, V., Backlund, J., Jansson, L., Kihlberg, J. & Holmdahl, R. T cells that are naturally tolerant to cartilage-derived type II collagen are involved in the development of collagen-induced arthritis. *Arthritis Res* **2**, 315-326 (2000).

- 43 Andersson, E. C. *et al.* Definition of MHC and T cell receptor contacts in the HLA-DR4-restricted immunodominant epitope in type II collagen and characterization of collagen-induced arthritis in HLA-DR4 and human CD4 transgenic mice. *Proc Natl Acad Sci U S A* **95**, 7574-7579 (1998).
- 44 Jardetzky, T. S. *et al.* Crystallographic analysis of endogenous peptides associated with HLA-DR1 suggests a common, polyproline II-like conformation for bound peptides. *Proc Natl Acad Sci U S A* **93**, 734-738 (1996).
- 45 Dessen, A., Lawrence, C. M., Cupo, S., Zaller, D. M. & Wiley, D. C. X-ray crystal structure of HLA-DR4 (DRA\*0101, DRB1\*0401) complexed with a peptide from human collagen II. *Immunity* **7**, 473-481 (1997).
- 46 Hammer, J. *et al.* Peptide binding specificity of HLA-DR4 molecules: correlation with rheumatoid arthritis association. *J Exp Med* **181**, 1847-1855 (1995).
- 47 Metsaranta, M., Toman, D., de Crombrughe, B. & Vuorio, E. Mouse type II collagen gene. Complete nucleotide sequence, exon structure, and alternative splicing. *J Biol Chem* **266**, 16862-16869 (1991).

## **CHAPTER 5**

### **Summary, conclusions, and future directions**

## 5.1 SUMMARY AND CONCLUSIONS

The objective of the current work was to explore the possibility of delivering macromolecules (e.g., peptides and proteins) that are conjugated to functional peptides to antigen presenting cells (APC) for the suppression of autoimmune diseases in the mouse model. Peptides and proteins have been used as carriers to target and deliver molecules to sites of action. Whereas over 200 protein drugs are currently on the market, a small fraction of those drugs are conjugated products.<sup>1</sup> Conjugating a drug to a macromolecule offers the advantage of being able deliver drug to a specific cell surface antigen with high affinity, thereby reducing any associated toxicity and increasing efficacy. Furthermore, conjugating peptides and proteins that have dual activities to modulate two or more receptors have shown promising results in animal models of autoimmune diseases.<sup>2</sup> Peptides and proteins (LABL and I-domain, respectively) derived from the alpha subunit of leukocyte function associated antigen-1 (LFA-1) bind to the first domain (D1) of intercellular adhesion molecule-1 (ICAM-1), an adhesion molecule that is normally upregulated during inflammatory processes.<sup>3-5</sup> A bifunctional peptide inhibitor (BPI) molecule called GAD-BPI is a conjugate between an antigenic peptide (GAD) and an LABL peptide. GAD-BPI could simultaneously bind to MHC-II and ICAM-1 to co-localize these two receptors on the surface of B cells from non-obese diabetic (NOD) mouse.<sup>6</sup> The proposed mechanism is that colocalizing these two receptors with the bifunctional peptide inhibitors (BPI) prevents the formation of the immunological synapse during the interaction of antigen presenting cells (APC) and T cells to alter T cell differentiation and proliferation from effector T cells to regulatory T cells (T-reg).<sup>7</sup>

In the first part of this work, we developed an I-domain antigen conjugate (IDAC) where I-domain was linked to multiple proteolipid protein (PLP) peptides for suppressing experimental autoimmune encephalomyelitis (EAE), an animal model for multiple sclerosis (MS). PLP<sub>139-151</sub> was conjugated to the lysine residues of I-domain via a maleimide linker with an average of 2.5 PLP<sub>139-151</sub> conjugations per protein molecule. Analysis of the secondary structure suggested that there was no difference in the secondary structure between IDAC and the naked I-domain protein. The applicability of IDAC to suppress EAE was tested using two different compounds, IDAC-1 and IDAC-3. The antigenic peptides of IDAC-3 had both the N- and C-termini capped to protect from exopeptidases, whereas IDAC-1 did not. In mice treated with two intravenous injections of IDAC-1 or IDAC-3 (26 nmol/injection), the onset and suppression of disease was inhibited more significantly in IDAC-3, suggesting that capping the ends of the peptide may increase its resistance to exopeptidases and therefore increasing its *in vivo* half-life. These studies were also the first to show that IDAC-3 could suppress the relapse of EAE when delivered in a vaccine-like manner. Cytokine studies suggested lower levels of IL-17 production, and higher levels of IL-10 in the IDAC-3-treated group, suggesting that IDAC-3 suppressed disease by shifting the immune balance away from Th17-mediated pathology by increasing involvement of T-reg cells.

In the third chapter, it was demonstrated that PLP conjugated to LABL (Ac-PLP-BPI-NH<sub>2</sub>-2) could be formulated in a colloidal gel and administered once subcutaneously (s.c.) to suppress EAE. We showed that Ac-PLP-BPI-NH<sub>2</sub>-2 could suppress EAE when injected s.c. three times in solution in a vaccine-like manner prior to the induction of disease. The rationale behind this work was to develop a one-time s.c. injection to mimic

the dosing schedule previously established in the Siahaan group.<sup>2,8</sup> A one-time injection is ideal for achieving a higher degree of compliance not observed with multi-dose vaccinations. Ac-PLP-BPI-NH<sub>2</sub>-2 was formulated into colloidal gels containing oppositely charged Poly(D,L-lactic-co-glycolic acid) (PLGA) particles. Biocompatible polysaccharides provided negatively charged (alginate) and positively charged (chitosan) coating for the PLGA. *In vitro* results suggested that the entire dose of Ac-PLP-BPI-NH<sub>2</sub>-2 was released by day 8. *In vivo* results indicated that a vaccine-like administration of Ac-PLP-BPI-NH<sub>2</sub>-2 in a colloidal gel formulation could suppress EAE as well as the relapse. Cytokine studies suggested that the mechanism of suppression was due to the shift of the immune balance away from a Th17-mediated response. Colloidal gels have been shown in these studies to be an attractive option in delivering peptide drugs to release in a controlled-release manner without the loss of peptide during formulation.

Finally, we investigated the utility of bifunctional peptide inhibitors to target other autoimmune diseases such as collagen induced arthritis (CIA), an animal model of rheumatoid arthritis (RA). Here, we conjugated different antigenic peptide sequences derived from collagen type II (CII<sub>256-270</sub>, CII<sub>707-721</sub>, and CII<sub>1237-1249</sub>) to LABL. It was found that prophylactic treatment with CII<sub>256-270</sub>-BPI and CII<sub>707-721</sub>-BPI suppressed CIA more effectively than their parent compound. The fact that CII<sub>1237-1249</sub>-BPI did not suppress paw inflammation suggested that the sequence of antigen is important for inducing tolerance in this model. Furthermore, cytokine data suggested that CII linked to LABL shifted the immune balance from a proinflammatory to a regulatory response. These studies suggested that the BPI technology can be translated to other appropriate animal models. Because BPI molecules were shown to be more effective in suppressing



autoimmune disease in different animal models than the parent antigenic peptides, it can be concluded that the adhesion peptide (LABL) has an important role in the *in vivo* activities of BPI molecules.

## **5.2 FUTURE DIRECTIONS**

### **5.2.1 Improving Delivery of IDAC to Suppress EAE**

Delivery of IDAC to the autoimmune animal model is still relatively new. Therefore, studies will need to be done to evaluate the effect of injections of IDAC-3 on the change or differentiation of immune cells. Furthermore, the effect of spreading the injections over a larger timespan as well as multiple injections (greater than 3) will be studied. In addition, the effect of increasing the dose while maintaining the same schedule of 2 injections will be evaluated. I-domain conjugated to a fluorophore (FITC) was observed to bind to and internalize after binding to LFA-1.<sup>9</sup> In the future, studies will be carried out to elucidate the potential mechanisms of action of IDAC molecules on the surface of APCs. Because IDAC-3 is a mixture of PLP<sub>139-151</sub>, mutation studies will be performed to elucidate the active IDAC species. This will be done by mutating several lysine residues to cysteine (Cys-I-domain) for selective conjugation to PLP<sub>139-151</sub> peptide. Finally, to address the issue of epitope spreading generally seen in MS, I-domain will be conjugated with other immunodominant epitopes, such as myelin oligodendrocyte glycoprotein (MOG), to create a multivalent I-domain protein.

### **5.2.2 Optimizing Ac-PLP-BPI-NH<sub>2</sub>-2 Formulation in Colloidal Gel**

Colloidal gel formulated with Ac-PLP-BPI-NH<sub>2</sub>-2 was shown to suppress autoimmune EAE. In the future, colloidal gels will be tested to study the effects of slowing or increasing the rate of peptide release. One way to do so is to formulate a higher amount of PLGA coated with positively charged chitosan polysaccharide relative to PLGA-alginate as Ac-PLP-BPI-NH<sub>2</sub>-2 has a net negative charge. Another way to do this is to adjust the ratio of polymer:peptide. Depending on the day of treatment (day -5 or day 4), a significant difference in the ability of colloidal gel formulated with Ac-PLP-BPI-NH<sub>2</sub>-2 to suppress EAE was observed. The difference in efficacy may be due to the difference in the timing of the production of regulatory and suppressor cells. Therefore, time-dependent cytokine studies need to be done to confirm the effect of schedule of injection on the efficacy of IDAC molecules.

### **5.2.3 Exploring the Mechanism of CIA Suppression**

Future studies in this area should include further investigation of the ability of CII-BPI to suppress CIA. Splenocytes will be isolated to study other cytokine markers, such as IL-17 and IL-10. Studies should include the investigation of observing the alteration in immunological synapse formation. It is also important to optimize the dose, dosing schedule, and utilization of a different route of delivery to better suppress CIA. Administering CII-BPI in a vaccine-like manner would also be valuable in investigating the ability of the peptide to shift the balance of the immune response to a regulatory phenotype prior to the induction of disease.

### 5.3 REFERENCES

- 1 Walsh, G. Biopharmaceutical benchmarks 2010. *Nat Biotechnol* **28**, 917-924 (2010).
- 2 Kobayashi, N., Kobayashi, H., Gu, L., Malefyt, T. & Siahaan, T. J. Antigen-specific suppression of experimental autoimmune encephalomyelitis by a novel bifunctional peptide inhibitor. *J Pharmacol Exp Ther* **322**, 879-886 (2007).
- 3 Lee, S. J. & Benveniste, E. N. Adhesion molecule expression and regulation on cells of the central nervous system. *J Neuroimmunol* **98**, 77-88 (1999).
- 4 Seidel, M. F., Keck, R. & Vetter, H. ICAM-1/LFA-1 expression in acute osteodestructive joint lesions in collagen-induced arthritis in rats. *J Histochem Cytochem* **45**, 1247-1253 (1997).
- 5 Stanley, P. & Hogg, N. The I domain of integrin LFA-1 interacts with ICAM-1 domain 1 at residue Glu-34 but not Gln-73. *J Biol Chem* **273**, 3358-3362 (1998).
- 6 Murray, J. S. *et al.* Suppression of type 1 diabetes in NOD mice by bifunctional peptide inhibitor: modulation of the immunological synapse formation. *Chem Biol Drug Des* **70**, 227-236 (2007).
- 7 Manikwar, P., Kiptoo, P., Badawi, A. H., Buyuktimkin, B. & Siahaan, T. J. Antigen-specific blocking of CD4-specific immunological synapse formation using BPI and current therapies for autoimmune diseases. *Med Res Rev*, (2011).
- 8 Kobayashi, N. *et al.* Prophylactic and therapeutic suppression of experimental autoimmune encephalomyelitis by a novel bifunctional peptide inhibitor. *Clin Immunol* **129**, 69-79 (2008).

- 9 Manikwar, P. *et al.* Utilization of I-domain of LFA-1 to Target Drug and Marker Molecules to Leukocytes. *Theranostics* **1**, 277-289 (2011).